

The initial mass function of simple and composite stellar populations

Pavel Kroupa^{1,2}

¹*Argelander-Institut für Astronomie, Universität Bonn, Auf dem Hügel 71, D-53121 Bonn, Germany*

²*The Rhine Stellar Dynamical Network*

Abstract. The distribution of stellar masses that form together, the initial mass function (IMF), is one of the most important astrophysical distribution functions. The determination of the IMF is a very difficult problem because stellar masses cannot be measured directly and because observations usually cannot assess all stars in a population requiring elaborate bias corrections. Nevertheless, impressive advances have been achieved during the last decade, such that the shape of the IMF is reasonably well understood from low-mass brown dwarfs (BDs) to very massive stars. The case can be made for a rather universal form that can be well approximated by a two-part power-law function in the stellar regime. However, there exists a possible hint for a systematic variation according to which the binary properties of very-low-mass stars (VLMSs) and BDs may be fundamentally different from those of late-type stars implying the probable existence of a discontinuity in the IMF, but the surveys also appear to suggest the number of BDs per star to be independent of the physical conditions of current Galactic star formation. Star-burst clusters and thus globular cluster may, however, have a much larger abundance of BDs. Very recent advances have allowed the measurement of the physical upper stellar mass limit, which also appears to be disconcertingly robust to variations in metallicity. Furthermore, it now appears that star clusters are formed in a rather organised fashion from low- to high stellar masses, such that the most-massive stars just forming terminate further star-formation within the particular cluster. Populations formed from many star clusters, *composite populations*, would then have steeper IMFs (fewer massive stars per low-mass star) than the simple populations in the constituent clusters. A near invariant star-cluster mass function implies the maximal cluster mass to correlate with the galaxy-wide star-formation rate. This then leads to the result that the composite-stellar IMFs vary in dependence of galaxy type, with potentially dramatic implications for theories of galaxy formation and evolution.

1. Introduction

The stellar initial mass function (IMF) is perhaps the most important macroscopic distribution function in astrophysics, because it defines the mass-spectrum of stars born together. The other fundamental function is the star-formation history of a stellar system. They are connected through complex microscopic physical processes that defy detailed treatment on galactic scales. Together they contain the essential information on the transformation of dark gas to shining

stars and the spectral energy distribution thereof. They also contain the essential information on the cycle of matter, which fraction of it is locked up for “ever” in feeble stars and sub-stellar objects, and how much of it is returned enriched with higher chemical elements to the interstellar medium or atmosphere of a galaxy.

Given the importance of the IMF a huge research effort has been invested to distill its shape and variability. The seminal contribution by Salpeter (1955) whilst staying in Canberra first described the IMF as a power-law, $dN = \xi(m) dm = k m^{-\alpha} = dN$, where dN is the number of stars in the mass interval $m, m + dm$ and k is the normalisation constant. By modelling the spatial distribution of the then observed stars with assumptions on the star-formation rate, Galactic-disk structure and stellar evolution time-scales, Salpeter arrived at the power-law index $\alpha = 2.35$ for $0.4 \lesssim m/M_{\odot} \lesssim 10$, which today is known as the “Salpeter IMF”.

This IMF form implies a diverging mass density for $m \rightarrow 0$, which was interesting since dark matter was speculated, until the early 1990’s, to possibly be made-up of faint stars or sub-stellar objects. Studies of the stellar velocities in the solar-neighbourhood also implied a large amount of missing, or dark, mass in the disk of the Milky Way (MW) (Bahcall 1984). Careful compilation in Heidelberg of the Gliese *Catalogue of Nearby Stars* beginning in the 1960’s (Jahreiß & Wielen 1997)¹, and the application at the beginning of the 1980’s of an innovative photographic pencil-beam survey-technique reaching deep into the Galactic field in Edinburgh by Reid & Gilmore (1982) significantly improved knowledge of the space density of VLMSs ($0.072 \lesssim m/M_{\odot} \lesssim 0.14$).

Major studies extending Salpeter’s work to lower and larger masses followed, showing that the mass function (MF) of Galactic-field stars turns over below one solar mass thus avoiding the divergence. Since stars with masses $m \lesssim 0.8 M_{\odot}$ do not evolve significantly over the age of the Galactic disk, the MF equals the IMF for these. While the work of Miller & Scalo (1979) relied on using the nearby stellar sample to define the IMF for $m < 1 M_{\odot}$, Scalo (1986) relied mostly on a more recent deep pencil-beam star-count survey. Scalo (1986) stands out as the most thorough and comprehensive analysis of the IMF in existence, laying down notation and ideas still in use today. The form of the IMF for low-mass stars was revised in the early 1990’s in Cambridge, especially through the quantification of significant non-linearities in the stellar mass–luminosity relation and evaluation of the bias due to unresolved binary systems (Kroupa et al. 1990, 1991, 1993). On the one hand this work led to a detailed understanding of the shape of the stellar luminosity function (LF) in terms of stellar physics, and on the other the difference between the results obtained by Miller & Scalo (1979) and Scalo (1986) for low-mass stars was resolved by this work through rigorous modelling of all biases affecting local trigonometric-based and distant photometric-parallax-based surveys, such as come from an intrinsic metallicity scatter, evolution along the main sequence and contraction to the main sequence. In doing so this work also included an updated local stellar sample *and* the then best-available deep pencil-beam survey by Stobie et al. (1989). As such it stands

¹The latest version of the catalogue can be found at <http://www.ari.uni-heidelberg.de/aricns/>, while <http://www.nstars.nau.edu/> contains the Nearby Stars (NStars) database.

unique today as being the only rigorous analysis of the late-type-star MF using simultaneously both the *nearby trigonometric parallax* and the *far, pencil-beam* star-count data. This study was further extended to an analysis of other ground-based pencil-beam surveys (Kroupa 1995a). Zheng et al. (2001) employed the HST to measure the LF through the entire thickness of the MW disk finding excellent agreement with the pencil-beam (photometric-parallax) LFs (Fig. 6 below). The results of Kroupa et al. (1993) ($\alpha \approx 1.3, 0.08 - 0.5 M_{\odot}$), were confirmed by Reid et al. (2002) using updated local star-counts that included Hipparcos parallax data. Indeed, the continued long-term observational effort on nearby stars by Neill Reid, John Gizis and collaborators forms one of the very major pillars of modern IMF work; continued discussion of controversial interpretations have much improved and sharpened our general understanding of the issues. A re-analysis of the nearby mass function of stars in terms of a log-normal form in the mass range $0.07 - 1 M_{\odot}$ was provided by Chabrier, finding agreement to the deep HST star-count data once unresolved multiple stars and a metal-deficient colour-magnitude relation for thick-disk M dwarfs are accounted for (Chabrier 2003b).

The Galactic-field IMF for $0.08 < m/M_{\odot} < 1$ can thus be regarded as being reasonably well-constrained, but some unresolved issues nevertheless remain. The exact form of the IMF is still under dispute. The mathematical necessity for the IMF to turn-over at some small mass and the corresponding empirical result by Miller & Scalo (1979) lead to the development of a theory of the IMF based on gravitational instabilities in the turbulent inter-stellar medium (Fleck 1982; Ferrini et al. 1983) and random hierarchical fragmentation (Zinnecker 1984), thereby accounting for the approximately log-normal shape of the IMF. While a log-normal form has often been adopted given the turnover near a few tenths of a solar mass (Miller & Scalo 1979; Chabrier 2001) and some theoretical ideas (e.g. Adams & Fatuzzo 1996; Chabrier 2003a), it has never been demonstrated that the log-normal form is consistent with the sharp peak in the stellar luminosity function (LF) near absolute visual and I-band magnitudes $M_V \approx 12, M_I \approx 8.5$, respectively. A power-law description together with a semi-empirical mass-luminosity relation has, in contrast, been found to fit the nearby and deep LFs well (Kroupa et al. 1993; Kroupa 1995a). Furthermore, most approaches have relied on using parametrised formulae, such as the multi-power-law form or the log-normal form, and so it would be important to develop a non-parametric method that allows inclusion of the biases through unresolved multiple systems. Such a method would be very useful for studying the shape of the IMF in star clusters.

In contrast to the Galactic-field sample, where stars of many ages and metallicities are mixed, star clusters offer the advantage that the stars have the same age and metallicity and distance. And so a very large effort has been invested to try to extract the IMF from open (Sanner & Geffert 2001; Piskunov et al. 2004; Moraux et al. 2004, e.g.) and embedded (Hillenbrand 1997; Muench et al. 2002; Luhman 2004, e.g.) clusters, as well as associations (Gouliermis et al. 2005). Here the continued methodologically consistent observational work on a number of different very young populations by Kevin Luhman and collaborators has had a major impact on our understanding of the IMF at low masses. On the theoretical side, the ever-improving modelling of stellar and BD atmospheres being pushed forward with excellent results no-

tably by the Lyon group (Isabelle Baraffe and Gilles Chabrier), has allowed consistently better constraints on the faint-star MF by a wide variety of observational surveys². Furthermore, the development of high-precision N -body codes that rely on complex mathematical and algorithmic procedures through the work of Sverre Aarseth and Seppo Mikkola (Aarseth 1999) and others has led to important progress on understanding the variation of the dynamical properties of stellar populations in individual clusters and the Galactic field (Kroupa 1995d; de La Fuente Marcos 1997; Kroupa 2001b; Kroupa et al. 2001; Portegies Zwart et al. 2001, 2002; Baumgardt & Makino 2003; Moraux et al. 2004; Hurley et al. 2005). In general, the MF found for clusters is consistent with the Galactic-field IMF for $m < 1 M_{\odot}$, but some problems remain. While a huge progress has been achieved in modelling cluster populations over time, it is for example still unclear as to why open clusters have a significant deficit of white dwarfs (Fellhauer et al. 2003). A further problem is posed by the rapid and violent early dynamical evolution of clusters (Lada et al. 1984; Goodwin 1997; Kroupa et al. 2001; Geyer & Burkert 2001; Moraux et al. 2004; Kroupa 2005) and the associated loss of a large fraction of the cluster population, and due to the density-dependent disruption of primordial binary systems. Young clusters have thus undergone a highly complex dynamical evolution which continues into old age (Baumgardt & Makino 2003) and are therefore subject to biases that can only be studied effectively with full-scale N -body methods, thus imposing a complexity of analysis that surpasses that for the Galactic-field sample.

For massive stars, the Scalo (1986) IMF is based on a combination of Galactic-field star-counts and OB association data and has a slope $\alpha \approx 2.7$ for $m \gtrsim 2 M_{\odot}$ with much uncertainty for $m \gtrsim 10 M_{\odot}$. The previous determination by Miller & Scalo (1979) also argued for a relatively steep field-IMF with $\alpha = 2.5, 1 \leq m/M_{\odot} \leq 10$ and $\alpha = 3.3, m > 10 M_{\odot}$. However, Massey's work at Tucson demonstrated, through extensive spectroscopic classification, that $\alpha = 2.35 \pm 0.1, m \gtrsim 10 M_{\odot}$ (Massey 1998), for a large variety of physical environments, namely OB associations and dense clusters for populations with metallicity ranging from near-solar-abundance to about 1/10th metal abundance (Fig. 1). Consequently, above about $0.5 M_{\odot}$ the empirical IMF can be described well by a single power-law form with the *Salpeter/Massey index*, $\alpha = 2.35$, therewith being remarkably invariant.³

While the case is often made that star-bursts may have an IMF that is overabundant in massive stars (e.g. Eisenhauer 2001), time-dependent mass segregation mimics just such an effect (Boily et al. 2005). Local well-resolved star-burst clusters also do not support top-heavy IMFs. Notable well-studied cases with masses in the range $10^4\text{--}5 M_{\odot}$ and central densities near 10^5 stars/pc³ are the

²Here it should be emphasised and acknowledged that the intensive and highly fruitful discourse between Guenther Wuchterl and the Lyon group has led to the important understanding that the classical evolution tracks computed in Lyon and by others are unreliable for ages less than a few Myr (Wuchterl & Tscharnuter 2003).

³Note that Scalo (1998) emphasises that the IMF remains poorly constrained owing to the small number of massive stars in any one sample. This is a true albeit conservative stand-point, and the present author prefers to accept Massey's result as a working hypothesis. This hypothesis that there exists a universal parent distribution function is tested in individual clusters and OB associations for possible significant deviations (cf. Pflamm-Altenburg & Kroupa 2006).

30 Dor cluster (R136) in the LMC, NGC 3603 in the MW, and the Arches cluster near the Galactic centre. The 30 Dor star-burst cluster (NGC 2070) has been found by Massey & Hunter (1998) to have a Salpeter MF for $2.8 \lesssim m/M_{\odot} \lesssim 120$, which is confirmed by Selman et al. (1999) who apply corrections for variable reddening. But they also note that the core of NGC 2070 is clearly mass-segregated with a flatter MF. For NGC 3603, Sung & Bessell (2004) find a highly mass-segregated system with a flat MF in the core, but the MF beyond the core has $\alpha = 1.9 \pm 0.1$, $m \gtrsim 1.6 M_{\odot}$, thus again being consistent with a Salpeter value. The Arches cluster is situated at a projected distance of 25 pc from the Galactic centre and is therefore in a very exotic environment being strongly influenced by tidal forces. Figer et al. (1999) and Stolte et al. (2002) find the innermost region of the cluster to have $\alpha \approx 1$, but at larger radii $\alpha \approx 2.7$. Kim et al. (2000) and Portegies Zwart et al. (2002) study the evolution of the Arches using N -body modelling and find that the cluster evolves rapidly, losing memory of its birth configuration within about 1 Myr. In particular, they find that the IMF in the Arches may have been quite normal.

This short discussion thus indicates that the evidence for a top-heavy IMF is not strong in well-resolved star-burst clusters, and that dynamical evolution of the clusters needs to be modelled in detail to understand possibly deviant *observed* IMF's. A highly interesting finding reported by Massey (1998, 2003) is that the OB stellar population found in the field of the LMC has a very steep MF, $\alpha \approx 4.5$, which can be interpreted to be due to the preferred formation of small groups or even isolated O and B-type stars. Another interpretation that would not need to resort to exotic star-formation events is the dynamical ejection of OB stars from dynamically unstable cores of young clusters. This may lead to such a steep IMF because simple estimates show that preferentially the less-massive members of a core are ejected (Clarke & Pringle 1992). This process needs to be studied using fully-consistent and high-precision N -body modelling of young clusters, to see if the observed distribution of field-OB stars can be accounted for with this process alone, or if indeed an exotic star-formation mode needs to be invoked to explain some of the observations.

The “secret” ingredient for uncovering the true nature of an IMF is thus the high-precision N -body experiment, which therewith achieves an importance well beyond merely the methodological (Kim et al. 2006; Pflamm-Altenburg & Kroupa 2006, e.g.).

Although we have essentially no knowledge about the low-mass end of the IMF in star-burst clusters, due to their rarity and thus generally large distances, today we do know that the MF of low-mass stars in globular clusters, that presumably formed as star-burst clusters, is quite similar to that of the solar-neighbourhood and in young open clusters. This suggests a remarkable invariance of the low-mass IMF (de Marchi & Paresce 1995a,b; Paresce et al. 1995, e.g.). The case has been made for a systematic variation with metallicity in the sense that the metal-poorer and older populations may have flatter MFs as expected from simple Jeans-mass arguments (Kroupa 2001b, eq. 22 below), but this suggestion remains speculative rather than conclusive because stellar-dynamical processes skew observed MFs (Kroupa 2001b; Baumgardt & Makino 2003).

The MF for BDs is even shallower, as two recent studies of the available solar-neighbourhood star-count data demonstrate, these constraints being consistent with those from young star clusters (Chabrier 2002; Allen et al. 2005). From their non-stellar binary properties (Martín et al. 2003; Bouy et al. 2003; Close et al. 2003) it is emerging, however, that BDs may not be a continuation of the stellar population. Although their formation is linked to that of their sibling stars, the IMF is likely to be discontinuous near the hydrogen-burning mass limit, and the overall result appears to be that about one BD is born per five stars (Kroupa & Bouvier 2003, § 5.2. below). We have thus had to realise that BDs contribute a negligible dynamical mass to any stellar population. Faint main-sequence stars account for most of the mass in the MW disk, and the need for dark matter in the MW disk also disappeared as improved kinematical data and analysis thereof became available (Kuijken 1991; Flynn & Fuchs 1994). Furthermore, the suggestion has been made by two independent teams, based on an extremely high-quality spectral analysis of solar-neighbourhood stars and by accounting for the relative death rate of stars, that the Galactic thick disk may be substantially more massive than is currently thought (Soubiran et al. 2003; Fuhrmann 2004). This would further reduce the mass discrepancy evident in the solar motion about the Galaxy.

Five very recent further developments have enriched the study of the mass-distribution of stars appreciably. Weidner & Kroupa (2004) demonstrated for the first time that the absence of stars more massive than about $150 M_{\odot}$ in R136 in the LMC must imply a physical mass limit to stars near $150 M_{\odot}$, with high statistical significance, unless $\alpha \gtrsim 2.8$ for $m \gtrsim 1 M_{\odot}$. Such a steep IMF may be the true mass-distribution if unresolved multiple systems are corrected for, but an affirmation of this and thus the negation of the physical stellar mass limit awaits a detailed investigation of this issue. Figer (2005) followed by performing the same analysis with his HST data on the Arches cluster confirming the same physical mass limit, and Oey & Clarke (2005) published a statistical analysis of a number of OB associations and clusters again confirming that a physical mass limit exists in the mass range $120 - 200 M_{\odot}$. Thus, stellar masses are limited near $0.072 M_{\odot}$ (Chabrier 2003a) and near $150 M_{\odot}$. The other notion recently re-affirmed is that star clusters appear to limit the masses of the most massive stars in them in such a way that more massive clusters permit higher masses of their most massive stars (Weidner & Kroupa 2006). The third very recent insight, resulting from the above two, is that the composite IMFs of whole galaxies must be steeper than the stellar IMF for $m \gtrsim 1 M_{\odot}$, because composite populations result from the addition of the stellar IMFs in the star clusters which themselves are distributed according to a power-law cluster mass function (Kroupa & Weidner 2003; Weidner & Kroupa 2005). This notion had been raised already by Vanbeveren (1982) and a similar ansatz has been followed by Oey & Clarke (1998) for the construction of HII LFs in galaxies, and the recent advances on this issue thus suggest that the discrepancy between Scalo's field-star IMF and Massey's stellar IMF in star clusters may have found a natural resolution (Kroupa & Weidner 2003). The fourth recent insight (Weidner et al. 2004) is that the star-formation rate of a galaxy dictates the mass of the most massive star cluster forming within it. This then implies the fifth recent result (Weidner & Kroupa 2006) that galaxies have different integrated (composite) IMFs. According to this picture, galaxies with a small stellar mass ($\lesssim 10^7 M_{\odot}$)

may, over their life-times, be significantly deficient in stars more massive than a few M_{\odot} .

Given these results, it thus becomes necessary to distinguish between *simple stellar populations* and *composite populations*. A simple population is found in a star cluster and consists of stars of equal age and metallicity. A composite population consists of more than one cluster. The *stellar IMF* refers to the IMF of stars in a simple population, while the *composite IMF*, or the *integrated galactic IMF* (IGIMF) is the IMF of a composite population, i.e. a population composed of many star clusters, most of which may be dissolved.

This treatise attempts to provide an overview of the general methods used to derive the IMF with special attention on the pitfalls that are typically encountered. The somewhat uncomfortable result until now is that there is no reliable, or confirmed, evidence for stellar-IMF differences in simple populations with different physical properties. While this must be recognised as being a problem, because elementary arguments would imply variations with different conditions, it does ease modelling of simple stellar systems. While the IMF for $0.08 \lesssim m/M_{\odot} \lesssim 1 M_{\odot}$ is by now quite well constrained, for massive stars the effects of unresolved multiple systems remains unknown⁴. Corrections for these may significantly affect the shape of the IMF with rather major implications for much of extragalactic and Galactic astrophysics. Understanding these corrections is thus of major importance. The very recent realisation that star-clusters limit the mass spectrum of their stars has interesting implications for the formation of stars in a cluster and leads to the insight that composite populations must show IMFs that differ from the stellar IMF in each cluster. A detailed analysis indicates that the composite IMF, i.e. the IGIMF, should vary between galaxies. With this finale, this treatise reaches the cosmological arena.

Other relatively recent reviews of the IMF are by Scalo (1998), Kroupa (2002), Chabrier (2003a). The proceedings of the “38th Herstmonceux Conference on the Stellar Initial Mass Function” (Gilmore & Howell 1998) and the proceedings of the “IMF50” meeting in celebration of Ed Salpeter’s 80th birthday (Corbelli et al. 2005) contain a wealth of important contributions to the field.

2. Some essentials

Assuming all binary and higher-order stellar systems can be resolved into individual stars in some population such as the solar neighbourhood and that only main-sequence stars are selected for, then the number of single stars per pc^3 in the mass interval m to $m + dm$ is $dN = \Xi(m) dm$, where $\Xi(m)$ is the present-day mass function (PDMF). The number of single stars per pc^3 in the absolute V-band magnitude interval M_P to $M_P + dM_P$ is $dN = -\Psi(M_P) dM_P$, where $\Psi(M_P)$ is the stellar luminosity function (LF) which is constructed by counting the number of stars in the survey volume per magnitude interval, and P signifies

⁴see also footnote 3

an observational photometric pass-band such as the V - or I -band. Thus

$$\Xi(m) = -\Psi(M_P) \left(\frac{dm}{dM_P} \right)^{-1}. \quad (1)$$

Note that the the minus sign comes-in because increasing mass leads to decreasing magnitudes, and that the LF constructed in one photometric pass band P can be transformed into another band P' by

$$\Psi(M_P) = \frac{dN}{dM_{P'}} \frac{dM_{P'}}{dM_P} = \Psi(M_{P'}) \frac{dM_{P'}}{dM_P} \quad (2)$$

if the function $M_{P'} = \text{fn}(M_P)$ is known.

Since the derivative of the stellar mass–luminosity relation (MLR), $m(M_P) = m(M_P, Z, \tau, \mathbf{s})$, enters the calculation of the MF, any uncertainties in stellar structure and evolution theory on the one hand (if a theoretical MLR is relied upon) or in observational ML-data on the other hand, will be magnified accordingly. This problem cannot be avoided if the mass function is constructed by converting the observed stellar luminosities one-by-one to stellar masses using the MLR and then binning the masses, because the derivative of the MLR nevertheless creeps-in through the binning process, because *equal luminosity intervals are not mapped into equal mass intervals*. The dependence of the MLR on the star’s chemical composition, Z , it’s age, τ , and spin vector \mathbf{s} , is explicitly stated here, since stars with fewer metals than the Sun are brighter (lower opacity), main-sequence stars brighten with time and loose mass, and rotating stars are dimmer because of the reduced internal pressure. Mass loss and rotation are significant factors for intermediate and especially high-mass stars (Penny et al. 2001).

The IMF follows by correcting the observed number of main sequence stars for the number of stars that have evolved off the main sequence. Defining $t = 0$ to be the time when the Galaxy that now has an age $t = \tau_G$ began forming, the number of stars per pc^3 in the mass interval $m, m + dm$ that form in the time interval $t, t + dt$ is $dN = \xi(m, t) dm \times b(t) dt$, where the expected time-dependence of the IMF is explicitly stated (§ 8.), and where $b(t)$ is the normalised SFH, $(1/\tau_G) \int_0^{\tau_G} b(t) dt = 1$. Stars that have main-sequence life-times $\tau(m) < \tau_G$ leave the stellar population unless they were born during the most recent time interval $\tau(m)$. The number density of such stars with masses in the range $m, m + dm$ still on the main sequence and the total number density of stars with $\tau(m) \geq \tau_G$, are, respectively,

$$\Xi(m) = \xi(m) \frac{1}{\tau_G} \times \begin{cases} \int_{\tau_G - \tau(m)}^{\tau_G} b(t) dt & , \quad \tau(m) < \tau_G, \\ \int_0^{\tau_G} b(t) dt & , \quad \tau(m) \geq \tau_G, \end{cases} \quad (3)$$

where the time-averaged IMF, $\xi(m)$, has now been defined. Thus, for low-mass stars $\Xi = \xi$, while for a sub-population of massive stars that has an age $\Delta t \ll \tau_G$, $\Xi = \xi(\Delta t/\tau_G)$ for those stars of mass m for which the main-sequence life-time $\tau(m) > \Delta t$, indicating how an observed high-mass IMF in an OB association, for example, has to be scaled to the Galactic-field IMF for low-mass stars.⁵ In

⁵assuming continuity of the IMF

this case the different spatial distribution via different disk-scale heights of old and young stars also needs to be taken into account, which is done globally by calculating the stellar surface density in the MW disk (Miller & Scalo 1979; Scalo 1986). Thus we can see that joining the cumulative low-mass star counts to the snap-shot view of the massive-star IMF is non-trivial and affects the shape of the IMF in the notorious mass range $\approx 0.8 - 3 M_{\odot}$, where the main-sequence life-times are comparable to the age of the MW disk. In a star cluster or association with an age $\tau_{\text{cl}} \ll \tau_{\text{G}}$, τ_{cl} replaces τ_{G} in eq. 3. Examples of the time-modulation of the IMF are $b(t) = 1$ (constant star-formation rate) or a Dirac-delta function, $b(t) = \tau_{\text{cl}} \times \delta(t - t_0)$ (all stars formed at the same time t_0).

Often used is the “logarithmic mass function” (Table 3 below),

$$\xi_{\text{L}}(m) = (m \ln 10) \xi(m), \quad (4)$$

where $dN = \xi_{\text{L}}(m) dlm$ is the number of stars with mass in the interval $lm, lm + dlm$ ($lm \equiv \log_{10} m$)⁶.

3. The massive stars

Studying the distribution of massive stars is complicated because they radiate most of their energy at far-UV wavelengths that are not accessible from Earth, and through their short main-sequence life-times, τ , that remove them from star-count surveys. For example, a $85 M_{\odot}$ star cannot be distinguished from a $40 M_{\odot}$ star on the basis of M_V alone (Massey 1998, 2003). Constructing $\Psi(M_V)$ in order to arrive at $\Xi(m)$ for a mixed-age population does not lead to success if optical or even UV-bands are used. Instead, spectral classification and broadband photometry for estimation of the reddening on a star-by-star basis has to be performed to measure the effective temperature, T_{eff} , and the bolometric magnitude, M_{bol} , from which m is obtained allowing the construction of $\Xi(m)$ directly (whereby $\Psi(M_{\text{bol}})$ and $\Xi(m)$ are related by eq. 1). Having obtained $\Xi(m)$ for a population under study, the IMF follows by applying eq. 3. A more straight-forward method often used (e.g. Hillenbrand 1997; Massey 1998, 2003) is to evolve each measured stellar mass to its initial value using theoretical stellar evolution tracks, and to construct $\xi(m)$ from this set of masses.

Massey (2003) stresses that studies that only rely on broad-band optical photometry consistently arrive at IMFs that are significantly steeper with $\alpha_3 \approx 3$ (see eq. 20 below), rather than $\alpha_3 = 2.2 \pm 0.1$ consistently found for a wide range of stellar populations. Indeed, the application of the same methodology by Massey on a number of young populations of different metallicity and density shows a remarkable uniformity of the IMF above about $10 M_{\odot}$ (Fig. 1).

The available IMF measurements do not take into account the bias through unresolved systems which may be substantial since the proportion of multiple stars is higher for massive stars than for low-mass Galactic-field stars (e.g. Duchêne et al. 2001). For example, in the Orion Nebula Cluster (ONC) each massive star has, on average, 1.5 companions (Preibisch et al. 1999), while in the cluster NGC 6231 García & Mermilliod (2001) find that 80 % of all O stars are

⁶Note that Scalo (1986) calls $\xi_{\text{L}}(m)$ the *mass function* and $\xi(m)$ the *mass spectrum*.

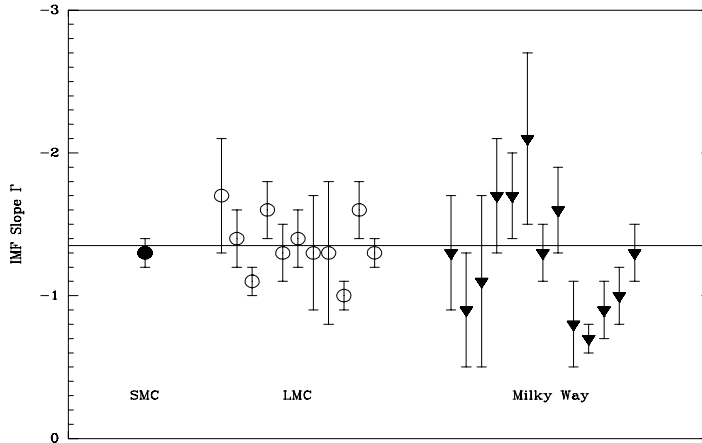


Figure 1. The IMF slope $\Gamma = 1 - \alpha$ determined in a homogeneous manner by Massey (2003) for OB associations and clusters in the MW, LMC and SMC. The Small Magellanic Cloud (SMC) has a metallicity $Z = 0.005$, the Large Magellanic Cloud (LMC) has $Z = 0.008$ and the Milky Way (MW) has $Z = 0.018$ within a distance of 3 kpc around the Sun. With kind permission from Massey (2003).

radial-velocity binaries. Sagar & Richtler (1991) estimate the binary-star bias on the IMF for stars in the mass range 2 to $14 M_{\odot}$ assuming each star has one companion. The IMF would steepen to the Scalo value $\alpha \approx 2.7$ for a measured $\alpha = 2.3$. This correction, however, depends on the distribution of companions that is not yet known very well (Preibisch et al. 1999; Duchêne et al. 2001). A larger value, $\alpha \approx 3 \pm 0.1$, is also suggested from a completely independent but indirect approach relying on the distribution of ultra-compact HII regions in the Galaxy (Casassus et al. 2000; Oey & Clarke 1998), but this may be a result of the composite nature of galaxy-wide populations (§ 8.). Clearly, the effect multiplicity has on the massive-star IMF needs further exploration.

Massive main-sequence stars have substantial winds flowing outwards with velocities of a few 100 to a few 1000 km/s (Kudritzki & Puls 2000). For example, $10^{-6.5} < \dot{M} < 10^{-6} M_{\odot}/\text{yr}$ for $m = 35 M_{\odot}$ with $\tau = 4.5$ Myr (Garcia-Segura et al. 1996), and $10^{-5.6} < \dot{M} < 10^{-5.8} M_{\odot}/\text{yr}$ for $m = 60 M_{\odot}$ with $\tau = 3.45$ Myr (Garcia-Segura et al. 1996). More problematical is that stars form rapidly rotating and are sub-luminous as a result of reduced internal pressure. But they decelerate significantly during their main-sequence life-time owing to the angular-momentum loss through their winds and become more luminous more rapidly than non-rotating stars (Maeder & Meynet 2000). A comparison of such models is available in Figs. 2 and 3. Evidently, for ages less than 2.5 Myr the models deviate only by 5–13 % from each other in mass, luminosity or temperature (Weidner & Kroupa 2006). Large deviations are evident for advanced stages of evolution though.

The mass–luminosity relation for a population of stars that have a range of ages is therefore broadened making mass estimates from M_{bol} uncertain by

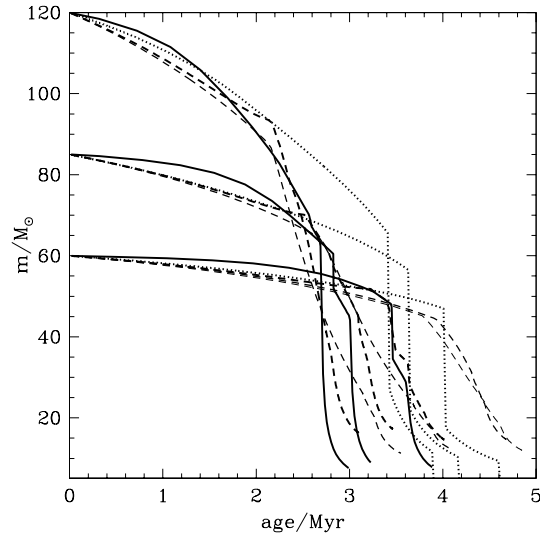


Figure 2. The mass-evolution of massive stars according to theoretical work: *Solid lines*: Geneva models (Schaller et al. 1992), *Dashed lines*: Geneva with rotation (Meynet & Maeder 2003, (thick: none, medium: 300 km/s, thin: 500 km/s); *Dotted lines*: stellar evolution package from Hurley based on the Pols non-rotating models (Hurley et al. 2000). From Weidner & Kroupa (2006).

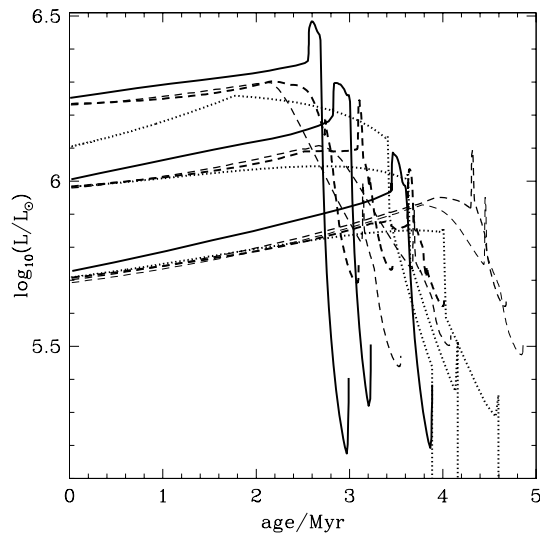


Figure 3. The luminosity-evolution of massive stars according to theoretical work. Line-types and initial masses are as in Fig. 2. From Weidner & Kroupa (2006)

up to 50 per cent (Penny et al. 2001), a bias that probably needs to be taken into account more thoroughly in the derivations of the IMF. Another problem is that $m \gtrsim 40 M_{\odot}$ stars may finish their assembly after burning a significant proportion of their central H so that a zero-age-main sequence may not exist for massive stars (Maeder & Behrend 2002). However, the agreement between slowly-rotating tidally-locked massive O-type binaries with standard non-rotating theoretical stellar models is very good (Penny et al. 2001).

3.1. The maximum stellar mass and cluster formation

A brief history: The empirically determined range of stellar masses poses important constraints on the physics of stellar formation, structure and stellar evolution, as well as on the feedback energy injected into a galaxy's atmosphere by a population of brand-new stars. The physical limit at low masses is now well established (§ 5.), and an upper mass limit appears to have been found recently.

A theoretical physical limitation to stellar masses has been known since many decades. Eddington (1926) calculated the limit which is required to balance radiation pressure and gravity, the *Eddington limit*: $L_{\text{Edd}}/L_{\odot} \approx 3.5 \times 10^4 m/M_{\odot}$. Hydrostatic equilibrium will fail if a star of a certain mass m has a theoretical luminosity that exceeds this limit, which is the case for $m \gtrsim 60 M_{\odot}$. It is not clear if stars above this limit cannot exist, as massive stars are not fully radiative but have convective cores. But more massive stars will lose material rapidly due to strong stellar winds. Schwarzschild & Härm (1959) inferred a limit of $\approx 60 M_{\odot}$ beyond which stars should be destroyed due to pulsations. But later studies suggested that these may be damped (Beech & Mitalas 1994). Stothers (1992) showed that the limit increases to $m_{\text{max}^*} \approx 120 - 150 M_{\odot}$ for more recent Rogers-Iglesia opacities and for metallicities $[\text{Fe}/\text{H}] \approx 0$. For $[\text{Fe}/\text{H}] \approx -1$, $m_{\text{max}^*} \approx 90 M_{\odot}$. A larger physical mass limit at higher metallicity comes about because the stellar core is more compact, the pulsations driven by the core having a smaller amplitude, and because the opacities near the stellar boundary can change by larger factors than for more metal-poor stars during the heating and cooling phases of the pulsations thus damping the oscillations. Larger physical mass limits are thus allowed to reach pulsational instability.

Related to the pulsational instability limit is the problem that radiation pressure also opposes accretion for proto-stars that are shining above the Eddington luminosity. Therefore the question remains how stars more massive than $60 M_{\odot}$ may be formed. Stellar formation models lead to a mass limit near $40 - 100 M_{\odot}$ imposed by feedback on a spherical accretion envelope (Kahn 1974; Wolfire & Cassinelli 1986; Wolfire & Cassinelli 1987). Some observations suggest that stars may be accreting material in discs and not in spheres (e.g. Chini et al. 2004). The higher density of the disc-material may be able to overcome the radiation at the equator of the proto-star. But it is unclear if the accretion-rate can be boosted above the mass-loss rate from stellar winds by this mechanism. Theoretical work on the formation of massive stars through disk-accretion with high accretion rates thereby allowing thermal radiation to escape pole-wards (e.g. Nakano 1989; Jijina & Adams 1996) indeed lessen the problem and allow stars with larger masses to form.

Another solution proposed is the merging scenario. In this case massive stars form through the merging of intermediate-mass proto-stars in the cores

of dense stellar clusters driven by core-contraction due to very rapid accretion of gas with low specific angular momentum, thus again avoiding the theoretical feedback-induced mass limit (Bonnell et al. 1998; Stahler et al. 2000). It is unclear though if the very large central densities required for this process to act are achieved in reality, but it should be kept in mind that an observable cluster is, by necessity, exposed from its natal cloud and is therefore likely to be always observed in an expanding phase (Kroupa 2005).

The search for a possible maximal stellar mass can only be performed in massive, star-burst clusters that contain sufficiently many stars to sample the stellar initial mass function beyond $100 M_{\odot}$. Observationally, the existence of a finite physical stellar mass limit was not evident until very recently. Indeed, observations in the 1980's of R136 in the Large Magellanic Cloud (LMC) suggested this object to be one single star with a mass of about $2000 - 3000 M_{\odot}$. Weigelt & Baier (1985) for the first time resolved the object into eight components using digital speckle interferometry, therewith proving that R136 is a massive star cluster rather than one single super-massive star. The evidence for any physical upper mass limit became very uncertain, and Elmegreen (1997) stated that “observational data on an upper mass cutoff are scarce, and it is not included in our models [of the IMF from random sampling in a turbulent fractal cloud]”. Although Massey & Hunter (1998) found stars in R136 with masses ranging up to $140 - 155 M_{\odot}$, Massey (2003) explains that the observed limitation is statistical rather than physical. We refer to this as the *Massey assertion*, i.e. that $m_{\max*} = \infty$. Meanwhile, Selman et al. (1999) found, from their observations, a probable upper mass limit in the LMC near about $130 M_{\odot}$, but they did not evaluate the statistical significance of this suggestion. Figer (2003) discussed the apparent cut-off of the stellar mass-spectrum near $150 M_{\odot}$ in the Arches cluster near the Galactic centre, but again did not attach a statistical analysis of the significance of this observation. Elmegreen (2000) also noted that random sampling from an unlimited IMF for all star-forming regions in the Milky Way (MW) would lead to the prediction of stars with masses $\gtrsim 1000 M_{\odot}$, unless there is a rapid turn-down *in the IMF* beyond several hundred M_{\odot} . However, he also stated that no upper mass limit to star formation has ever been observed, a view also emphasised by Larson (2003).

Thus, while theory clearly expected a physical stellar upper mass limit, the observational evidence in support of this was very unclear. This, however, changed in 2004.

Empirical results Given the observed rather sharp drop-off of the IMF in R136 near $150 M_{\odot}$, Weidner & Kroupa (2004) studied the *Massey assertion* in some detail.

R136 has an age ≤ 2.5 Myr (Massey & Hunter 1998) which is young enough such that stellar evolution will not have removed stars through supernova explosions. It has a metallicity of $[\text{Fe}/\text{H}] \approx -0.5$ dex (de Boer et al. 1985).

From the radial surface density profile Selman et al. (1999) estimated there to be 1350 stars with masses between 10 and $40 M_{\odot}$ within 20 pc of the 30 Doradus region, within the centre of which lies R136. Massey & Hunter (1998) and Selman et al. (1999) found that the IMF can be well-approximated by a Salpeter power-law with exponent $\alpha = 2.35$ for stars in the mass range 3 to $120 M_{\odot}$. This corresponds to 8000 stars with a total mass of $0.68 \times 10^5 M_{\odot}$.

Extrapolating down to $0.1 M_{\odot}$ the cluster would contain 8×10^5 stars with a total mass of $2.8 \times 10^5 M_{\odot}$. Using a standard IMF with a slope of $\alpha = 1.3$ (instead of the Salpeter value of 2.35) between 0.1 and $0.5 M_{\odot}$ this would change to 3.4×10^5 stars with a combined mass of $2 \times 10^5 M_{\odot}$, for an average mass of $0.61 M_{\odot}$ over the mass range $0.1 - 120 M_{\odot}$. Based on the observations by Selman et al. (1999), Weidner & Kroupa (2004) assumed that R136 has a mass in the range $5 \times 10^4 \leq M_{\text{R136}}/M_{\odot} \leq 2.5 \times 10^5$. This mass range can be used to investigate the expected number of stars above mass m ,

$$N(> m) = \int_m^{m_{\text{max}^*}} \xi(m') dm', \quad (5)$$

with the mass in stars of the whole (originally embedded) cluster being

$$M_{\text{ecl}} = \int_{m_{\text{low}}}^{m_{\text{max}^*}} m' \xi(m') dm', \quad (6)$$

where $m_{\text{low}} = 0.01 M_{\odot}$ and $m_{\text{max}^*} = \infty$ (the Massey assertion). Here the assumption is that the cluster is still compact despite having-blown out its residual gas. There are two unknowns ($N(> m)$ and k) that can be solved for using the two equations above.

Using the *standard stellar IMF* (eq. 20 below), $N(> m)$ is plotted in Fig. 4 for the two mass estimates of the cluster. The solid vertical line indicates $150 M_{\odot}$, the approximate maximum mass observed in R136 (Massey & Hunter 1998). Weidner & Kroupa (2004) found that $N(> 150 M_{\odot}) = 40$ stars are missing if $M_{\text{ecl}} = 2.5 \times 10^5 M_{\odot}$, while $N(> 150 M_{\odot}) = 10$ stars are missing if $M_{\text{ecl}} = 5 \times 10^4 M_{\odot}$. The probability that no stars are observed although 10 are expected, assuming $m_{\text{max}^*} = \infty$, is $P = 4.5 \times 10^{-5}$. Weidner & Kroupa (2004) concluded that the observations of the massive stellar content of R136 suggest a physical stellar mass limit near $m_{\text{max}^*} = 150 M_{\odot}$.

Furthermore, Weidner & Kroupa (2004) deduced that the *Massey assertion* would be correct for both cluster masses if the IMF had a slope $\alpha_3 \gtrsim 2.8$. Such a steep slope would make the observed limit consistent with random selection from the IMF, and it may be the true power-law index if unresolved multiple systems among O stars are corrected for, but this awaits a detailed study. A further caveat comes from unresolved multiple systems which would allow an $m_{\text{max}^*, \text{true}}$ as small as $\approx m_{\text{max}^*}/2$ if $\alpha_3 \approx 2.35$.

Similar results were obtained by Don Figer for the Arches cluster. The Arches is a star-burst cluster within 30 pc in projected distance from the Galactic centre. It has a mass $M \approx 1 \times 10^5 M_{\odot}$ (Bosch et al. 2001), age 2 – 2.5 Myr (Najarro et al. 2004) and $[\text{Fe}/\text{H}] \approx 0$ (Najarro et al. 2004). It is thus a counterpart to R136 in that the Arches is metal rich and was born in a very different tidal environment to R136.

Using his HST observations of the Arches, Figer (2005) performed the same analysis as Weidner & Kroupa (2004) did for R136. The Arches appears to be dynamically evolved, with substantial mass loss through the strong tidal forces (Portegies Zwart et al. 2002) and the stellar mass function with $\alpha = 1.9$ is thus flatter than the Salpeter IMF. Using his updated IMF measurement, Figer calculated the expected number of stars above $150 M_{\odot}$ to be 33, while

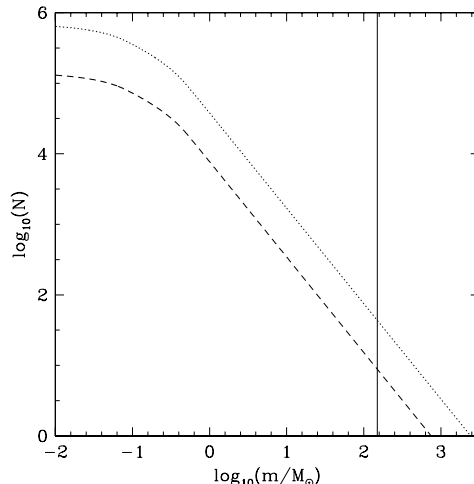


Figure 4. Number of stars above mass m for R136 with different mass estimates (dotted line: $M_{\text{R136}} = 2.5 \times 10^5 M_{\odot}$, dashed line: $M_{\text{R136}} = 5 \times 10^4 M_{\odot}$, (Selman et al. 1999). The vertical solid line marks $m = 150 M_{\odot}$. Taken from Weidner & Kroupa (2004).

a Salpeter IMF would predict there to be 18 stars. Observing no stars but expecting to see 18 has a probability of $P = 10^{-8}$, again strongly suggesting $m_{\text{max}^*} \approx 150 M_{\odot}$.

Given the importance of knowing if a finite physical upper mass limit exists and how it varies with metallicity, Oey & Clarke (2005) studied the massive-star content in 9 clusters and OB associations in the MW, the LMC and the SMC. They predicted the expected masses of the most massive stars in these clusters for different upper mass limits (120, 150, 200, 1000 and 10000 M_{\odot}). For all populations they found that the observed number of massive stars supports with high statistical significance the existence of a general upper mass cutoff in the range $m_{\text{max}^*} \in (120, 200 M_{\odot})$.⁷

The general indication thus is that a physical stellar mass limit near $150 M_{\odot}$ seems to exist. While biases due to unresolved multiples that may steepen the IMF and/or reduce the true maximal mass need to be studied further, the absence of variations of m_{max^*} with metallicity poses a problem. A constant m_{max^*} would only be apparent for a true variation as proposed by the theoretical models, *if metal-poor environments have a larger stellar multiplicity*, the effects of which would have to compensate the true increase of m_{max^*} with metallicity.

Maximal stellar mass in clusters Above we have seen that there seems to exist a universal physical stellar mass limit. However, an elementary argument suggests that star-clusters must also limit the masses of their constituent

⁷More recent work on the physical upper mass limit can be found in Koen (2006); Maíz Apellániz et al. (2006).

stars: A pre-star-cluster gas core with a mass M_{core} can, obviously, not form stars with masses $m > \epsilon M_{\text{core}}$, where $\epsilon \approx 0.33$ is the star-formation efficiency (Lada & Lada 2003). Thus, given a freshly hatched cluster with stellar mass M_{ecl} , stars in that cluster cannot surpass masses $m_{\text{max}} = M_{\text{ecl}}$, which is the identity relation corresponding to a “cluster” consisting of one massive star. Assuming the stellar IMF is a continuous density distribution function and that clusters are filled with stars distributed according to the stellar IMF, this can be generalised by stating that each cluster can have only one most massive star,

$$1 = \int_{m_{\text{max}}}^{m_{\text{max}}^*} \xi(m') dm', \quad (7)$$

with

$$M_{\text{ecl}}(m_{\text{max}}) = \int_{m_{\text{low}}}^{m_{\text{max}}} m' \xi(m') dm' \quad (8)$$

as a further condition, as above. These two equations need to be solved numerically and give the semi-analytical relation $m_{\text{max}} = \mathcal{F}(M_{\text{ecl}})$ (Weidner & Kroupa 2004). It is plotted in Fig. 5 as the thick-solid curve.

A compilation of clusters from the literature for which the cluster mass and the initial mass of the heaviest star can be estimated (Weidner & Kroupa 2006) shows that the cluster mass indeed appears to have a limiting influence on the stellar mass within it. The observational data are plotted in Fig. 5, finding rather excellent agreement with the semi-analytical description above.

However, it would be undisputed that a stochastic sampling effect from the IMF must be present when stars form. This can be mimicked in the computer by performing various Monte-Carlo experiments (Weidner & Kroupa 2006). The Monte-Carlo experiments are conducted in three different ways,

- pure random sampling (*random sampling*)
- mass constrained random sampling (*constrained sampling*)
- mass constrained random sampling with sorted adding (*sorted sampling*)

For the *random sampling model*, 10 million clusters are randomly taken from a cluster distribution with a power-law index of $\beta_N = 2.35$ between 12 and 2.5×10^7 stars. The relevant distribution function is the embedded-cluster star-number function (ECSNF),

$$dN_{\text{ecl}} \propto N^{-\beta_N}, \quad (9)$$

which is the number of clusters containing $N \in [N', N' + dN')$ stars. Each cluster is then filled with N stars randomly from the standard IMF (eq. 20 without a mass limit, or by imposing the physical stellar mass limit, $m \leq 150 M_{\odot}$). The stellar masses are added to get the cluster mass, M_{ecl} . For each cluster the maximal stellar mass is searched for. For each cluster in a mass bin $M_{\text{ecl}} - \Delta M_{\text{ecl}}/2, M_{\text{ecl}} + \Delta M_{\text{ecl}}/2$ the average m_{max} is calculated, and the set of average m_{max} values define the relation

$$m_{\text{max}} = m_{\text{max}}^{\text{ran}}(M_{\text{ecl}}). \quad (10)$$

For the *constrained sampling model*, 5×10^7 clusters are randomly taken from the embedded-cluster mass function (ECMF),

$$\xi_{\text{ecl}}(M_{\text{ecl}}) \propto M_{\text{ecl}}^{-\beta}, \quad (11)$$

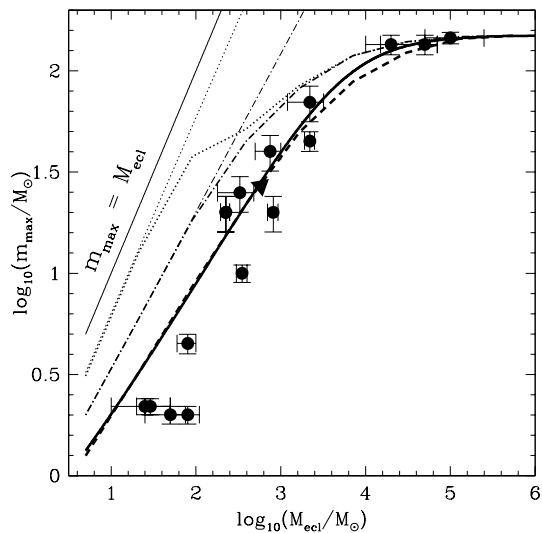


Figure 5. The *thick solid line* shows the dependence of the mass of the most-massive star in a cluster on the cluster mass according to the semi-analytical model. The *thick dashed line* shows the mean maximum stellar mass for sorted sampling. The *dot-dashed lines* are mass-constrained random-sampling results with a physical upper mass limit of $m_{\max*} = 150 M_{\odot}$ (*thick line*) and $10^6 M_{\odot}$ (*thin line*). Pure random sampling models are plotted as *dotted lines*. The *thick one* is sampled to $m_{\max*} = 150 M_{\odot}$ while the *thin one* up to $10^6 M_{\odot}$. The *thin solid line* shows the identity relation, where a “cluster” consists only of one star. The *dots* with error bars are observed clusters, while the *triangle* is a result from a star-formation simulation with an SPH code (Bonnell et al. 2003). Taken from Weidner & Kroupa (2006).

between $5 M_\odot$ (the minimal, Taurus-Auriga-type, star-forming “cluster” counting ≈ 15 stars) and $10^7 M_\odot$ (an approximate maximum mass for a single stellar population that consists of one metallicity and age, Weidner et al. 2004) and again with $\beta = 2.35$. Note that $\beta_N \approx \beta$ because the ECSNF and the ECMF only differ by a nearly-constant average stellar mass. Then stars are taken randomly from the standard IMF and added until they reach or surpass the respective cluster mass, M_{ecl} . Afterwards the clusters are searched for their maximum stellar mass. For each cluster in a mass bin $M_{\text{ecl}} - \Delta M_{\text{ecl}}/2, M_{\text{ecl}} + \Delta M_{\text{ecl}}/2$ the average m_{max} is calculated, and the set of average m_{max} values define the relation

$$m_{\text{max}} = m_{\text{max}}^{\text{con}}(M_{\text{ecl}}). \quad (12)$$

For the *sorted sampling model* again 5×10^7 clusters are randomly sampled from the ECMF (eq. 11) between $5 M_\odot$ and $10^7 M_\odot$ and with $\beta = 2.35$. However, this time the number N of stars which are to populate the cluster is estimated from $N = M_{\text{ecl}}/m_{\text{av}}$, where $m_{\text{av}} = 0.36 M_\odot$ is the average stellar mass for the standard IMF (eq. 20) between $0.01 M_\odot$ and $150 M_\odot$. These stars are added to give $M_{\text{ecl,ran}}$,

$$M_{\text{ecl,ran}} = \sum_N m_i,$$

such that $m_i \leq m_{i+1}$. If $M_{\text{ecl,ran}} < M_{\text{ecl}}$ in this first step, an additional number of stars, ΔN , is picked randomly from the IMF, where $\Delta N = (M_{\text{ecl}} - M_{\text{ran}})/m_{\text{av}}$ (we assume $m_{\text{av}} = \text{constant}$). Again these stars are added to obtain an improved estimate of the desired cluster mass,

$${}^2M_{\text{ecl,ran}} = \sum_{N+\Delta N} m_i, \quad m_i \leq m_{i+1}.$$

This is done such that ${}^2M_{\text{ecl,ran}} \approx M_{\text{ecl}}$ (for details of the method see Weidner & Kroupa 2006). The procedure is repeated until all clusters from the ECMF are ‘filled’. They are then also searched for the most massive star in each cluster, as above. For each cluster in a mass bin $M_{\text{ecl}} - \Delta M_{\text{ecl}}/2, M_{\text{ecl}} + \Delta M_{\text{ecl}}/2$ the average m_{max} is calculated, and the set of average m_{max} values define the relation

$$m_{\text{max}} = m_{\text{max}}^{\text{sort}}(M_{\text{ecl}}). \quad (13)$$

All three relations are plotted in Fig. 5. We noted already that the observations follow the semi-analytic relation remarkably well. Furthermore, Fig. 5 also suggests that the different Monte-Carlo schemes can be selected for. Thus, the sorted-sampling algorithm leads to virtually the same results as the semi-analytical relation, and it fits the data very well indeed. The correspondence of the sorted-sampling algorithm to the semi-analytical result is not really surprising, because the algorithm is Monte-Carlo integration of the same problem. The constrained-sampling and random-sampling algorithms, on the other hand, can be excluded with very high confidence by performing statistical tests on the observational data that are reported in detail in Weidner & Kroupa (2006).

On a historical note, Larson (1982) had pointed out that more massive and dense clouds correlate with the mass of the most massive stars within them and he estimated that $m_{\text{max}} = 0.33 M_{\text{cloud}}^{0.43}$ (masses are in M_\odot). An updated

relation was derived by Larson (2003) by comparing m_{\max} with the stellar mass in a few clusters, $m_{\max} \approx 1.2 M_{\text{cluster}}^{0.45}$. Both are flatter than the semi-analytical relation, and therefore do not fit the data in Fig. 5 as well (Weidner & Kroupa 2006). Elmegreen (1983) constructed a relation between cluster mass and its most massive star based on an assumed equivalence between the luminosity of the cluster population and its binding energy, for a Miller-Scalo IMF. This function is even shallower than the one estimated by Larson (2003) relation. Assuming $m_{\max*} = \infty$, Elmegreen (2000) solved eqs 7 and 8 above for a single Salpeter power-law stellar IMF finding a $m_{\max}(M_{\text{ecl}})$ relation quite consistent with the data in Fig. 5 (Weidner & Kroupa 2006).

Implications: stellar astrophysics and the formation of star clusters We are now in the happier situation that a physical stellar mass limit seems to have been found. But the absence of clear variation of this limit with metallicity poses a potential problem, although it may be too early to make definite statements. Further observational work on many more very young and massive clusters is needed to ascertain the findings reported here, and to quantify the multiplicity properties of massive stars, as noted above.

That the sorted-sampling algorithm for making star clusters fits the observational maximal-stellar-mass–star-cluster-mass data so well would appear to imply that *clusters form in an organised fashion*. The physical interpretation of the algorithm (i.e. of the Monte-Carlo integration) is that as a pre-cluster core contracts under self gravity the gas densities increase and local density fluctuations in the turbulent medium lead to low-mass star formation, perhaps similar to what is seen in Taurus-Aurigae. As the contraction proceeds and before feedback from young stars begins to disrupt the cloud, star-formation activity increases in further density fluctuations with larger amplitudes thereby forming more massive stars. The process stops when the most massive stars that have just formed supply sufficient feedback energy to disrupt the cloud (Elmegreen 1983). Thus, less-massive pre-cluster cloud-cores would die at a lower maximum stellar mass than more massive cores. But in all cases stellar masses are limited, $m \leq m_{\max}(M_{\text{ecl}}) \leq m_{\max*}$.

This scenario is nicely consistent with the hydrodynamic cluster formation calculations presented by Bonnell et al. (2003) and Bonnell et al. (2004), as is reported in more detail in Weidner & Kroupa (2006). We note here that Bonnell et al. (2004) found their theoretical clusters to form hierarchically from smaller sub-clusters, and together with continued competitive accretion this leads to the relation $m_{\max} \propto M_{\text{ecl}}^{2/3}$ in excellent agreement with the compilation of observational data. While this agreement is stunning, the detailed outcome of the currently available SPH modelling in terms of stellar multiplicities is not right (Goodwin et al. 2004; Goodwin & Kroupa 2005), and feedback that ultimately dominates the process of star-formation, given the generally low star-formation efficiencies observed in cluster-forming volumes, is not yet incorporated in the modelling. This poses a severe computational hurdle because radiation transfer requires the correct treatment of atomic processes in remote regions of space that are exchanging radiation (eg. Baes et al. 2005).

Caveats Unanswered questions regarding the formation and evolution of massive stars remain. There may be stars with $m \geq m_{\max*}$ which implode “in-

visibly” after 1 or 2 Myr. The explosion mechanism sensitively depends on the presently still rather uncertain mechanism for shock revival after core collapse (e.g. Janka 2001). Since such stars would not be apparent in massive clusters older than 2 Myr they would not affect the empirical maximal stellar mass, and $m_{\text{max*},\text{true}}$ would be unknown at present.

Furthermore, and as stated already above, stars are often in multiple systems. Especially massive stars seem to have a binary fraction of 80% or even larger (García & Mermillod 2001) and apparently tend to be in binary systems with a preferred mass-ratio near unity. Thus, if all O stars would be in equal-mass binaries, then $m_{\text{max*},\text{true}} \approx m_{\text{max*}}/2$.

Finally, it is disconcerting that $m_{\text{max*}} \approx 150 M_{\odot}$ appears to be the same for low-metallicity environments ($[\text{Fe}/\text{H}] = -0.5$, R136) and metal-rich environments ($[\text{Fe}/\text{H}] = 0$, Arches), in apparent contradiction to the theoretical values (Stothers 1992). Clearly, this issue needs further study.

4. Low-mass stars

There are three well-tried approaches to determine $\Psi(M_V)$ in eq. 1 (Kroupa 2001c). The first two are applied to Galactic-field stars, and the third to star clusters. The sample of Galactic-field stars close to the Sun is especially important because it is the most complete and well-studied stellar sample at our disposal.

4.1. Galactic-field stars

Galactic-field stars have an average age of about 5 Gyr and represent a mixture of many star-formation events. The IMF deduced for these is therefore a time-averaged composite IMF. For $m \lesssim 1.3 M_{\odot}$ the composite IMF equals the simple-stellar IMF (§ 8.), and so it is an interesting quantity for at least two reasons: For the mass-budget of the Milky-Way disk, and as a bench-mark against which the IMFs measured in presently occurring star-formation events can be compared to distill possible variations about the mean.

The first and most straightforward method consists of creating a local volume-limited catalogue of stars. Completeness of the modern *Jahreiss–Gliese Catalogue of Nearby Stars* extends to about 25 pc for $m \gtrsim 0.6 M_{\odot}$, trigonometric distances having been measured using the Hipparcos satellite, and only to about 5 pc for less massive stars for which we still rely on ground-based trigonometric parallax measurements⁸. The advantage of the LF, $\Psi_{\text{near}}(M_V)$, created using

⁸ Owing to the poor statistical definition of $\Psi_{\text{near}}(M_V)$ for $M_V \gtrsim 10$, $m \lesssim 0.5$, it is important to increase the sample of nearby stars, but controversy exists as to the maximum distance to which the VLMS census is complete. Using spectroscopic parallax it has been suggested that the local census of VLMSs is complete to within about 15 % to distances of 8 pc and beyond (Reid & Gizis 1997). However, Malmquist bias allows stars and unresolved binaries to enter such a flux-limited sample from much larger distances (Kroupa 2001c). The increase of the number of stars with distance using trigonometric distance measurements shows that the nearby sample becomes incomplete for distances larger than 5 pc and for $M_V > 12$ (Jahreiss 1994; Henry et al. 1997). The incompleteness in the northern stellar census beyond 5 pc and within 10 pc amounts to about 35 % (Jao et al. 2003), and recently discovered companions (e.g. Delfosse et al. 1999; Beuzit et al. 2004) to known primaries in the distance range 5 <

this catalogue is that virtually all companion stars are known, that it is truly distance limited and that the distance measurements are direct.

The second method is to make deep pencil-beam surveys using photographic plates or CCD cameras to extract a few hundred low-mass stars from a hundred-thousand stellar and galactic images. This approach leads to larger stellar samples, especially so since many lines-of-sight into the Galactic field ranging to distances of a few 100 pc to a few kpc are possible. The disadvantage of the LF, $\Psi_{\text{phot}}(M_V)$, created using this technique is that the distance measurements are indirect relying on photometric parallax. Such surveys are flux limited rather than volume limited and pencil-beam surveys which do not pass through virtually the entire stellar disk are prone to Malmquist bias (Stobie et al. 1989). This bias results from a spread of luminosities of stars that have the same colour because of their dispersion of metallicities and ages, leading to intrinsically more luminous stars entering the flux-limited sample and thus biasing the inferred absolute luminosities and the inferred stellar space densities. Furthermore, binary systems are not resolved in the deep surveys.

The local, *nearby LF* and the Malmquist-corrected deep *photometric LF* are displayed in Fig. 6. They differ significantly for stars fainter than $M_V \approx 11.5$ which caused significant controversy in the past (Kroupa 1995a). That the local sample has a spurious but significant over-abundance of VLMSs can be ruled out by virtue of the large velocity dispersion in the disk, ≈ 30 pc/Myr. Any significant overabundance of stars within a sphere with a radius of 30 pc would disappear within one Myr, and cannot be created by any physically plausible mechanism from a population of stars with stellar ages spanning the age of the Galactic disk. The shape of $\Psi_{\text{phot}}(M_V)$ for $M_V \gtrsim 12$ is confirmed by many independent photometric surveys. That all of these could be making similar mistakes, such as in colour transformations, becomes unlikely on consideration of the LFs constructed for completely independent stellar samples, namely star clusters (Fig. 7).

Eq. 1 shows that any non-linear structure in the MLR is mapped into observable structure in the LF, provided the MF does not have compensating structure. Such a conspiracy is implausible because the MF is defined through the star-formation process, but the MLR is a result of the internal constitution of stars. The MLR, its derivative and deviations of models from observational data are shown in Figs. 8 and 9, respectively. It is apparent that the slope is very small at faint luminosities leading to large uncertainties in the MF near the hydrogen burning mass limit.

The physics underlying the non-linearities of the MLR are due to an interplay of changing opacities, the internal stellar structure and the equation of state of the matter deep inside the stars. Starting at high masses ($m \gtrsim \text{few } M_{\odot}$), as the mass of a star is reduced H^- opacity becomes increasingly important through the short-lived capture of electrons by H-atoms resulting in reduced stellar luminosities for intermediate and low-mass stars. The $m(M_V)$ relation becomes less steep in the broad interval $3 < M_V < 8$ leading to the Wielen dip

$d < 12$ pc indeed suggest that the extended sample may not yet be complete. Based on the work by Reid et al. (2003) and Reid et al. (2003), Luhman (2004) however argues that the incompleteness is only about 15 %.

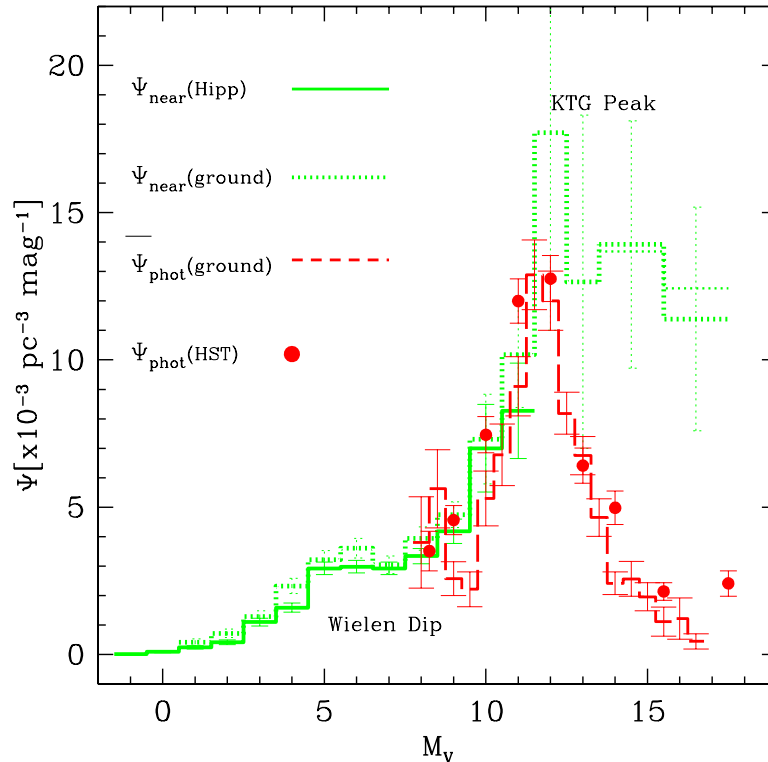


Figure 6. Stellar luminosity functions (LFs) for solar-neighbourhood stars. The photometric LF corrected for Malmquist bias and at the mid-plane of the Galactic disk (Ψ_{phot}) is compared with the nearby LF (Ψ_{near}). The average, ground-based $\bar{\Psi}_{\text{phot}}$ (dashed histogram, data pre-dating 1995, Kroupa 1995a) is confirmed by Hubble-Space-Telescope (HST) star-count data which pass through the entire Galactic disk and are thus less prone to Malmquist bias (solid dots, Zheng et al. 2001). The ground-based volume-limited trigonometric-parallax sample (dotted histogram) systematically overestimates Ψ_{near} due to the Lutz-Kelker bias, thus lying above the improved estimate provided by the Hipparcos-satellite data (solid histogram, Jahreiß & Wielen 1997; Kroupa 2001c). The depression/plateau near $M_V = 7$ is the *Wielen dip*. The maximum near $M_V \approx 12$, $M_I \approx 9$ is the *KTG peak*. The thin dotted histogram at the faint end indicates the level of refinement provided by recent stellar additions (Kroupa 2001c) demonstrating that even the immediate neighbourhood within 5.2 pc of the Sun probably remains incomplete at the faintest stellar luminosities.

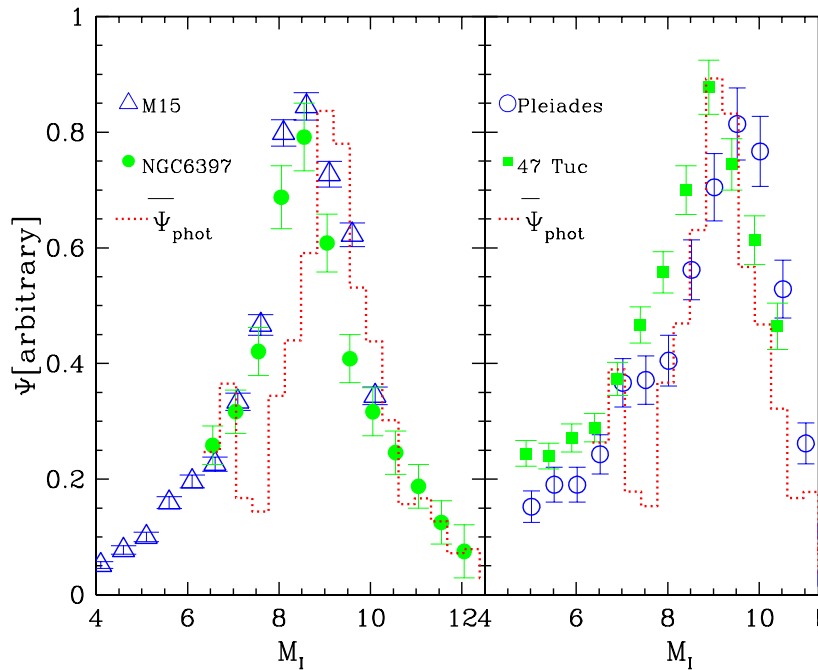


Figure 7. I -band LFs of stellar *systems* in four star clusters: globular cluster (GC) *M15* (de Marchi & Paresce 1995a, distance modulus $\Delta m = m - M = 15.25$ mag); GC *NGC 6397* (Paresce et al. 1995, $\Delta m = 12.2$); young Galactic cluster *Pleiades* (Hambly et al. 1991, $\Delta m = 5.48$); GC *47 Tuc* (de Marchi & Paresce 1995b, $\Delta m = 13.35$). The dotted histogram is $\bar{\Psi}_{\text{phot}}(M_I)$ from the upper panel, transformed to the I -band using the linear colour–magnitude relation $M_V = 2.9 + 3.4(V - I)$ (Kroupa et al. 1993) and $\Psi_{\text{phot}}(M_I) = (dM_V/dM_I) \Psi_{\text{phot}}(M_V)$ (eq. 2).

(Fig. 6). The $m(M_V)$ relation steepens near $M_V = 10$ because the formation of H_2 in the very outermost region of main-sequence stars causes the onset of convection up to and above the photo-sphere leading to a flattening of the temperature gradient and therefore to a larger effective temperature as opposed to to an artificial case without convection but the same central temperature. This leads to brighter luminosities and full convection for $m \leq 0.35 M_\odot$. The modern Delfosse data beautifully confirm the steepening in the interval $10 < M_V < 13$ predicted in 1990, and the dotted MLR demonstrates the effects of suppressing the formation of the H_2 molecule by lowering its dissociation energy from 4.48 eV to 1 eV (Kroupa et al. 1990). The $m(M_V)$ relation flattens again for $M_V > 14$, $m < 0.2 M_\odot$ as degeneracy in the stellar core becomes increasingly important for smaller masses limiting further contraction (Hayashi & Nakano 1963; Chabrier & Baraffe 1997). Therefore, owing to the changing conditions within the stars with changing mass, a pronounced local maximum in $-dm/dM_V$ results at $M_V \approx 11.5$, postulated in 1990 to be the origin of the maximum in Ψ_{phot} near $M_V = 12$ (Kroupa et al. 1990).

The implication that the LFs of all stellar populations should show such a feature, although realistic metallicity-dependent stellar models were not available yet, was noted (Kroupa et al. 1993). The subsequent finding that all known stellar populations have such a maximum in the LF (Figs. 6 and 7) constitutes one of the *most impressive achievements of stellar-structure theory*. Different theoretical $m(M_V)$ relations have the maximum in $-dm/dM_V$ at different M_V , suggesting the possibility of testing stellar structure theory near the critical mass $m \approx 0.35 M_\odot$, where stars become fully convective (Kroupa & Tout 1997; Brocato et al. 1998). But since the IMF also defines the LF the shape and location cannot be unambiguously used for this purpose unless it is postulated that the IMF is invariant.

A study of the position of the maximum in the I -band LF has been undertaken by von Hippel et al. (1996) and Kroupa & Tout (1997) finding that the observed position of the maximum shifts to brighter magnitude with decreasing metallicity, as expected from theory (Figs. 10 and 11).

In addition to the non-linearities in the $m(M_P)$ relation, unresolved multiple systems affect the MF derived from the photometric LF, in particular since no stellar population is known to exist that has a binary proportion smaller than 50 per cent, apart possibly from dynamically highly evolved globular clusters. Suppose an observer sees 100 systems. Of these 40, 15 and 5 are binary, triple and quadruple, respectively, these being realistic proportions. There are thus 85 companion stars which the observer is not aware of if none of the multiple systems are resolved. Since the distribution of secondary masses for a given primary mass is not uniform but typically increases with decreasing mass (Malkov & Zinnecker 2001), the bias is such that low-mass stars are significantly underrepresented in any survey that does not detect companions (Kroupa et al. 1991; Holtzman et al. 1998; Luhman et al. 1998; Malkov & Zinnecker 2001). Also, if the companion(s) are bright enough to affect the system luminosity noticeably then the estimated photometric distance will be too small, artificially enhancing inferred space densities which are, however, mostly compensated for by the larger distances sampled by binary systems in a flux-limited survey, together with an exponential density fall-off perpendicular

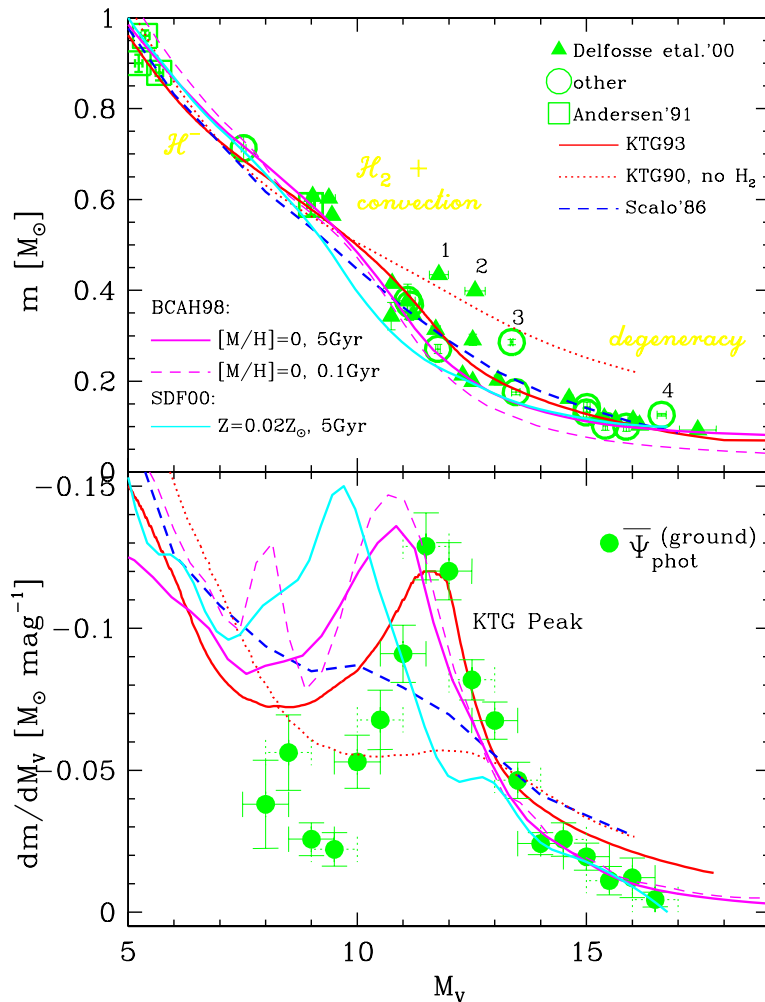


Figure 8. The mass-luminosity relation (MLR, upper panel) and its derivative (lower panel) for late-type stars. *Upper panel:* The most recent observational data (solid triangles and open circles, Delfosse et al. 2000; open squares, Andersen 1991) are compared with the empirical MLR of Scalo (1986) and the semi-empirical KTG93-MLR (Kroupa et al. 1993). The under-luminous data points 1,2 are GJ2069Aa,b and 3,4 are Gl791.2A,B. All are probably metal-rich by ~ 0.5 dex (Delfosse et al. 2000). Recent theoretical MLRs from Baraffe et al. (1998) (BCAH98) and Siess et al. (2000) (SDF00) are also shown. The observational data (Andersen 1991) show that $\log_{10}[m(M_V)]$ is approximately linear for $m > 2 M_\odot$. *Lower panel:* The derivatives of the same relations plotted in the upper panel are compared with $\bar{\Psi}_{\text{phot}}$ from Fig. 6. Note the good agreement between the location, amplitude and width of the KTG peak in the LF and the extremum in dm/dM_V .

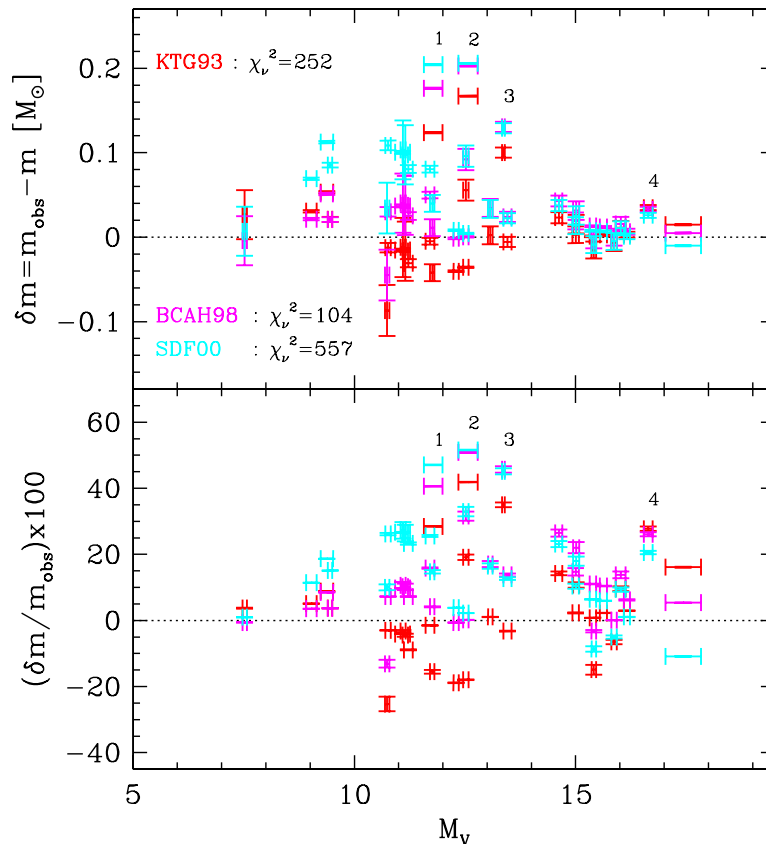


Figure 9. Deviations of the MLRs ($\delta m = m_{\text{obs}} - m(M_V)$) from the empirical data with errors ϵ_m shown in Fig. 8 in M_\odot (upper panel) and in percent (lower panel with uncertainties $-(m(M_V)/m_{\text{obs}}^2) \times \epsilon_m$). Reduced χ_ν^2 ($\nu = 26$ for 31 data points, ignoring the four outliers) values indicate the formal goodness-of-fit. Formally, none of the MLRs available is an acceptable model for the data. This is not alarming though, because the models are for a single-metallicity, single-age population while the data span a range of metallicities and ages typical for the solar-neighbourhood stellar population, as signified by $\delta m \gg \epsilon_m$ in most cases. The χ_ν^2 values confirm that the BCAH98 models (Baraffe et al. 1998) and the semi-empirical KTG93 MLR (Kroupa et al. 1993) provide the best-matching MLRs. Note that the KTG93 MLR was derived from mass-luminosity data prior to 1980, but by using the shape of the peak in $\Psi_{\text{phot}}(M_V)$ as an additional constraint the constructed MLR became robust. The lower panel demonstrates that the deviations of observational data from the model MLRs are typically much smaller than 30 per cent, excluding the putatively metal-rich stars (1–4).

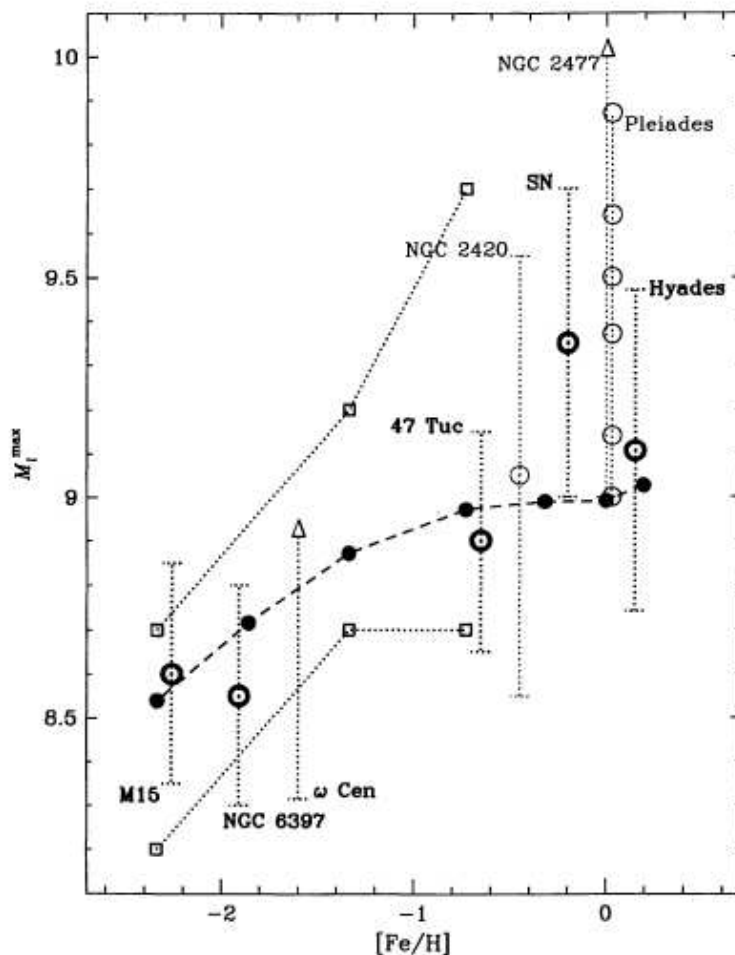


Figure 10. The position of the maximum in $-dm/dM_I$ as a function of metallicity of the theoretical mass–luminosity data of Kroupa & Tout (1997) is shown as solid dots. The open squares represent bounds by the stellar-structure models of D’Antona & Mazzitelli (1996), and the open circles are observational constraints for different populations (e.g. SN for the composite solar-neighbourhood population, Pleiades for the simple population of an intermediate-age cluster). Thick circles are more certain than the thin circles, and for the Pleiades a sequence of positions of the LF-maximum is given, from top to bottom, with the following combinations of (distance modulus, age): (5.5, 70 Myr), (5.5, 120 Myr), (5.5, main sequence), (6, 70 Myr), (6, 120 Myr), (6, main sequence). For more details see Kroupa & Tout (1997).

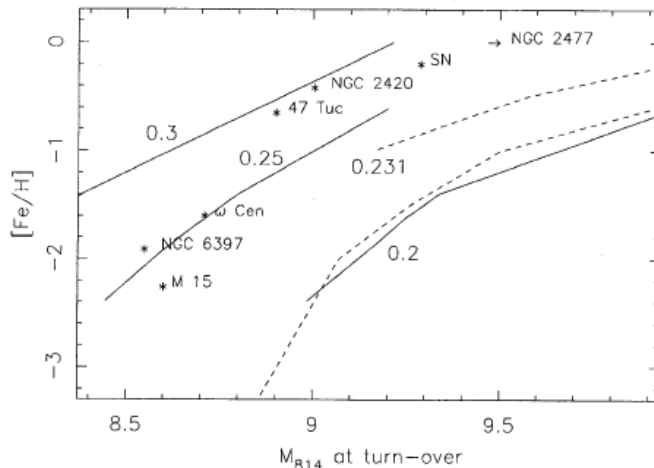


Figure 11. Similar to Fig. 10 but from von Hippel et al. (1996), their fig.5: The absolute I -band-equivalent magnitude of the maximum in the LF as a function of metallicity for different populations. The solid and dashed lines are loci of constant mass ($0.2, 0.231, 0.3 M_{\odot}$) according to theoretical stellar structure calculations. See von Hippel et al. (1996) for more details.

to the Galactic disk (Kroupa 2001c). A faint companion will also be missed if the system is formally resolved but the companion lies below the flux limit of the survey.

Comprehensive star-count analysis of the solar neighbourhood that incorporate unresolved binary systems, metallicity and age spreads and the density fall-off perpendicular to the Galactic disk show that the IMF can be approximated by a two-part power-law with $\alpha_1 = 1.3 \pm 0.7, 0.08 < m/M_{\odot} \leq 0.5$, $\alpha_2 = 2.2, 0.5 < m/M_{\odot} \leq 1$, a result obtained for two different MLRs (Kroupa 2001c). The index α_2 is constrained tightly owing to the well-constrained Ψ_{near} , the well-constrained empirical MLR in this mass range and because unresolved binary systems do not significantly affect the solar-neighbourhood LF in this mass range because primaries with $m \gtrsim 1 M_{\odot}$ are rare and are not sampled.

Fig. 12 demonstrates models of the single-star and system LFs for the KTG93 MLR shown in Fig. 8. The significant difference between the single-star and system LFs is evident, being most of the explanation of the disputed⁹

⁹The discrepancy evident in Fig. 12 between the nearby LF, Ψ_{near} , and the photometric LF, Ψ_{phot} , invoked a significant dispute as to the nature of this discrepancy. On the one hand (Kroupa 1995a) the difference is thought to be due to unseen companions in the deep but low-resolution surveys used to construct Ψ_{phot} , with the possibility that photometric calibration for VLMSs may remain problematical so that the exact shape of Ψ_{phot} for $M_V \gtrsim 14$ is probably uncertain. On the other hand (Reid & Gizis 1997) the difference is thought to come from non-linearities in the $V - I, M_V$ colour-magnitude relation used for photometric parallax. Taking into account such structure it can be shown that the photometric surveys underestimate stellar space densities so that Ψ_{phot} moves closer to the extended estimate of Ψ_{near} using a sample of stars within 8 pc or further. While this is an important point, the extended Ψ_{near} is incomplete

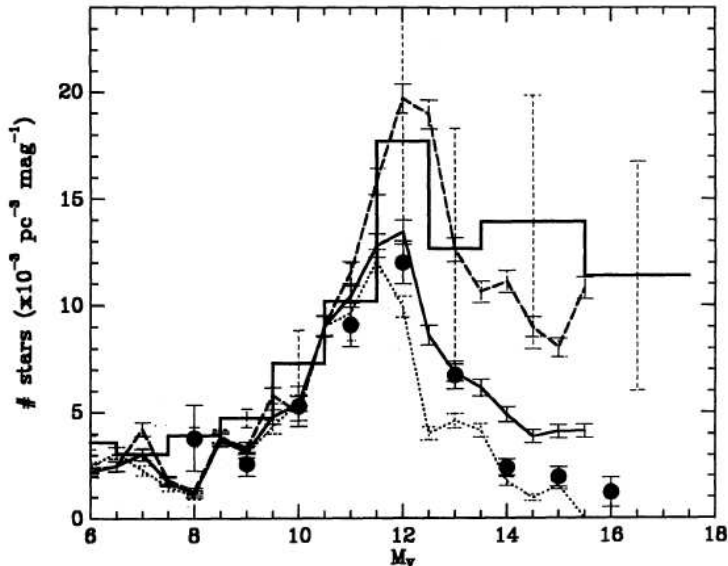


Figure 12. Comparison of the model field luminosity function (curves) of a single-metallicity and single-age population that is without measurement errors, with observations in the photometric V-band (a comparison of the corresponding LFs in bolometric magnitudes can be found in Kroupa 1995e). *The model* assumes the standard stellar IMF, eq. 20 below. The model single star luminosity function is normalised to the nearby luminosity function at $M_V \approx 10$, $M_{bol} \approx 9$, giving the normalisation constant in the MF k , and the plot shows $k\Psi_{mod,sing}$ (long dashed curve), $k\Psi_{mod,sys}(t = 0)$ (dotted curve, without pre-main sequence brightening) and $k\Psi_{mod,sys}(t = 1 \text{ Gyr})$ (solid curve). Note that the solid curve is the luminosity function for a realistic model of the Galactic field population of systems consisting of 48 per cent binaries which have a period distribution consistent with the empirical G-, K-, and M-dwarf period distribution, the mass ratio distributions for G-dwarf systems as observed (Duquennoy & Mayor 1991), and the overall mass-ratio distribution given by fig. 2 in Kroupa et al. (2003), where a concise description of the “standard star-formation model” can be found. *The observed* nearby stellar luminosity function, Ψ_{near} , which is not corrected for Malmquist-type bias (tables 2 and 8 in Kroupa (1995a) and which is smoothed by using larger bin widths at the faint end, as detailed in section 4 of that paper, is plotted as the solid-line histogram. The filled circles represent the best-estimate Malmquist corrected photometric luminosity function, $\bar{\Psi}_{phot}$, Fig. 6. By correcting for Malmquist bias (Stobie et al. 1989) the LF becomes that of a single-age, single-metallicity population. Taken from Kroupa (1995e).

discrepancy between the observed Ψ_{near} and Ψ_{phot} . Note though that the observed photometric LF contains triple and quadruple systems that are not accounted for by the model. Note also that the photometric LF has been corrected for Malmquist bias and so constitutes the system LF in which the broadening due to a metallicity and age spread and photometric errors has been largely removed. It is therefore directly comparable to the model system LF, and both indeed show a very similar KTG peak. The observed nearby LF, on the other hand, has not been corrected for the metallicity and age spread nor for trigonometric distance errors, and so it appears broadened. The model single-star LF, in contrast, does not, by construction, incorporate these, and thus appears with a more pronounced maximum. Such observational effects can be incorporated rather easily into full-scale star-count modelling (Kroupa et al. 1993). The deviation of the model system LF from the observed photometric LF for $M_V \gtrsim 14$ may indicate a change of the pairing properties of the VLMS or BD population (§ 5.).

Since the nearby LF is badly defined statistically for $M_V \gtrsim 13$, the resulting model, such as shown in Fig. 12, is a *prediction* of the true, single-star LF that should become apparent once the immediate solar-neighbourhood sample has been enlarged significantly through the planned space-based astrometric survey GAIA (Gilmore et al. 1998), followed by an intensive follow-up imaging and radial-velocity observing programme scrutinising every nearby candidate for unseen companions (Kroupa 2001c). Despite such a monumental effort, the structure in $\Psi_{\text{near}}^{\text{GAIA}}$ will be smeared out due to the metallicity and age spread of the local stellar sample, a factor to be considered seriously.

4.2. Star clusters

Star clusters offer populations that are co-eval, equi-distant and that have the same chemical composition, but as a compensation of these advantages the extraction of faint cluster members is very arduous because of contamination by the background Galactic-field population. The first step is to obtain photometry of everything stellar in the vicinity of a cluster and to select only those stars that lie near one or a range of isochrones, taking into account that unresolved binaries are brighter than single stars. The next step is to measure proper motions and radial velocities of all candidates to select only those high-probability members that have coinciding space motion with a dispersion consistent with the a priori unknown but estimated internal kinematics of the cluster. Since nearby clusters for which proper-motion measurements are possible appear large on the sky, the observational effort is horrendous. For clusters such as globulars that are isolated the second step can be omitted, but in dense clusters stars missed due to crowding need to be corrected for. The stellar LFs in clusters turn out to have the same general shape as Ψ_{phot} (Fig. 7), with the maximum being

(see footnote 8) and theoretical colour-magnitude relations do not have the required degree of non-linearity. The observational colour-magnitude data also do not conclusively suggest a feature with the required strength (Baraffe et al. 1998). Furthermore, Ψ_{phot} agrees almost perfectly with the LFs measured for star clusters of solar and population I metallicity (Fig. 7) so that it appears unlikely that non-linearities in the colour-magnitude relation are the dominant source of the discrepancy.

slightly off-set depending on the metallicity of the population (Figs. 10 and 11). A 100 Myr isochrone (the age of the Pleiades) is also plotted in Fig. 8 to emphasise that for young clusters additional structure (in this case another maximum near $M_V = 8$ in the LF is expected via eq. 1). This is verified for the Pleiades cluster (Belikov et al. 1998), and is due to stars with $m < 0.6 M_\odot$ not having reached the main-sequence yet (Chabrier & Baraffe 2000).

LFs for star clusters are, like Ψ_{phot} , system LFs because binary systems are not resolved in the typical star-count survey. The binary-star population evolves due to encounters, and after a few initial crossing times only those binary systems survive that have a binding energy larger than the typical kinetic energy of stars in the cluster. A further complication with cluster LFs is that star clusters preferentially loose single low-mass stars across the tidal boundary as a result of ever-continuing re-distribution of energy during encounters while the retained population has an increasing binary proportion and increasing average stellar mass. The global PDMF thus flattens with time with a rate proportional to the fraction of the cluster lifetime and, for highly evolved initially rich open clusters, it evolves towards a delta function near the turnoff mass, the mass-loss rate being a function of Galactocentric distance. This is a major problem for aged open clusters (initially $N < 10^4$ stars) with life-times of only a few 100 Myr (Kroupa 1995c).

These processes are now well quantified (Kroupa 2001a; Portegies Zwart et al. 2001), and Fig. 13 shows that a dynamically very evolved cluster such as the Hyades has been depleted significantly in low-mass stars. Even so, the binary-star correction that needs to be applied to the LF in order to arrive at the single-star present-day LF is significant¹⁰.

A computationally challenging investigation of the systematic changes of the MF in evolving clusters of different masses has been published by Baumgardt & Makino (2003). Baumgardt & Makino quantify the depletion of the clusters of low-mass stars through stellar-dynamical processes with a hitherto not available quality and conclusively show that highly evolved clusters have a very substantially skewed present-day MF (Fig. 14). If the cluster ages are expressed in fractions, τ_f , of the overall cluster lifetime, which depends on the initial cluster mass, its concentration and orbit, then different clusters on different orbits lead to virtually the same present-day MFs at the same τ_f . Their results were obtained for clusters that are initially in dynamical equilibrium and that do not contain binary stars (these are computationally highly demanding), so that future analysis, including initially non-virialised clusters and a high primordial binary fraction (Goodwin & Kroupa 2005), will be required to further refine these excellent results.

The first realistic calculations of the formation of an open star cluster such as the Pleiades demonstrate that the binary properties of stars remaining in the cluster are comparable to those observed even if all stars initially form in binary systems with Taurus-Auriga-like properties (Kroupa et al. 2001, 2003). They also demonstrate the complex and counter-intuitive interplay between the initial concentration, mass segregation at the time of residual gas expulsion, and

¹⁰Note that a *system* can be a binary star or a single star, and that the *single-star* LF is the LF obtained by counting all stars independently of whether they are in systems or single.

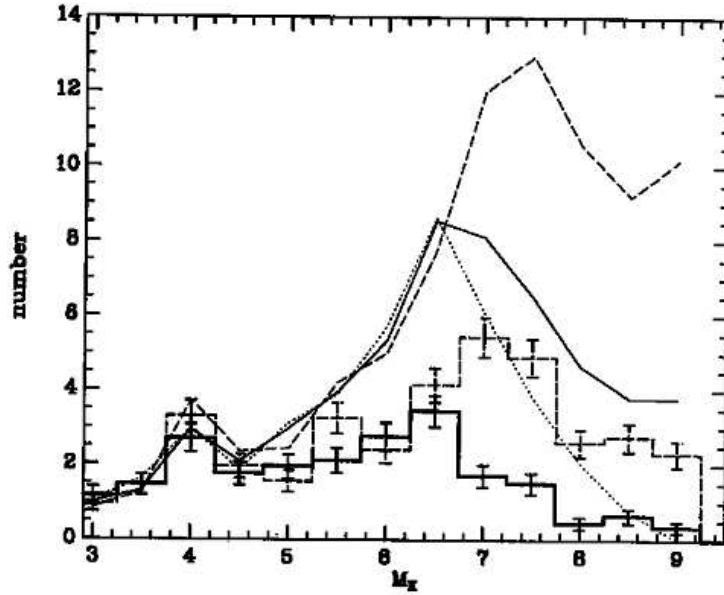


Figure 13. Models of the K -band single-star and system LFs in an ensemble of 20 dynamically highly evolved clusters (thin and thick histograms, respectively). Each cluster model consists initially of 200 binaries with a half-mass radius of 0.85 pc, and the LFs are shown at an age of 480 Myr (44 initial crossing times) and count all stars and systems within the central sphere with a radius of 2 pc. The clusters are random renditions from the same parent distributions (binary-star orbital parameters, IMF, stellar positions and velocities) and are initially in dynamical equilibrium. The upper dashed curve is the initial single-star LF (KTG93 MLR and standard IMF, eq. 20 below) and the solid curve is the model Galactic-field LF of systems. This is an accurate representation of the Galactic-field population in terms of the IMF and mixture of single and binary stars, and is derived by stars forming in clusters such as shown here that dissolve with time. Both of these LFs are identical to the ones shown in Fig. 12. The dotted curve is the initial system LF (100 % binaries). From Kroupa (1995c).

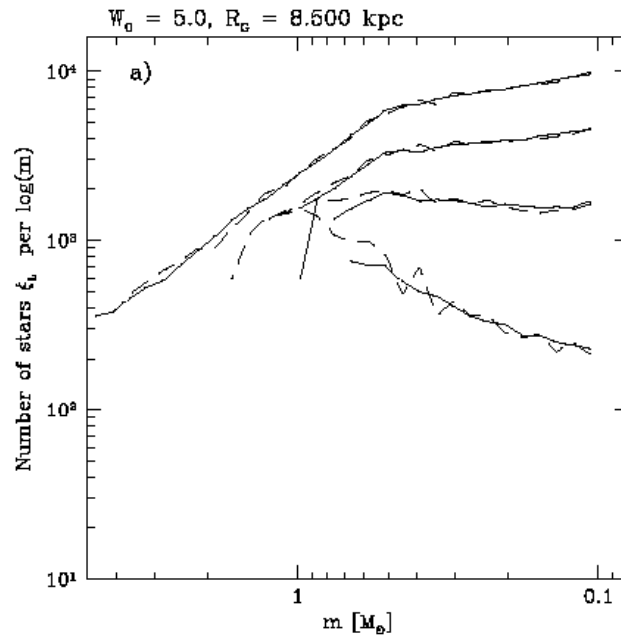


Figure 14. Present-day mass functions in a King-model cluster with concentration $W_0 = 5$ on a circular orbit about the MW centre with radius 8.5 kpc. Shown are the MFs of all bound stars at ages corresponding to $\tau_f = 0\%$, 30% , 60% and 90% of the cluster life-time (from top to bottom). For each age the solid line represents one computation with 1.28×10^5 stars, the dashed lines show the sum of four clusters each with 8000 stars (scaled to the same number of stars as the massive computation). Results for other circular and eccentric orbits and cluster concentrations are virtually indistinguishable. From Baumgardt & Makino (2003).

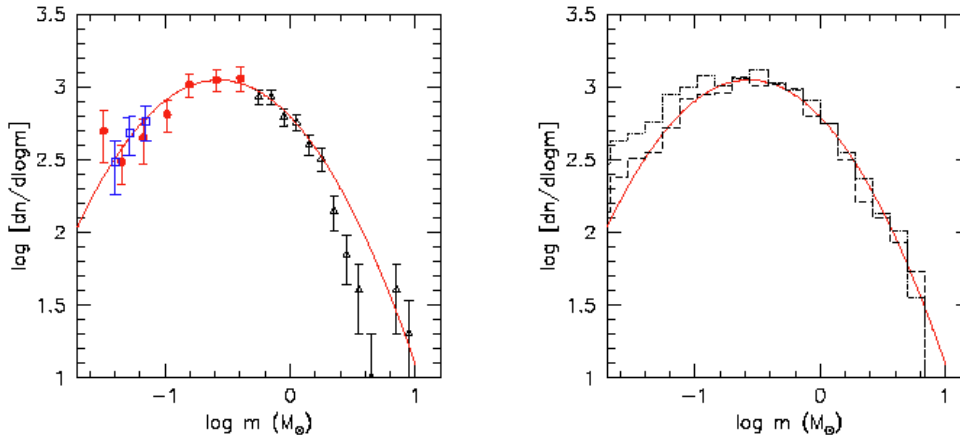


Figure 15. The observed MF in the Pleiades cluster. *Left panel:* The symbols are observational data (for details see Moraux et al. 2004) and the curve is a log-normal fit. *Right panel:* The solid curve is the same log-normal fit. Theoretical system MFs for two initial models of the Pleiades cluster according to Kroupa et al. (2001) are plotted at an age of 100 Myr. These models assume the young cluster to be deeply embedded in gas, with a star-formation efficiency of 33 %, a gas-expulsion time-scale shorter than the crossing time and to contain 10^4 stars and BDs. Model A (dashed histogram) has an initial central number density $\rho_C = 10^{4.8}$ stars/pc³, while model B (dotted histogram) has $\rho_C = 10^{5.8}$ stars/pc³. The embedded phase lasts 0.6 Myr, and during this time mass segregation develops in the initially denser cluster model B. Note that these models are not a fit but a prediction of the Pleiades MF, assuming it had a standard IMF (eq. 20). From Moraux et al. (2004).

the final ratio of the number of BDs to stars (Fig. 15). Thus, the modelling by Kroupa et al. (2001) shows that an initially denser cluster evolves to significant mass segregation when the gas explosively leaves the system. Contrary to naive expectation, according to which a mass-segregated cluster should lose more of its least massive members during expansion after gas expulsion, the ensuing violent relaxation of the cluster retains more free-floating BDs than the less-dense model. This comes about because BDs are split from the stellar binaries more efficiently in the denser cluster. These issues remain an active area of research, because at least two changes need to be made to the modelling: on the one hand, BDs need to be treated as an extra population (Kroupa et al. 2003; Kroupa & Bouvier 2003) so that the above discovered free-floating BDs that result from the disruption of star-BD binaries will not be available, and on the other hand some observations suggest that star clusters may form highly mass-segregated (but see Fig. 17). The mass-dependent loss of stars thus definitely remains an issue to be studied.

From the above work it is now established that even clusters as young as the Pleiades are significantly evolved because clusters of all masses form from highly concentrated embedded morphologies (Kroupa 2005). Also, the low-mass stars in clusters as young as the Pleiades or M35 (Fig. 16 below) have not yet reached the main sequence, so that pre-main sequence stellar-evolution calculations have

to be resorted to when transforming measured luminosities to stellar masses via the MLR.

For ages younger than a few Myr this becomes a serious problem: Classical pre-main sequence theory, which assumes hydrostatic contraction of spherical non-, sometimes slowly-rotating stars from idealised initial states breaks down because of the overlap with the star formation processes that defies detailed treatment. Stars this young remember their accretion history, invalidating the application of classical pre-main sequence stellar evolution tracks, a point made explicitly clear by the excellent work of Wuchterl and collaborators (Wuchterl & Klessen 2001; Wuchterl & Tscharnuter 2003), and are in any case rotating rapidly and non-spherical. Such realistic pre-main sequence tracks are not available yet.

Nevertheless, owing to the lack of an alternative, research of the IMF in very young clusters has to resort to spectroscopic classification of individual stars to place them on a theoretical isochrone of existing classical theory to estimate masses (e.g. Meyer et al. 2000; Luhman 2004; Barrado y Navascués et al. 2004; Slesnick et al. 2004). In such cases the age spread becomes comparable to the age of the cluster (eq. 3). Binary systems are mostly not resolved.

A few results are shown in Figs. 16 and 17. While the usual argument is for an invariant IMF (Kroupa 2001a, 2002; Chabrier 2003a), as is apparent for most population II stars (e.g. fig.5 in Chabrier 2003a), Fig. 16 shows that some appreciable differences in measured MFs are evident. The M35 MF appears to be highly deficient in low-mass stars. This clearly needs further study because M35 and the Pleiades appear to be otherwise fairly similar in terms of age, metallicity (M35 is somewhat less metal-rich than the Pleiades) and the size of the survey volume.

Taking the ONC as the best-studied example of a very young and nearby rich cluster (age ≈ 1 Myr, distance ≈ 450 pc; $N \approx 5000 - 10000$ stars and BDs; Hillenbrand & Carpenter 2000; Luhman et al. 2000; Muench et al. 2000; Kroupa 2000; Slesnick et al. 2004), Fig. 16 shows how the shape of the deduced IMF varies with improving (but still classical) pre-main sequence contraction tracks. This demonstrates that any sub-structure cannot, at present, be relied upon to reflect possible underlying physical mechanisms of star formation.

For the much more massive and long-lived globular clusters ($N \gtrsim 10^5$ stars) theoretical stellar-dynamical work shows that the MF measured for stars near the cluster's half-mass radius is approximately similar to the global PDMF, while inwards and outwards of this radius the MF is flatter (smaller α_1) and steeper (larger α_1), respectively, owing to dynamical mass segregation (Vesperini & Heggie 1997). However, mass loss from the cluster flattens the global PDMF such that it no longer resembles the IMF anywhere (Fig. 14), for which evidence has been found in some cases (Piotto & Zoccali 1999). The MFs measured for globular clusters must therefore generally be flatter than the IMF, which is indeed born-out by observations (Fig. 20 below). However, again the story is by no means straightforward, because globular clusters have significantly smaller binary fractions than population II clusters (Ivanova et al. 2005), and so the binary-star correction is smaller for globular cluster MFs. Therefore, and as already pointed out by Kroupa (2001b), it appears quiet realistically possible that population II IMFs were in fact flatter (smaller α_1) than population I IMFs, as would be

qualitatively expected from simple fragmentation theory (§ 7. below). Clearly, this issue needs detailed investigation which, however, is computationally extremely highly demanding, requiring the use of state-of-the art N -body codes and special-purpose hardware.

The IMFs obtained for nearby and young star clusters as well as for globular clusters are summarised in Table 1.

5. Very low-mass stars and brown dwarfs

These are stars near to the hydrogen-burning mass limit (VLMS) or below (BD), in which case they are not massive enough to achieve sufficiently high central pressures and temperatures to stabilise against continued contraction by burning H and thus indefinitely cool to unobservable luminosities and temperatures. Observationally it is very difficult to distinguish between VLMSs and BDs, because a sufficiently young BD may have colours and spectral features corresponding to a VLMS. BDs were studied as theoretical objects in 1963 by Hayashi & Nakano (1963), who performed the first truly self-consistent estimate of the minimum hydrogen burning mass limit by computing the luminosity at the surface and the energy release rate by nuclear burning. Modern theory of the evolution and internal constitution of BDs has advanced considerably owing to the inclusion of an improved equation of state and realistic model-atmospheres that take into account absorption by many molecular species as well as dust allowing the identification of characteristic photometric signatures (Chabrier & Baraffe 2000). The first BDs were detected in 1995, and since then they have been found in the solar neighbourhood and in young star clusters (Basri 2000) allowing increasingly sophisticated estimates of their mass distribution.

For the solar neighbourhood, near-infrared large-scale surveys have now identified many dozens of BDs probably closer than 25 pc (Allen et al. 2005). Since these objects do not have reliable distance measurements an ambiguity exists between their ages and distances, and only statistical analysis that relies on an assumed star-formation history for the solar neighbourhood can presently constrain the IMF (Chabrier 2002), finding a 60 % confidence interval $\alpha_0 = 0.3 \pm 0.6$ for $0.04 - 0.08 M_\odot$ approximately for the Galactic-field BD IMF (Allen et al. 2005).

Surveys of young star clusters have also discovered BDs by finding objects that extend the colour–magnitude relation towards the faint locus while being kinematical members. Given the great difficulty of this endeavour, only a few clusters now possess constraints on the MF. The Pleiades star cluster has proven especially useful, given its proximity ($d \approx 127$ pc) and young age ($\tau_{cl} \approx 100$ Myr). Results indicate $\alpha_0 \approx 0.5 - 0.6$ (Table 1). Estimates for other clusters (ONC, σ Ori, IC 348; Table 1) also indicate $\alpha_0 \lesssim 0.8$. In their table 1, Allen et al. (2005) summarise the available measurements for 11 populations finding that $\alpha_0 \approx 0 - 1$.

5.1. BD binaries

The above estimates of the IMF suffer under the same bias affecting stars, namely unseen companions. BD–BD binary systems are known to exist (Basri 2000), in the field (Bouy et al. 2003; Close et al. 2003) and in clusters (Martín et al.

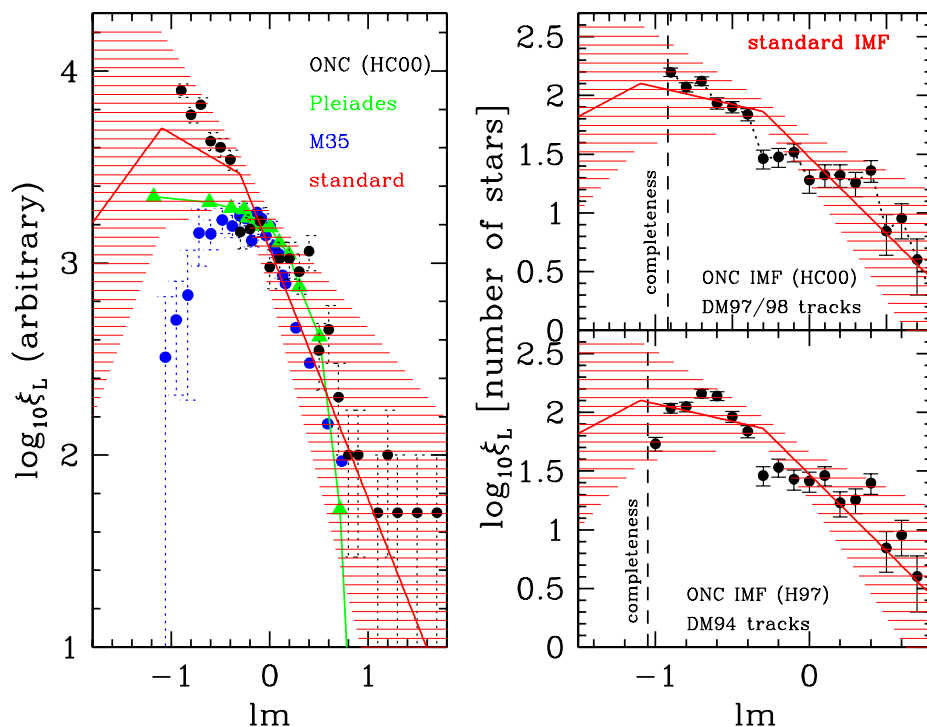


Figure 16. *Left panel:* The measured system mass functions ($lm \equiv \log_{10}(m/M_{\odot})$) in the ONC (Hillenbrand & Carpenter 2000): optical data, $r \leq 2.5$ pc, $\tau_{\text{cl}} < 2$ Myr, $[\text{Fe}/\text{H}] = -0.02$ (Esteban et al. 1998) in the Pleiades (Hambly et al. 1999): $r \leq 6.7$ pc, $\tau_{\text{cl}} \approx 100$ Myr, $[\text{Fe}/\text{H}] = +0.01$, and in M35 (Barrado y Navascués et al. 2001): $r \leq 4.1$ pc, $\tau_{\text{cl}} \approx 160$ Myr, $[\text{Fe}/\text{H}] = -0.21$, where r is the approximate radius of the survey around the cluster centre and τ_{cl} the nuclear age. The strong decrease of the M35 MF below $m \approx 0.5 M_{\odot}$ remains present despite using different MLRs (e.g. DM97, as in the right panel). None of these MFs are corrected for unresolved binary systems. The standard single-star IMF (eq. 20) is plotted as the three straight lines. *Right panel:* The shape of the ONC IMF differs significantly for $m < 0.22 M_{\odot}$ if different pre-main sequence evolution tracks, and thus essentially different theoretical MLRs, are employed (DM stands for tracks calculated by D’Antona & Mazzitelli, see Hillenbrand & Carpenter 2000 for details.)

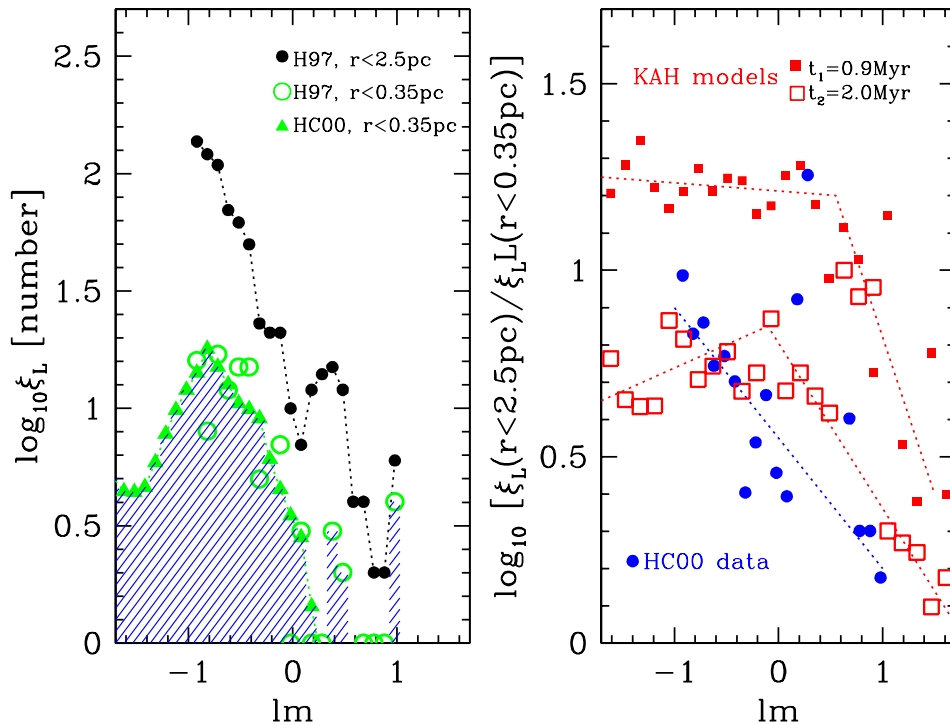


Figure 17. *Left panel:* Mass segregation is very pronounced in the ONC, as is evident by comparing the MF for all stars within $r = 2.5$ pc with the MF for all stars with $r < 0.35$ pc (Hillenbrand & Carpenter 2000, HC00) ($lm \equiv \log_{10}(m/M_{\odot})$). For both samples the reddening $A_V < 2.5$ mag (Hillenbrand 1997, H97, is for an optical and spectroscopic survey, whereas HC00 is a near-infrared survey). *Right panel:* The ratio, $\xi_L(r < 2.5 \text{ pc})/\xi_L(r < 0.35 \text{ pc})$, of the MFs shown in the left panel increases significantly with decreasing mass, demonstrating the significant depletion of low-mass stars in the central region of the ONC. Stellar-dynamical models of the ONC (Kroupa et al. 2001) approximately reproduce this trend at an age of 2 Myr for the standard IMF (eq. 20, whereby the system masses of surviving binary systems are counted instead of the individual stars many of which are in unresolved binaries) even if no initial mass segregation is assumed (at $t = 0$, $\xi_L(r < 2.5 \text{ pc})/\xi_L(r < 0.35 \text{ pc}) = \text{constant}$). The model snapshots shown are from model B in Kroupa et al. (2001) under the assumption that prior to gas-expulsion, 2–1.4 Myr ago, the central stellar density was $\rho_C = 10^{5.8}$ stars/ pc^3 . The dotted lines are eye-ball fits to the plotted data.

2003). Their frequency is not yet very well constrained since detailed scrutiny of individual objects is time-intensive on large telescopes. But the results show conclusively that the semi-major axis distribution of VLMSs and BDs is much more compact than that of M dwarfs, K dwarfs and G dwarfs. Bouy et al. (2003); Close et al. (2003); Martín et al. (2003); Phan-Bao et al. (2005) all find that BD binaries with semi-major axis $a \gtrsim 15$ AU are very rare. Using Monte-Carlo experiments on published multiple-epoch radial-velocity data of VLMSs and BDs, Maxted & Jeffries (2005) deduce an overall binary fraction between 32 and 45 % with a semi-major-axis distribution that peaks near 4 AU and is truncated at about 20 AU. In the Pleiades cluster where their offset in the colour–magnitude diagram from the single-BD locus makes them conspicuous, Pinfield et al. (2003) find the BD binary fraction may be as high as 60 %.

The truncated semi-major-axis distribution of BDs may be a result of binary-disruption in dense clusters of an initial stellar-like distribution. Kroupa et al. (2003) test this notion by setting-up the hypothesis that BDs form according to the same pairing rules as stars, the *star-like hypothesis*. This ought to be true since objects with masses $0.04 - 0.072 M_{\odot}$ should not have very different pairing rules than stars that span a much larger range of masses ($0.1 - 1 M_{\odot}$) but show virtually the same period-distribution function (the M-, K- and G-dwarf samples, Fischer & Marcy 1992; Mayor et al. 1992; Duquennoy & Mayor 1991, respectively). Thus, the hypothesis is motivated by observed orbital distribution functions of stellar binaries not being sensitive to the primary mass, which must come about if the overall physics of the formation problem is similar. Further arguments for a star-like origin of BDs comes from the detection of accretion onto and disks about very young BDs, and that the BDs and stars in Taurus-Auriga have indistinguishable spatial and velocity distributions (White & Basri 2003).

Kroupa et al. (2001, 2003) perform N -body calculations of ONC- and Taurus-Auriga-like stellar aggregates to predict the semi-major-axis distribution functions of BD–BD, star–BD and star–star binaries. These calculations demonstrate that the binary proportion among BDs is smaller than among low-mass stars after a few crossing times, owing to their weaker binding energies. The distribution of separations, however, extends to similar distances as for stellar systems ($a \approx 10^3$ AU), disagreeing completely with the observed distribution. The star-like hypothesis thus predicts far too many wide BD–BD binaries. This can also be seen from the distribution of binding energies of real BD binaries. It is very different to that of stars by having a low-energy cut-off, ${}^{\text{BD}}E_{\text{bin,cut}} \approx -10^{-0.9} M_{\odot} (\text{pc/Myr})^2$, that is much higher than that of the M dwarfs, ${}^{\text{M}}E_{\text{bin,cut}} \approx -10^{-3} M_{\odot} (\text{pc/Myr})^2$ (Fig. 18). This is a very strong indicator for some fundamental difference in the dynamical history of BDs which sets a different energy scale than for stars.

Furthermore, the theoretical distributions contain a substantial number of star–BD pairs, which also disagrees with the observational constraints that have found very few BD companions to nearby stars (Basri 2000; Phan-Bao et al. 2005). Basically, if BDs form exactly like stars, then the number of star–BD binaries would be significantly larger than is observed, since for example G-dwarfs prefer to pair with M-dwarfs. The observed general absence of BD companions is referred to as the *BD desert* (Zucker & Mazeh 2001), since stellar companions

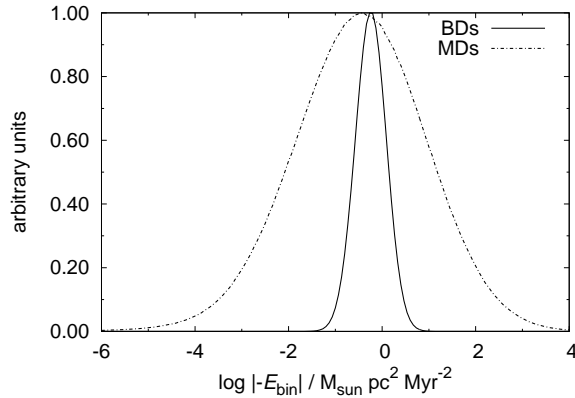


Figure 18. The distribution of binding energies, $E_{\text{bin}} = -G m_1 m_2 / (2a)$, of BDs (solid line) compared to those of M dwarfs (dot-dashed line). The BD distribution is computed by adopting the semi-major-axis, a , distribution from Close et al. (2003) and choosing 10^7 BD masses, $m_i \in (0.04 - 0.1 M_\odot)$, from a power-law MF with $\alpha_0 = 0.3$. The M dwarf energy distribution is computed by assuming the a -distribution from Fischer & Marcy (1992) (which is practically identical to that of G dwarfs) and choosing 10^7 masses, $m_i \in (0.1 - 0.5 M_\odot)$, from a power-law MF with $\alpha_1 = 1.3$. The BD distribution is incomplete to the right of the solid line because tight BD pairs could not be discovered by the available surveys (Bouy et al. 2003; Close et al. 2003; Maxted & Jeffries 2005).

and planets are found at such separations (Halbwachs et al. 2000; Vogt et al. 2002). A few very wide systems with BD companions can form during the final stages of dissolution of a small cluster (de La Fuente Marcos 1998), and three such common proper-motion pairs have perhaps been found (Gizis et al. 2001).

Finally, the star-like hypothesis predicts far too few star–star binaries in Taurus-Auriga, where binary disruption has not been active. Kroupa et al. (2003) thus conclude that the observed BD population is incompatible with their hypothesis, such that BDs need to be treated as a separate, or extra, population.

5.2. The number of BDs per star

Briceño et al. (2002) report that Taurus-Auriga appears to form significantly fewer BDs per star than the ONC. Both systems are very different physically but have similar ages of about 1 Myr. This finding was interpreted to be the first possible direct evidence of a variable IMF, being nicely consistent qualitatively with the Jean-mass,

$$M_J \propto \rho^{-1/2} T^{3/2}, \quad (14)$$

being larger in Taurus-Auriga than in the ONC because its gas density, ρ , is smaller by one–two orders of magnitude, while the temperatures, T , are similar to within a factor of few.

Given this exciting finding, Kroupa et al. (2003) computed N -body models of the stellar aggregates in Taurus-Auriga in order to investigate the hypothesis that BDs form star-like. They find that the same initial number of BDs per

star in Taurus-Auriga and in the ONC actually leads to different observed ratios because BD–BD and star–BD binaries are disrupted more efficiently in the ONC; the observer thus sees many more BDs there than in the comparatively dynamically unevolved Taurus-Auriga groups. But, as already noted above, this approach fails because the Kroupa et al. (2003) model has too many wide BD–BD binaries, and also it predicts too many star–BD binaries. Given this problem, Kroupa & Bouvier (2003) study the production rate of BDs per star assuming BDs are a separate population, such as ejected embryos (Reipurth & Clarke 2001). Again they find that both, the physically very different environments of Taurus-Auriga and the ONC, can have produced the same ratios (about one BD per 4–5 stars) if BDs are ejected embryos with a dispersion of ejection velocities of about 2 km/s.

Based on some additional observations, Luhman (2004) revised the Briceño et al. (2002) results by finding that the number of BDs per star had been underestimated in Taurus-Auriga. Since the new spectroscopic study of Slesnick et al. (2004) also revised the number of BDs per star in the ONC downwards, Luhman (2004) retracts the significance of the claimed difference of the ratio in Taurus-Auriga and the ONC. Is a universal, invariant, BD production scenario still consistent with the updated numbers?

Let the true ratio of the number of BDs per late-type star be

$$R \equiv \frac{N(0.02 - 0.08 M_{\odot})}{N(0.15 - 1.0 M_{\odot})} \equiv \frac{N_{\text{BD,tot}}}{N_{\text{st,tot}}}. \quad (15)$$

Note that here stars more massive than $10 M_{\odot}$ are not counted because this would not make much sense given that Taurus-Auriga is mostly producing late-type stars given the limited gas mass available. But the observed ratio is

$$R = \frac{N_{\text{BD,obs}}}{N_{\text{st,obs}}} = N_{\text{BD,tot}}(\mathcal{B} + \mathcal{U}) \frac{(1 + f)}{N_{\text{st,tot}}}, \quad (16)$$

since the observed number of BDs, $N_{\text{BD,obs}}$ is the total number produced multiplied by the fraction of BDs that are gravitationally bound to the population (\mathcal{B}) plus the unbound fraction, \mathcal{U} , which did not yet have enough time to leave the survey area. These fractions can be computed for dynamical models of the Taurus-Auriga and ONC and depend on their mass and the dispersion of velocities of the BDs. This velocity dispersion can either be the same as that of the stars if BDs form like stars, or larger if they are ejected embryos (Reipurth & Clarke 2001). The observed number of “stars” is actually the number of systems such that the total number of individual stars is $N_{\text{st,tot}} = (1 + f) N_{\text{st,obs}}$, where $f \equiv N_{\text{st,bin}}/N_{\text{st,sys}}$ is the binary fraction and $N_{\text{st,bin}}$ is the number of binary systems in a sample of $N_{\text{st,sys}}$ stellar systems. Note that here no distinction is made between single or binary BDs. For Taurus-Auriga, Luhman (2004) observes $R_{\text{TA,obs}} = 0.25$ from which follows

$$R_{\text{TA}} = 0.18 \quad \text{since} \quad f_{\text{TA}} = 1, \mathcal{B} + \mathcal{U} = 0.35 + 0.35 \quad (17)$$

(Kroupa et al. 2003). According to Slesnick et al. (2004), the revised ratio for the ONC is $R_{\text{ONC,obs}} = 0.28$ so that

$$R_{\text{ONC}} = 0.19 \quad \text{because} \quad f_{\text{ONC}} = 0.5, \mathcal{B} + \mathcal{U} = 1 + 0 \quad (18)$$

(Kroupa et al. 2003). Note that the regions around the stellar groupings in Taurus-Auriga not yet surveyed should contain about 30 % of all BDs, while all BDs are retained in the ONC.

Therefore, the updated numbers imply that about *one BD is produced per five late-type stars*, and that the dispersion of ejection velocities is $\sigma_{\text{ej}} \approx 1.3$ km/s. These numbers are an update of those given in Kroupa et al. (2003), but the results have not changed much. Note that a BD with a mass of $0.06 M_{\odot}$ and a velocity of 1.3 km/s has a kinetic energy of $10^{-1.29} M_{\odot} (\text{pc/Myr})^2$ which is rather comparable to the cut-off in BD-BD binding energies (Fig. 18). *This supports the notion that most BDs may be mildly ejected embryos.*

BDs can come in different flavours (Kroupa & Bouvier 2003): star-like BDs, ejected embryos, collisional BDs and photo-evaporated BDs. As seen above, star-like BDs appear to be very rare, because BDs do not mix with stars in terms of pairing properties; some mechanism ensures the two types of object are kept separated. Ejected embryos appear to be a promising production channel, as noted above. Kroupa & Bouvier (2003) discount the collisional removal of accretion envelopes for the production of unfinished stars because this process is far too slow, or rare. The removal of accretion envelopes through photo-evaporation can occur, but only within the immediate vicinity of an O star and never in Taurus-Auriga (Whitworth & Zinnecker 2004). However, Kroupa & Bouvier (2003) show that the radius within which photo-evaporation may be able to remove substantial fractions of an accretion envelope within 10^5 yr is comparable to the cluster size in star-burst clusters that contain thousands of O stars. In such clusters photo-evaporated BDs may be very common. Globular clusters may then be full of BDs.

Returning to the local star-forming regions, it thus now appears that the very different physical environments evident in Taurus-Auriga and the ONC produce the same number of BDs per late-type star, so that there is no evidence for differences in the IMF across the hydrogen burning mass limit. There is also no substantial evidence for a difference in the stellar IMF in these two star-forming regions, contrary to the assertion by Luhman (2004). Fig. 19 shows the IMF in Taurus-Auriga: it is similar to the standard IMF (eq. 20 below), provided corrections for the high multiplicity are made. And in turn, the standard IMF is comparable to that seen in the ONC (Fig. 16). The caveat that the classical pre-main sequence evolution tracks, upon which the observational mass determinations rely, are not really applicable for such young ages (§ 4.2.) needs to be kept in mind though.

6. The Shape of the IMF

From the above discourse it thus becomes apparent that the distribution of stars by mass is a power-law with exponent or index $\alpha_2 \approx 2.35$ for stellar masses $m \gtrsim 0.5 M_{\odot}$. There exists a physical stellar mass limit, $m_{\text{max}^*} \approx 150 M_{\odot}$ such that $m \leq m_{\text{max}^*}$ (§ 3.1.). The distribution of stars below the K/M dwarf transition mass, $0.5 M_{\odot}$, can also be described by a power law, but with exponent $\alpha_1 \approx 1.3$ (§ 4.). Given the latest results described in § 5., the mass-distribution below the mass $m_1 \in (0.072 - 0.14) M_{\odot}$ is uncertain, but measurements indicate a power-law with exponent $0 < \alpha_0 < 1$. Because the binary properties of

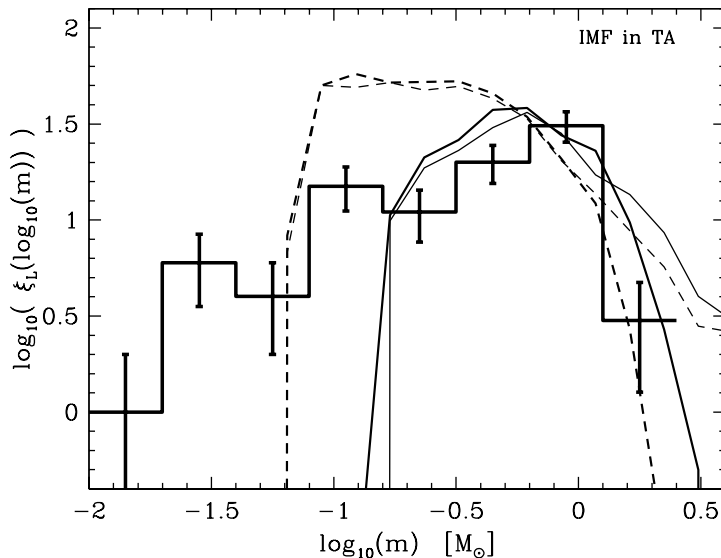


Figure 19. The thick histogram shows the Taurus-Auriga MF observed by Luhman et al. (2003), and the dashed curves are the standard IMF (eq. 20). The solid curves are the model from Kroupa et al. (2003) assuming all stars are in unresolved binary systems. The model shown by thick curves assumes stars only form in the mass interval $0.07 - 1.5 M_{\odot}$, while the thin curves are for stars in the mass range $0.07 - 50 M_{\odot}$. BDs would be part of the model as an extra population matched by the thick histogramme but are not explicitly shown in the model. The binary-star model (solid lines) is in good agreement with the observed MF in the stellar regime. For details see Kroupa et al. (2003). Note the discontinuity in the IMF evident between the dashed curve and the solid histogramme at $10^{-1.2} M_{\odot}$.

VLMSs and BDs differ substantially from those in the low-mass star regime, it can be argued that VLMSs and BDs need to be considered as a separate population that is linked-to, but different from stars. This would then open the likelihood that the IMF is discontinuous near m_1 , as may already be evident in Fig. 19. And so fitting a functional description of the mass distribution with the continuity constraint would be wrong. For this reason it would appear to be dangerous, and in the worst case unphysical, to use one single function such as the log-normal form to attempt to describe the mass distribution from the fragmentation limit¹¹, $m_0 \approx 0.01 M_\odot$, through to the physical stability limit $m_{\max*}$. Indeed, Chabrier (2003a) already noted (i) that a single log-normal function over the entire stellar mass range is not compatible with the data, a power-law form for $m > 1 M_\odot$ being required, and (ii) that the continuous IMF predicts too many VLMSs and BDs by a factor of about three.

With these recent insights (power-law IMF over two orders of magnitude in mass and probable discontinuity near the sub-stellar mass limit), little of the argument for the advantages of a log-normal or any other mathematical form (Table 3 below) remains. Indeed, any such other mathematical form has the little nastiness that the tails of the distribution react to changes in the parametrisation in a way perhaps not wanted when testing models. To give an example: a single log-normal form would change the slope of the IMF at large masses even if only the LF for late-type stars is to be varied. The standard (eq. 20) two-part power-law stellar IMF, on the other hand, would allow changes to the index at low masses without affecting the high-mass end, and the addition of further power-law segments is mathematically convenient. The standard two-part power-law stellar IMF also captures the essence of the physics of star formation, namely a featureless power-law form for the largest range of stellar masses and a turnover near some fraction of a solar mass which probably is a result of increasing inefficiency of star formation (§ 7.). The overall shape of the IMF then sets the characteristic or average stellar mass.

6.1. The standard or average IMF

The various constraints arrived at above are summarised by a multi-part power-law,

$$\xi(m) = k \begin{cases} \left(\frac{m}{m_1}\right)^{-\alpha_0} & , \quad m_0 < m \leq m_1 & , \quad n = 0, \\ \left(\frac{m}{m_1}\right)^{-\alpha_1} & , \quad m_1 < m \leq m_2 & , \quad n = 1, \\ \left[\prod_{i=2}^{n \geq 2} \left(\frac{m_i}{m_{i-1}}\right)^{-\alpha_{i-1}}\right] \left(\frac{m}{m_n}\right)^{-\alpha_n} & , \quad m_n < m \leq m_{n+1} & , \quad n \geq 2, \end{cases} \quad (19)$$

¹¹When a cloud collapses its density increases but its temperature remains constant as long as the opacity remains low enough to enable the contraction work to be radiated away. The Jeans mass (eq. 14) consequently decreases and further fragments with smaller masses form. When, however, the density increases to a level such that the cloud core becomes optically thick, then the temperature increases, and the Jeans mass follows suit. Thus an opacity-limited minimum fragmentation mass is arrived at (Low & Lynden-Bell 1976; Boss 1986; Kumar 2003).

where k contains the desired scaling and the mass-ratios ensure continuity, with

$$\begin{aligned} \alpha_0 &= +0.3 \pm 0.7 & , & \quad 0.01 \leq m/M_\odot < 0.08 & , & \quad n = 0, \\ \alpha_1 &= +1.3 \pm 0.5 & , & \quad 0.08 \leq m/M_\odot < 0.50 & , & \quad n = 1, \\ \alpha_2 &= +2.3 \pm 0.7 & , & \quad 0.5 \leq m/M_\odot \lesssim 150 & , & \quad n = 2. \end{aligned} \quad (20)$$

The uncertainties are discussed in § 6.2.

This two-part power-law stellar IMF is referred to as the *standard* or *canonical stellar IMF*. It is also the *average IMF* since it rests upon a derivation from local star-counts for $m < 1 M_\odot$ that sample star-formation over the age of the MW disk (about 10 Gyr), and upon an averaging of the results obtained by the surveys of many OB associations and massive clusters for $> \text{few } M_\odot$ (Fig. 1). Eq. 20 is therefore a good bench-mark against which individually-derived IMFs can be compared to study possible systematic changes of the IMF with changing physical conditions.

A larger value for $\alpha_3 \approx 2.7$ in the *stellar IMF* may be closer to the truth than the above canonical Salpeter/Massey value ($\alpha_3 = 2.3$) when binary-companions are corrected for (§ 3., Sagar & Richtler 1991), in this case arriving at the *KTG93 IMF* (Kroupa et al. 1993),

$$\begin{aligned} \alpha_0 &= +0.3 \pm 0.7 & , & \quad 0.01 \leq m/M_\odot < 0.08 & , & \quad n = 0, \\ \alpha_1 &= +1.3 \pm 0.5 & , & \quad 0.08 \leq m/M_\odot < 0.50 & , & \quad n = 1, \\ \alpha_2 &= +2.3 \pm 0.3 & , & \quad 0.5 \leq m/M_\odot < 1 & , & \quad n = 2, \\ \alpha_3 &= +2.7 \pm 0.7 & , & \quad 1 \leq m/M_\odot & , & \quad n = 3. \end{aligned} \quad (21)$$

Note that in this case the observational data would not constrain the physical upper stellar mass limit (Weidner & Kroupa 2004). A detailed study of systematic biases affecting power-law index measurements based on binned data is under way and will allow deeper insights into these issues (Maíz Apellániz et al. 2005).

Note that $\alpha_3 = 2.7$ (the Scalo index) was also derived by Scalo (1986) for the MW disk population of massive stars such that the three-part-power law KTG93 IMF needs to be identified with the *composite IMF* introduced in § 8.. Whether the stellar IMF needs to be changed away from the Salpeter/Massey value ($\alpha_3 = 2.3$) because of corrections for unresolved multiples, and by how much the composite IMF then differs from the stellar IMF above $1 M_\odot$, thus needs to be studied in more detail.

6.2. The alpha plot

A convenient way for summarising various studies of the IMF is by plotting independently-derived power-law indices in dependence of the stellar mass over which they are fitted (Scalo 1998; Kroupa 2001b, 2002; Hillenbrand 2004). Fig. 20 plots such data: The shape of the IMF is mapped by plotting measurements of α at $\langle lm \rangle = (lm_2 - lm_1)/2$ obtained by fitting power-laws, $\xi(m) \propto m^{-\alpha}$, to logarithmic mass ranges lm_1 to lm_2 (not indicated here for clarity). Circles and triangles are data compiled by Scalo (1998); Kroupa (2001b) for MW and Large-Magellanic-Cloud (LMC) clusters and OB associations, as well as newer data, some of which are emphasised using different symbols (and colours) (Table 1). Unresolved multiple systems are not corrected for in all these

data including the MW-bulge data. The standard stellar IMF (eq. 20, corrected for unseen binary-star companions for $m < 1 M_\odot$) is the two-part power-law (thick short-dashed lines).

Note that the M dwarf ($0.1 - 0.5 M_\odot$) MFs for the various clusters are systematically flatter (smaller α_1) than the standard IMF, which is mostly due to unresolved multiple systems in the observed values. Some of the data do coincide with the standard IMF though, and Kroupa (2001b) argues that on correcting these for unresolved binaries the underlying true single-star IMF ought to have $\alpha_1 \approx 1.8$. This may indicate a systematic variation of α_1 with metallicity because the data are young clusters that are typically more metal-rich than the average Galactic field population for which $\alpha_1 = 1.3$ (cf. eq. 22 below)

A power-law extension into the BD regime with a smaller index ($\alpha_0 = +0.3$) is shown as a third thick short-dashed segment, but this part of the mass distribution may not be a continuous extension of the stellar distribution, as noted above. The upper and lower thin short-dashed lines are the estimated 99 % confidence range on α_i (eq. 20). Other binary-star-corrected solar-neighbourhood-IMF measurements are indicated as (magenta) dotted error-bars (Table 1). Note that for $m > 1 M_\odot$ correction for unseen companions may steepen the standard IMF to $\alpha \approx 2.7$.

The long-dash-dotted horizontal lines in Fig. 20 labelled “SN” are those IMFs with $\alpha_3 = 0.70(1.4)$ but $\alpha_0, \alpha_1, \alpha_2$ as in eq. 20, for which 50 % of the stellar (including BD) mass is in stars with $8 - 50(8 - 120) M_\odot$, respectively. It is noteworthy that none of the available clusters, not even including the starburst clusters (Table 1), has such a top-heavy IMF. Any hypothetical cluster so dominated by massive stars would disperse due to the mass loss from the supernova explosions.

The vertical dotted lines in Fig. 20 delineate the four mass ranges (eq. 20), and the shaded areas highlight those stellar mass regions where the derivation of the IMF is additionally complicated especially for Galactic field stars: for $0.08 < m/M_\odot < 0.15$ long pre-main sequence contraction times (Chabrier & Baraffe 2000) make the conversion from an empirical LF to an IMF (eq. 1) dependent on the precise knowledge of stellar ages and the SFH, and for $0.8 < m/M_\odot < 2.5$ uncertain main-sequence evolution, Galactic-disk age and the SFH of the MW disk do not allow accurate IMF determinations (Binney et al. 2000).

6.3. The distribution of data points in the alpha-plot

The first thing to note about the data distribution in the alpha-plot is that there is (unfortunately) no clear systematic difference in IMF determinations with metallicity nor density of the population (cf. Fig. 1).

In order to understand the origin and nature of the dispersion of power-law indices evident in the alpha plot, Kroupa (2001b) investigates the dispersion of α values for a given mass interval theoretically. The result is that the dispersion can be understood in terms of statistical sampling from a universal IMF (as also found by Elmegreen 1997, 1999) together with stellar-dynamical biases. Given such a theoretical investigation, it is now possible to compare the theoretical distribution of α values for an ensemble of star clusters with the observational data. This is done for stars with $m > 2.5 M_\odot$ in Fig. 21 where the open (green) histogram shows the distribution of observational data from Fig. 20. The (blue)

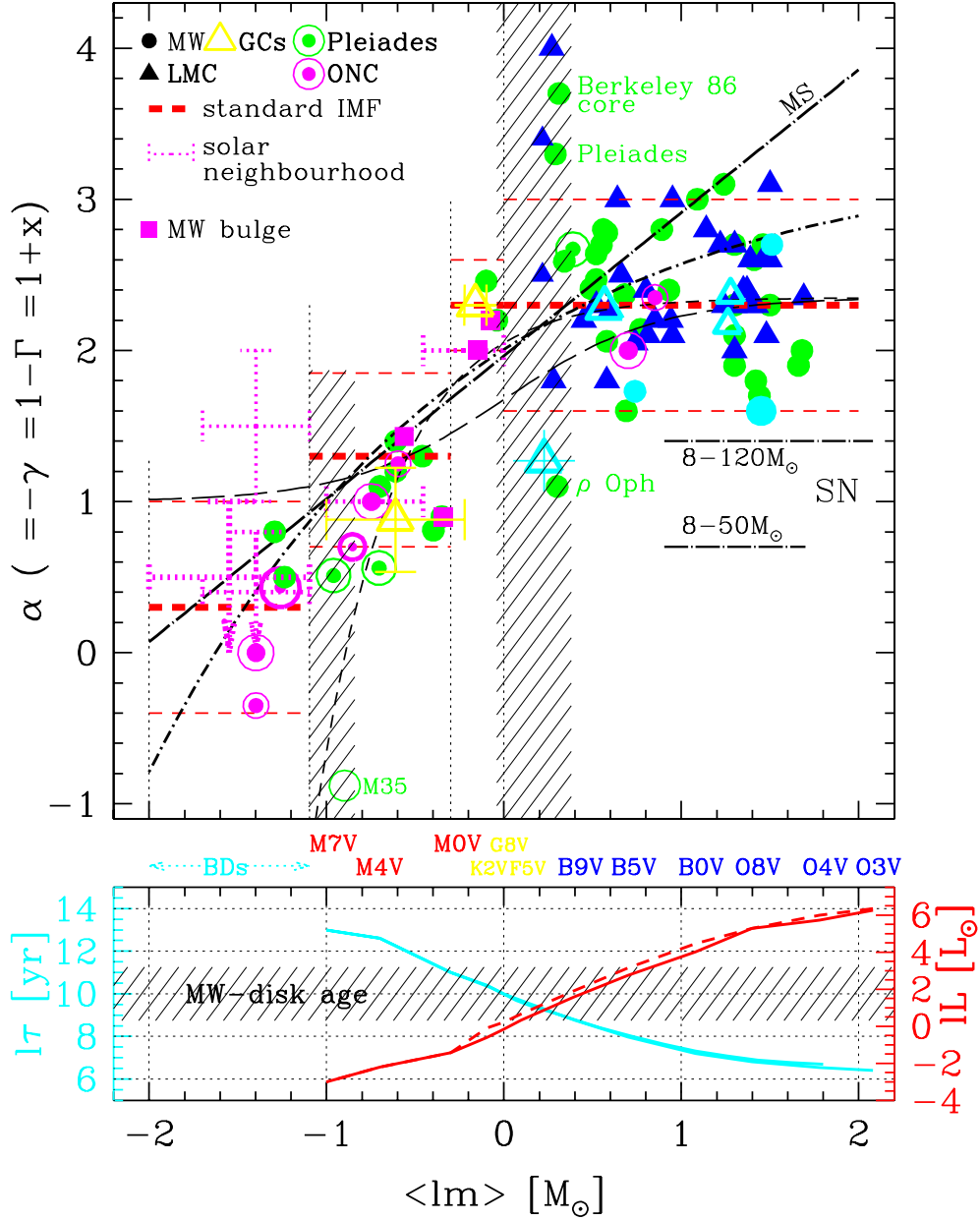


Figure 20. The alpha plot (upper panel), and bolometric MLR, $lL(lm)$, stellar main-sequence life-time, $l\tau$, and possible range of Milky-Way (MW) disk ages shown as the shaded region (lower panel). Notation: $lm \equiv \log_{10}(m/M_{\odot})$, $l\tau \equiv \log_{10}(\tau/\text{yr})$, $lL \equiv \log_{10}(L/L_{\odot})$. For more details see text.

shaded histogram is the theoretical ensemble of 12 star clusters containing initially 800 to 10^4 stars that are “observed” at 3 and 70 Myr: stellar companions are merged to give the system MFs, which are used to measure α , but the input single-star IMF is in all cases the standard form (eq. 20). The dotted curves are Gaussians with the same average α and standard deviation in α obtained from the histograms. Fixing $\alpha_f = \langle \alpha \rangle$ and using only $|\alpha| \leq 2\sigma_\alpha$ for the observational data gives the narrow thin (red) dotted Gaussian distribution which describes the Salpeter peak extremely well (not by construction).

The interesting finding is thus that the observational data have a very pronounced Salpeter/Massey peak, with broad near-symmetric wings. This indicates that there are no serious biases that should skew the distribution. For example, if the observational sample contained clusters or associations within which the OB stars have a low binary fraction compared to others that have a very high multiplicity fraction, we would expect the binary-deficient cases to deviate towards low α values. Likewise, energetic dynamical ejections from cluster cores would skew the IMF towards more massive stars (reduced α) while mass segregation has a similar effect.

In contrast, the theoretical data show (i) a distribution with a mean shifted to smaller $\alpha \approx 2.2$ that has (ii) a larger width than the observational one. The input standard Salpeter/Massey index is not really evident in the theoretical data, and if these were the observational data then it is likely that the astronomical community would strongly argue for the case that the IMF shows appreciable variations. It is peculiar that the empirical data are so much better behaved, since all the additional complications (theoretical stellar models, rotating/non-rotating stars) are not modelled in the theoretical data. The elucidation of the reason for the difference between the much more “well-behaved” observational data and the theoretical data will need further theoretical work which will have to attempt to re-produce the observational procedure as exactly as is possible.

6.4. Mass density and some other numbers

The nearby Hipparcos LF, $\Psi_{\text{near}}(\text{Hipp})$, has $\rho = (5.9 \pm 0.3) \times 10^{-3}$ stars/pc³ in the interval $M_V = 5.5 - 7.5$ corresponding to the mass interval $m_2 = 0.891 - 0.687 M_\odot$ (Kroupa 2001c) using the KTG93 MLR (Fig. 8). $\int_{m_1}^{m_2} \xi(m) dm = \rho$ yields $k = 0.877 \pm 0.045$ stars/(pc³ M_\odot). The number fractions, mass fractions and Galactic-field mass densities contributed by stars in different mass-ranges are summarised in Table 2.

The local mass density made up of interstellar matter, $\rho^{\text{gas}} \approx 0.04 \pm 0.02 M_\odot/\text{pc}^3$, and stellar remnants, $\rho^{\text{rem}} \approx 0.003 M_\odot/\text{pc}^3$ (Weidemann 1990), or $\rho^{\text{rem}} \approx 0.005 M_\odot/\text{pc}^3$ (Chabrier 2003a and references therein). Giant stars contribute about $0.6 \times 10^{-3} M_\odot/\text{pc}^3$ (Haywood et al. 1997), so that main-sequence stars make up about half of the baryonic matter density in the local Galactic disk (Table 2). BDs, which for some time were regarded as candidates for contributing to the dark-matter problem, do not constitute a dynamically important mass component of the Galaxy, even when eq. 20 is extrapolated to $0.0 M_\odot$ giving $\rho^{\text{BD}} = 3.3 \times 10^{-3} M_\odot/\text{pc}^3$. This is corroborated by dynamical analysis of local stellar space motions that imply there is no dark matter in the Milky-Way disk (Flynn & Fuchs 1994), and the revision of the thick-disk mass

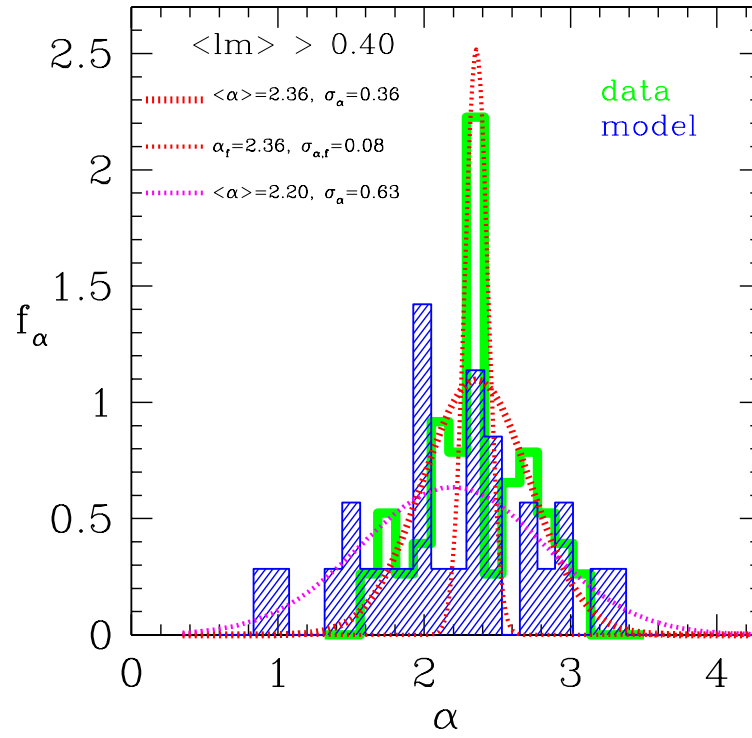


Figure 21. Distribution of α values for massive stars. See text for details.

density to larger values (Fuhrmann 2004; Soubiran et al. 2003) further reduces the need for dark matter within the solar circle (cf Chabrier 2003a).

Table 2 also shows that a star cluster loses about 13 per cent of its mass through stellar evolution within 10 Myr if $\alpha_3 = 2.3$ (turnoff-mass $m_{t0} \approx 20 M_\odot$), or within 300 Myr if $\alpha_3 = 2.7$ (turnoff-mass $m_{t0} \approx 3 M_\odot$). After 5 Gyr the mass loss through stellar evolution alone amounts to about 45 per cent if $\alpha_3 = 2.3$ or 29 per cent if $\alpha_3 = 2.7$. Mass loss through stellar evolution therefore poses no risk for the survival of star clusters for the IMFs discussed here, since the mass-loss rate is small enough for the cluster to adiabatically re-adjust. A star-cluster would be threatened through mass loss from supernova explosions if $\alpha \approx 1.4$ for $8 < m/M_\odot \leq 120$ which would mean a mass-loss of 50 per cent within about 40 Myr when the last supernova explodes. It is remarkable that none of the measurements has found such a low α for massive stars (Fig. 20).

6.5. Other IMF forms

As already discussed at the beginning of this section, the standard or canonical power-law IMF (eq. 20) provides a good description of the data combined with mathematical ease and physical meaning. A strong advantage of this parametrisation is that each section can be changed without affecting another part of the IMF, as stated above. As an explicit example, should the BD MF be revised, α_0 can be adopted accordingly without affecting the rest of the mass distribution in the well-tested stellar regime.

But additional forms are in use and are preferred for some investigations: In Fig. 20 the quasi-diagonal (black) lines are alternative analytical forms summarised in Table 3. Of these the generalised Rosin-Rammler function (eq. *Ch* in Table 3, thick short-dash-dotted curve) best represents the data, apart from a deviation for $m \gtrsim 10 M_\odot$, which Chabrier (2003a) fixes by adopting a Salpeter/Massey power-law extension for $m > 1 M_\odot$. Interpretation of m_o in terms of a characteristic mass poses difficulties. The popular Miller-Scalo log-normal IMF (eq. *MS* in Table 3) deviates even more strongly from the empirical data at high masses. Larson's eq. *Lb* in Table 3 fits rather well, except that it may predict too many BDs. Finally, the *effective initial mass function for galactic disks* proposed by Hollenbach et al. (2005) (eq. *Holl*) reproduces the data in the alpha-plot quite well (fig. 1 in Hollenbach et al. 2005), and is not incorporated into Fig. 20 here. Note however that a *composite IMF* ought to be steeper (have a larger α) at high masses (§ 8.).

The closed functional IMF formulations (eqs. *MS*, *La*, *Lb*, *Ch*, *Holl*) have the advantage that possible variations of the IMF with physical conditions can be studied more naturally than with a multi-power-law form, because they typically have a characteristic mass that can be varied directly.

7. Variation of the IMF and theoretical aspects

Is the scatter of data points in the alpha-plot (Fig. 20) a result of IMF variations? For this to be conclusively convincing would require a measurement to lie further from the standard IMF than the conservative uncertainty range adopted in eq. 20 and shown in the figure. However, the adopted uncertainties on α_i in eq. 20 stem from the scatter in the alpha plot, so that this argument is circular.

An independent indication of the uncertainties inherent to IMF determinations can be obtained by comparing IMF estimates of the same cluster by different authors. This is demonstrated for the well-studied Pleiades, ONC and for 30 Dor (Table 1, Fig. 20). Overall, the uncertainties in α are about ± 0.5 which is also about the scatter evident in all the data, so that there is no indication of significant outliers (except in the shaded regions, see below). Substantial differences for VLMSs and BDs are evident for the extremely young ONC allowing an estimate of likely non-physical variations in the alpha plot. Data reduction at these low masses is hampered by variability, variable reddening, spurious detections (Slesnick et al. 2004). It is clear that because the procedure of measuring $\alpha(lm)$ is not standardised and because the IMF is not a single power-law, author–author variations occur simply due to the use of different mass ranges when fitting power-laws. Here the work by Maíz Apellániz et al. (2005), who is addressing such issues, is important.

Significant departures from the standard IMF only occur in the shaded areas of the alpha plot. These are, however, not reliable. The upper mass range in the shaded area near $1 M_{\odot}$ poses the problem that the star-clusters investigated have evolved such that the turn-off mass is near to this range. Some clusters such as ρ Oph are so sparse that more massive stars did not form. In these cases the shaded range is close to the upper mass limit leading to possible stochastic stellar-dynamical biases since the most massive stars meet near the core of a cluster due to mass segregation, but three-body or higher-order encounters there can cause expulsions from the cluster. Furthermore, ρ Oph is still forming, leading to unknown effects that are likely to enhance variations in the first derivative of the IMF (i.e. in α values). Dynamical ejections are probably the cause for the “OB field-star” MF which has $\alpha \approx 4.5$ and is interpreted to be the result of isolated high-mass star-formation in small clouds (Massey 1998). Precise proper-motion measurements have, however, shown that even the best candidates for this isolated population have very high space motions (Ramspeck et al. 2001) which are the result of energetic stellar-dynamical ejections when massive binary systems interact in the cores of star-clusters in normal but intense star-forming regions, thus posing important constraints on the properties of OB binary systems (Clarke & Pringle 1992; Kroupa 2001a; Pflamm-Altenburg & Kroupa 2006).

The shaded area near $0.1 M_{\odot}$ poses the problem that the VLMSs are not on the main sequence for most of the clusters studied, and are again prone to bias through mass-segregation by being underrepresented within the central cluster area that is easiest to study observationally. Especially the latter is probably biasing the M35 datum, but some effect with metallicity may be operating, especially so since M35 appears to have a smaller α near the H-burning mass limit than the Pleiades cluster which has a similar age but has a larger abundance of metals (Fig. 16). The M35 cluster ought to be looked at again with telescopes.

To address stellar-dynamical biases, an extensive theoretical library of binary-rich star clusters has been assembled (Kroupa 2001b) covering 150 Myr of stellar-dynamical evolution taking into account stellar evolution and assuming the standard IMF (eq. 20) in all cases. This extends the notion raised by Elmegreen (1999) that the scatter seen in the empirical alpha-plot may be due to finite– N sampling from a universal IMF that can be interpreted as a probability density

distribution. Evaluating the MF within and outside of the clusters, at different times and for clusters containing initially $800 - 10^4$ stars, leads to a theoretical alpha-plot which reproduces the spread in $\alpha(lm)$ values evident in the empirical alpha-plot quite well. This verifies the conservative uncertainties adopted in the standard IMF (eq. 20) but also implies that the scatter in the empirical alpha-plot around the standard IMF cannot be interpreted as true variations. This work also addresses the bias due to unresolved binary systems, with the result that typical open clusters ought to be underrepresented in VLMSs. This bias is incorporated in the definition of the standard IMF, as is evident in the empirical alpha-plot.

One peculiar feature of the empirical alpha-plot that merits further study is the distribution of α data for $m > 2.5 M_\odot$ (§ 6.3.). A histogram of the empirical data (Fig. 21) shows a narrow peak positioned at the Salpeter value, with symmetric broad wings. The empirical data are not distributed normally. The aforementioned theoretical alpha-plot shows a very different distribution, the width being *larger* than for the empirical data. Interestingly, the spread, $\sigma_{\alpha,f} = 0.08$, of the narrow peak in the empirical data is very similar to the uncertainties quoted by Massey in an extensive and consistent observational determination of the IMF for massive stars, $\alpha = 2.2 \pm 0.1$ (Fig. 1). If $\alpha = 2.3 \pm 0.1$ is adopted for massive stars, then the measurement $\alpha = 1.6 \pm 0.1$ for the massive but difficult-to-observe Arches cluster near the Galactic centre (Table 1) would definitely mean an IMF that is top-heavy for this extreme population. But as discussed in § 1., the Arches is suffering heavily from the tidal forces that strip its less massive members so that the PDMF is likely skewed towards massive stars. Kim et al. (2006) indeed verify the near-Salpeter/Massey IMF in the Arches cluster. *The question thus remains if the non-Gaussian distribution of empirical α values contains information on a possible physical variation of the IMF.*

Two other well-studied massive star-burst clusters have $\alpha \approx \text{Salpeter/Massey}$ (30 Dor and NGC 3603, Table 1) implying no clear evidence for a bias that resolved star-burst clusters prefer smaller α and thus more massive stars relatively to the number of low-mass stars. Low-mass stars are known to form in 30 Dor (Sirianni et al. 2000), although their MF has not been measured yet due to the large distance of about 55 kpc. From the ONC we know that the entire mass spectrum $0.05 \lesssim m/M_\odot \lesssim 60$ is represented roughly following the standard IMF (Fig. 16, Pflamm-Altenburg & Kroupa 2006). The Pleiades appears to have had an IMF very similar to the standard one (Fig. 15), although for massive stars a steeper IMF with $\alpha_3 \approx 2.7$ appears to be suggested by the theoretical work (Moraux et al. 2004).

The available evidence is thus that low-mass stars and massive stars form together even in extreme environments without, as yet, convincing demonstration of a variation of the number ratio. This is also supported by an impressive observational study (Luhman et al. 2000; Luhman 2004) of many close-by star-forming regions using one consistent methodology to avoid author–author variations. The result is that the IMF does not show measurable differences from low-density star-forming regions in small molecular clouds ($n = 0.2 - 1$ stars/pc³ in ρ Oph) to high-density cases in giant molecular clouds ($n = (1-5) \times 10^4$ stars/pc³ in the ONC). This result extends to the populations in the truly exotic ancient and metal-poor dwarf-spheroidal satellite galaxies which are speculated to be

severely dominated by dark matter but definitely constitute star-forming conditions very different from present-day events. Two such close companions to the Milky Way have been observed (Grillmair et al. 1998; Feltzing et al. 1999) finding the same MF as in globular clusters for $0.5 \lesssim m/M_{\odot} \lesssim 0.9$ and thus no very evident differences to the standard IMF.

However, there are peculiar indications of top-heavy IMFs such as in some massive star-burst clusters in the M82 galaxy. Spectroscopy of the unresolved M82-F cluster derives, via the inferred velocity dispersion, a mass and from the luminosity a mass-to-light ratio that is significantly smaller than the ratio expected from the standard IMF for such a young (about 60 Myr) population. The implication is that the M82-F population may be significantly depleted in low-mass stars, provided the velocity dispersion is representative of the entire cluster. A possibility that will have to be addressed using stellar-dynamical modelling of forming star clusters is that M82-F may have lost low-mass stars due to tidal shocking (Smith & Gallagher 2001). Highly pronounced mass segregation which leads to a dynamically decoupled central core of OB stars is an important mechanism for reducing the measured mass-to-light ratio (Boily et al. 2005), while rapid expulsion of residual gas from forming clusters enhances the measured mass-to-light ratios (Goodwin & Bastian 2006).

The proclamation by Briceño et al. (2002) that Taurus-Auriga is producing significantly fewer BDs per star than the ONC, and thus for a possible first robust indication of a variable IMF, was found to not be the correct interpretation by Kroupa et al. (2003); Kroupa & Bouvier (2003) and was retracted by Luhman (2004) based on newer data. A new analysis of these actually shows that Taurus-Auriga and the ONC are producing the same number of BDs per star, about 0.2 (§ 5.). Nevertheless, the discussion in § 5. shows that BDs probably need to be treated as a separate population such that the IMF may be discontinuous near the stellar/sub-stellar mass limit. Since BDs may come in four flavours, Kroupa & Bouvier (2003) suggest that the photo-evaporated sort could far outweigh the others in star-burst clusters, so that globular clusters could contain a larger fraction of BDs per star than the current modest Galactic clusters.

Differences in the metallicity, Z , of the population also do not lead to observable variations of the IMF for massive stars (Massey 2003, Fig. 1). The mass of the most massive star, $m_{\max*} \approx 150 M_{\odot}$, is independent of Z . Thus the distribution of masses for massive stars does not appear to be affected by the metallicity of the star-forming gas and therefore radiation pressure on dust grains during star-assembly cannot be a physical mechanism establishing $m_{\max*}$ (§ 3.).

However, there may be an effect for VLMSs. Present-day star-forming clouds typically have somewhat higher metal-abundances ($[\text{Fe}/\text{H}] \approx +0.2$) compared to 5 Gyr ago ($[\text{Fe}/\text{H}] \approx -0.3$) (Binney & Merrifield 1998) which is the mean age of the population defining the standard IMF. The data in the empirical alpha-plot indicate that some of the younger clusters may have a single-star MF that is somewhat steeper (larger α_1) than the standard IMF if unresolved binary-stars are corrected for (Fig. 20). This may mean that clouds with a larger $[\text{Fe}/\text{H}]$ produce relatively more low-mass stars (Kroupa 2001b) which is tentatively supported by the typically but not significantly flatter MFs in globular clusters (Piotto & Zoccali 1999) that have $[\text{Fe}/\text{H}] \approx -1.5$, and the recent

finding that the old and metal-poor ($[\text{Fe}/\text{H}] = -0.6$) thick-disk population also has a flatter MF below $0.3 M_{\odot}$ with $\alpha_1 \approx 0.5$ (Reylé & Robin 2001). If such a systematic effect is present, then for $m \lesssim 0.7 M_{\odot}$ and to first order,

$$\alpha \approx 1.3 + \Delta\alpha [\text{Fe}/\text{H}], \quad (22)$$

with $\Delta\alpha \approx 0.5$, being similar to the adopted uncertainty on α . Theoretical considerations do suggest that for sufficiently small metallicity a gas cloud cannot cool efficiently causing the Jeans mass required for gravitational collapse to be larger. In particular, the first stars ought to have large masses owing to this effect and the generally higher ambient temperatures at early cosmological epochs (Larson 1998; Bromm et al. 2001). Finding the remnants of these poses a major challenge.

An easier target is measuring the IMF for low-mass and VLMSs in metal-poor environments, such as young star-clusters in the Small Magellanic Cloud. That metallicity does play a role is becoming increasingly evident in the planetary-mass regime in that the detected exo-planets occur mostly around stars that are more metal-rich than the Sun (Vogt et al. 2002; Zucker & Mazeh 2001).

While the Jeans-mass argument (eq. 14) should be useful as a general indication of the rough mass scale where fragmentation of a contracting gas cloud occurs, the concept clearly breaks down when considering the stellar masses that form in star clusters. The central regions of these are denser, formally leading to smaller Jeans masses which is the opposite of the observed trend, where even in very young clusters massive stars tend to be located in the inner regions. More complex physics is clearly involved. Stars may, to a certain extent, regulate their own mass by outflows (Adams & Laughlin 1996), and the coagulation of proto-stars probably plays a significant role in the densest regions where the cloud-core collapse time, τ_{coll} , is longer than the fragment collision time-scale, τ_{cr} . The collapse of a fragment to a proto-star takes no longer than $\tau_{\text{coll}} \approx 0.1$ Myr (Wuchterl & Klessen 2001), so that

$$t_{\text{cr}}/\text{Myr} \approx 42 \left(\frac{(R/\text{pc})^3}{(M_{\text{ecl}}/M_{\odot})} \right)^{\frac{1}{2}} < 0.1 \text{ Myr}, \quad (23)$$

where R is the half-mass radius of a Plummer-sphere model, implies $M/R^3 > 10^5 M_{\odot}/\text{pc}^{-3}$. Such densities, where proto-stellar interactions are expected to affect the emerging stellar mass-spectrum, are found in the centres of very dense and rich embedded star clusters such as the ONC before they expand as a result of gas expulsion (Kroupa et al. 2001; Vine & Bonnell 2003). Thus, only for massive stars is the form of the IMF probably affected by coagulation, which may explain why massive stars are usually centrally concentrated in very young clusters (Bonnell et al. 1998; Klessen 2001). However, the observed mass segregation in very young clusters cannot as yet be taken as conclusive evidence for primordial mass segregation and coagulation, unless precise N -body computations of the embedded cluster are performed for each case in question. For example, models of the ONC show that the degree of observed mass segregation can be established dynamically within about 2 Myr (Fig. 17) despite the embedded and much denser configuration having no initial mass segregation. The notion behind such an assumption is that star clusters fragment heavily sub-clustered (Megeath et al. 1996; Bontemps et al. 2001; Klessen 2001), and each

sub-cluster may form a few OB stars with a few hundred associated lower-mass stars (Table 2), so that the overall morphology may resemble a system without significant initial mass segregation. The theoretical time-scale, $t_2 - t_1$ in Fig. 17, for mass segregation to be established can be shortened by decreasing the relaxation time. This can be achieved by reducing the number of stars in the model, for example. But it may prove impossible to find agreement at the same time with the density profile and kinematics because the ONC is probably expanding rapidly now. Clearly this issue requires more study.

The origin of most stellar masses is indicated by a remarkable discovery for the low-mass ρ Oph cluster in which star-formation is on-going. Here the pre-stellar and proto-star MF are indistinguishable and both are startlingly similar to the standard IMF, even in showing the same flattening of the power-law at $0.55 M_\odot$ (Motte et al. 1998; Bontemps et al. 2001). The pre-stellar cores have sizes and densities that are in agreement with the Jeans-instability argument for the conditions in the ρ Oph cloud, so that cloud-fragmentation due to the collapse of density fluctuations in a dissipating turbulent interstellar medium (Nordlund & Padoan 2003; Padoan & Nordlund 2002; Mac Low & Klessen 2004; Tilley & Pudritz 2004; Padoan & Nordlund 2004) appears to be the most-important mechanism shaping the stellar IMF for masses $0.5 \lesssim m/M_\odot \lesssim$ a few M_\odot , the shape of the IMF being determined by the spectrum of density fluctuations in the molecular cloud. Similar results have been obtained for the Serpens clouds and for the clouds in Taurus–Auriga (Testi & Sargent 1998; Onishi et al. 2002, respectively). The majority of stellar masses making up the standard IMF thus do not appear to suffer significant subsequent modifications such as competitive accretion (Bonnell et al. 2001), proto-stellar mergers or even self-limitation through feedback processes. The work of Padoan & Nordlund (2002) demonstrates that, under certain reasonable assumptions, the mass function of gravitationally unstable cloud cores deriving from the power-spectrum of a super-sonic turbulent medium leads to the observed standard IMF above $1 M_\odot$. The flattening at lower masses is a result of a reduction of the star-formation efficiency because at small masses only the densest cores can survive sufficiently long to collapse.

The intriguing result from ρ Oph, Serpens and Taurus–Auriga, in which the stellar, proto-stellar and pre-stellar clump mass spectra are similar to the stellar IMF (eq. 20), is consistent with the independent finding that the properties of binary systems in the Galactic field can be understood if most stars formed in modest, ρ Oph-type clusters with primordial binary properties as observed in Taurus–Auriga (Kroupa 1995b), and with the independent result derived from an analysis of the distribution of local star clusters that most stars appear to stem from such modest clusters (Adams & Myers 2001). However, the standard IMF is also similar to the IMF in the ONC (Fig. 16) implying that fragmentation of the pre-cluster cloud proceeded similarly.

The impressive computations by Bonnell & Bate (2002) and collaborators of dense clusters indeed not only predict the observed $m_{\max}(M_{\text{ecl}})$ relation (Fig. 5), but they also show that a Salpeter/Massey power-law IMF is obtained as a result of competitive accretion and the merging of stars near the cluster core driven by accretion onto it. The reason as to why the IMF is so invariant above a few M_\odot

may thus be that the various physical processes all conspire to give the same overall scale-free result.

This still leaves the origin and nature of VLMSs and BDs unclear. As the discussion in § 5. suggests, VLMSs and BDs probably need to be considered a different or extra population which does not mix well, in terms of pairing, with stars. Maxted & Jeffries (2005) demonstrate that virtually *all* currently available theoretical work on the formation of BDs is excluded by the data. Together with the realisation that existing star-formation theory fails to reproduce the binary properties of young stars (Goodwin et al. 2004; Goodwin & Kroupa 2005), this suggests that our theories lack major ingredients that probably are related to stellar feedback processes. That VLMS and BD binaries have a significantly higher energy scale than stellar binaries does, however, suggest that their formation may be linked to a dense environment which they probably leave abruptly.

8. Composite stellar population

We have thus seen that while a conclusive theoretical formulation of the IMF is still wanting, we do have some good ideas about its origin and a good impression of its shape, and empirically there is not a strong case for systematic variation of the IMF with physical conditions. It is thus reasonable to assume that the stellar IMF is invariant.

The natural assumption has often been made that independent of the star-formation mode, the stellar distribution is sampled randomly from the invariant IMF (e.g. Elmegreen 2004). Thus, for example, 10^5 clusters, each with 20 stars, would have the same composite (i.e. combined) IMF as one cluster with 2×10^6 stars.

However, the existence of the $m_{\max}(M_{\text{ecl}})$ relation (§ 3.1.) has profound consequences for *composite populations*. It immediately implies, for example, that 10^5 clusters, each with 20 stars, *cannot* have the same composite (i.e. combined) IMF as one cluster with 2×10^6 stars, because the small clusters can never make stars more massive than about $1.5 M_{\odot}$ (Fig. 5). Thus, galaxies, that are composite stellar populations consisting of many star clusters, most of which may be dissolved, would have steeper composite, or integrated galactic IMFs (IGIMFs), than the stellar IMF in each individual cluster (Vanbeveren 1982; Kroupa & Weidner 2003).

The IGIMF is an integral over all star-formation events in a given star-formation “epoch” $t, t + \delta t$,

$$\xi_{\text{IGIMF}}(m; t) = \int_{M_{\text{ecl},\min}}^{M_{\text{ecl},\max}(SFR(t))} \xi(m \leq m_{\max}(M_{\text{ecl}})) \xi_{\text{ecl}}(M_{\text{ecl}}) dM_{\text{ecl}}. \quad (24)$$

Here $\xi(m \leq m_{\max}) \xi_{\text{ecl}}(M_{\text{ecl}}) dM_{\text{ecl}}$ is the stellar IMF contributed by $\xi_{\text{ecl}} dM_{\text{ecl}} \propto M_{\text{ecl}}^{-\beta} dM_{\text{ecl}}$ clusters with mass near M_{ecl} . $M_{\text{ecl},\max}$ follows from the maximum star-cluster-mass *vs* global-star-formation-rate-of-the-galaxy relation,

$$M_{\text{ecl},\max} = \text{fn}(SFR) \quad (25)$$

(eq. 1 in Weidner & Kroupa 2005, as derived by Weidner et al. 2004). $M_{\text{ecl},\text{min}} = 5 M_{\odot}$ is adopted in the standard modelling and corresponds to the smallest star-cluster units observed. At time t the SFR is

$$SFR(t) = \frac{M_{\text{tot}}}{\delta t}, \quad (26)$$

where

$$M_{\text{tot}} = \int_{M_{\text{ecl},\text{min}}}^{M_{\text{ecl},\text{max}}} M_{\text{ecl}} \xi_{\text{ecl}}(M_{\text{ecl}}) dM_{\text{ecl}} \quad (27)$$

is the total stellar mass assembled in time δt which Weidner et al. (2004) define to be a “star-formation epoch”, within which the ECMF is sampled to completion. This formulation leads naturally to the observed $M_{\text{ecl},\text{max}}(SFR)$ correlation if the ECMF is invariant, $\beta \approx 2.35$ and if the “epoch” lasts about $\delta t = 10$ Myr. Thus, the embedded cluster mass function is fully sampled in 10 Myr intervals, independent of the SFR. This time-scale compares very well indeed to the star-formation time-scale in normal galactic disks measured by Egusa et al. (2004) using an entirely independent method, namely from the offset of HII regions from the molecular clouds in spiral-wave patterns. The time-integrated IGIMF then follows from

$$\xi_{\text{IGIMF}}(m) = \int_0^{\tau_{\text{G}}} \xi_{\text{IGIMF}}(m; t) dt, \quad (28)$$

where τ_{G} is the age of the galaxy under scrutiny.

Note that $\xi_{\text{IGIMF}}(m)$ is the mass function of all stars ever to have formed in a galaxy, and can be used to estimate the total number of supernovae ever to have occurred, for example. $\xi_{\text{IGIMF}}(m; t)$, on the other hand, includes the time-dependence through a dependency on $SFR(t)$ of a galaxy and allows one to compute the time-dependent evolution of a stellar population over the life-time of a galaxy.

Because more-massive stellar clusters are observed to form for higher SFRs (eq. 25), the ECMF is sampled to larger masses in galaxies that are experiencing high SFRs, leading to IGIMFs that are flatter than for low-mass galaxies that have had only a low-level of star-formation activity. Weidner & Kroupa (2005) show that the sensitivity of the IGIMF power-law index for $m \gtrsim 1 M_{\odot}$ towards SFR variations increases with decreasing SFR .

Thus, galaxies with a small mass in stars can either form with a very low continuous SFR (appearing today as low-surface-brightness but gas-rich galaxies) or with a brief initial SF burst (dE or dSph galaxies). The IGIMF ought to vary significantly among such galaxies (Fig. 22). In all cases, however, the IGIMFs are invariant for $m \lesssim 1.3 M_{\odot}$ which is the maximal stellar mass in $5 M_{\odot}$ “clusters” (Fig. 5). Low-surface-brightness galaxies would therefore appear chemically young, while the dispersion in chemical properties ought to be larger for dwarf galaxies than for larger galaxies (Goodwin & Pagel 2005; Weidner & Kroupa 2005; Köppen et al. 2007). Another interesting implication is that the number of supernovae per star would be significantly smaller over cosmological times than predicted by an invariant Salpeter IMF (Goodwin & Pagel 2005, Fig. 23).

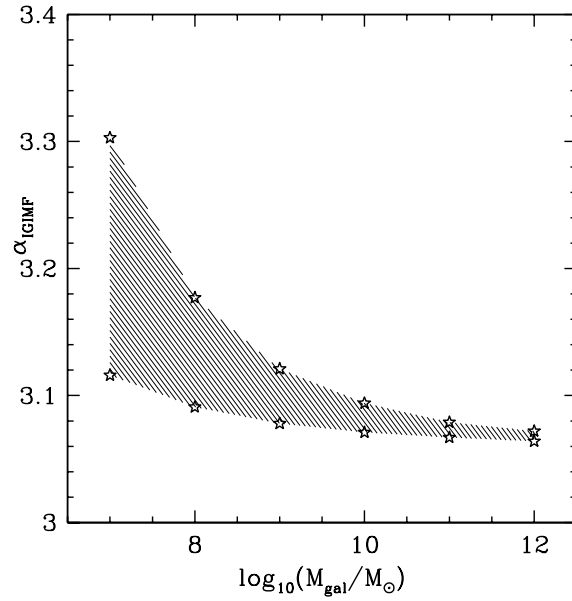


Figure 22. The power-law index α_{IGIMF} of the IGIMF above $1.3 M_{\odot}$ as a function of the stellar mass of a galaxy, which determines the average SFR over a Hubble time. The lower bound is for an initial SF burst that forms the entire stellar galaxy, while the upper bound is for a constant SFR over a Hubble time. In all cases the input stellar IMF is the standard form (eq. 20). Note that the detailed results depend on the adopted form of the ECMF (cf. Fig. 23). For further details see Weidner & Kroupa (2005).

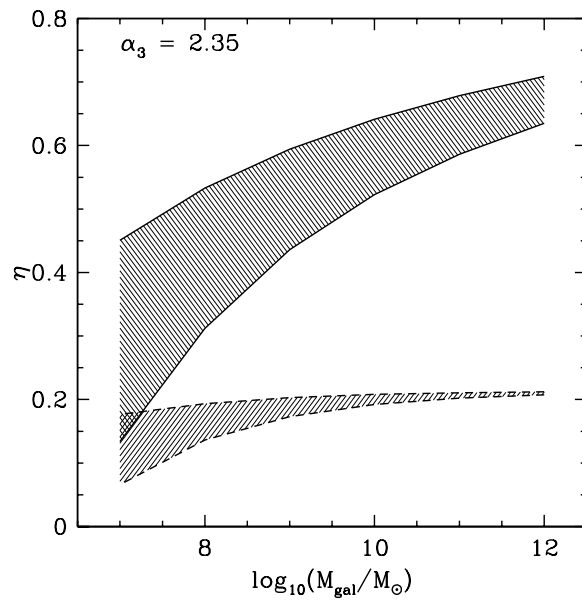


Figure 23. The number of supernovae per star in the IGIMF divided by the number of supernovae per star in the standard IMF, η , as a function of the stellar galaxy mass. The upper shaded area is for an ECMF with $\beta = 2$, while the lower shaded area assumes $\beta = 2.35$. The upper bound for each shaded region is for an initial SF burst model, while the lower bounds are for a constant SFR over a Hubble time. For further details see Weidner & Kroupa (2005).

These new insights should lead to a revision of theoretical work on galaxy formation that typically until now relied on an invariant IMF. Empirical evidence in favour of or against the notion of a galaxy-variable IGIMF is being studied and will ultimately lead to a refinement of the ideas.

9. Concluding comments

Spectacular advances have been achieved over the past decade in the field of IMF research and this affects a vast area of astrophysics.

The stellar IMF appears to be extra-ordinarily universal. It is described by eq. 20. The evidence for top-heavy IMFs comes from either unresolved clusters or clusters that are very difficult to observe. The most significant uncertainty that remains at high masses despite the presence of exquisite data is the exact shape of the IMF for massive stars, because the biases due to unresolved multiple systems and due to stellar rotation have not been studied in sufficient detail. The true IMF may be closer to the Scalo value $\alpha_3 \approx 2.7$ rather than being Salpeter/Massey. For sub-stellar masses more data are necessary to improve constraints on α_0 and to better quantify any claims for a variation of the IMF. Further problems are inadequate stellar models for stars younger than a few Myr, and the under-representation of stellar-dynamical modelling which, however, is an absolute necessity in the search for IMF variations among clusters.

Among intriguing recent results are that the BDs appear to be a distinct population from that of low-mass stars; their pairing properties have a different energy scale. This sets the stage for a probable discontinuity in the IMF near the stellar/sub-stellar boundary which has already probably been detected. This then questions the validity of fitting continuous log-normal functions across the VLMS/BD barrier. Furthermore, the IMF does appear to have a physical maximum stellar mass that has now been found empirically. Stars with $m \gtrsim 150 M_\odot$ do not appear to exist, unless they implode invisibly shortly after being formed. In addition, by realising that star clusters are the true fundamental building blocks of a galaxy, we merely need to add up all clusters and their (invariant) IMFs to arrive at the integrated galactic initial mass function. The IGIMF varies according to the star-formation history of the galaxy. This formulation now allows us to compute the IGIMF, as a function of time, for galaxies that are converting their gas supply only slowly to stars, or for galaxies that like to eat it up all at once. The implications are that equally-old galaxies can have very different chemical compositions ranging from young to evolved, and that the cosmological supernova II rate may be significantly smaller and dependent on galaxy type than if an invariant Salpeter IMF is assumed. Galaxy-formation and evolution computations with this latter assumption are not likely to be correct.

Thus, the IMF research as presented here has advanced onto cosmological issues, whereby many details still need to be worked out. But the most intimately connected research field, namely star formation, is being tested rather dramatically. The brilliant computational results that have been becoming available have led to a beautiful agreement with the observed maximum-stellar-mass *vs* cluster-mass correlation and reproduce the general shape of the IMF. However, different ideas (competitive accretion, coagulation and simply the distribution of gravitationally unstable regions in turbulent clouds) all lead to virtually the

same type of theoretical IMF. Detailed computations of the formation of stars actually get it all wrong - the primordial-binary properties cannot yet be described, and the failure of modern theory is especially evident in the BD regime, where virtually all current ideas are being excluded by the data. The failures of modern theory are not surprising though, because the primary process driving star-formation is injection of feedback energy, the consistent inclusion of which goes beyond currently available computational resources. On the bright side, the convergence of different mechanisms to the same Salpeter/Massey IMF may be interpreted to simply mean that the shape of the IMF for $m \gtrsim 0.5 M_{\odot}$ is indeed invariant to the physics, as is observed.

Acknowledgments. I would like to thank the organisers for this splendid meeting, Carsten Weidner, Christopher Tout and Gerry Gilmore for very stimulating and important contributions, and Ingo Thies and Jörg Dabringhausen for help with some of the material. I am especially indebted to Sverre Aarseth whose immense tutoring allowed me to do the numerical dynamics work. I would also like to thank M.R.S. Hawkins who had introduced me to this field in about 1987 whilst I visited the Siding-Spring Observatory as a summer vacation scholar at the ANU. Mike gave me a delightful lecture on the low-mass LF one night when I visited his observing run to learn about modern, state-of-the-art Schmidt-telescope surveying *before* I embarked on post-graduate work. This research was much later supported through DFG grants KR1635/2, KR1635/3 and a Heisenberg fellowship, KR1635/4, and currently KR1635/13.

	α mass range [M_{\odot}]	α mass range [M_{\odot}]	α mass range [M_{\odot}]
Orion Nebula cluster, ONC			
Muench et al. (2000)	-0.35	+1.25	+2.35
<i>magenta small open circles with central dot</i>	0.02 – 0.08	0.08 – 0.80	0.80 – 63.1
<i>magenta large open circles with central dot</i>	+0.00	+1.00	+2.00
	0.02 – 0.08	0.08 – 0.40	0.4 – 63.10
Hillenbrand & Carpenter (2000) (HC00)	+0.43		
<i>magenta large thick open circle</i>	0.02 – 0.15		
<i>with central dot</i>			
Luhman et al. (2000)	+0.70		
<i>magenta small thick open circle</i>	0.035 – 0.56		
<i>with central dot</i>			
Pleiades			
Moraux et al. (2001)	+0.51 ± 0.15		
<i>green circles with central dot</i>	0.04 – 0.30		
Hambly et al. (1999), from Barrado y Navascués et al. (2001)	+0.56	+2.67	
<i>green circles with central dot</i>	0.065 – 0.60	0.6 – 10.0	
σ Ori			
Béjar et al. (2001)	0.8 ± 0.4		
<i>green solid circle</i>	0.013 – 0.20		
M35			
Barrado y Navascués et al. (2001)	-0.88 ± 0.12	0.81 ± 0.02	2.59 ± 0.04
<i>green solid circle¹</i>	0.08 – 0.2	0.2 – 0.8	0.8 – 6.0
IC 348			
Najita et al. (2000) for MLR from Baraffe et al. (1998)	+0.5		
<i>green solid circle</i>	0.015 – 0.22		
NGC 2264			
Park et al. (2000)			+2.7
<i>green solid circle</i>			2.0 – 6.3
5 LMC regions			
Parker et al. (2001)			+2.3 ± 0.2
<i>blue solid triangle</i>			5 – 60
NGC 1818 in LMC			
Santiago et al. (2001), outer region		+2.5	
<i>blue solid triangle</i>		0.9 – 3	
NGC 1805 in LMC			
Santiago et al. (2001), outer region		+3.4	
<i>blue solid triangle</i>		0.9 – 3	

Table 1. *continued*

	α mass range [M_{\odot}]	α mass range [M_{\odot}]	α mass range [M_{\odot}]
30 Dor* in LMC			
Selman et al. (1999), $r > 3.6$ pc <i>cyan small open triangle</i>			$+2.37 \pm 0.08$ 3 – 120
Selman et al. (1999), $1.1 < r/\text{pc} < 4.5$ <i>cyan small open triangle</i>			$+2.17 \pm 0.05$ 2.8 – 120
Sirianni et al. (2000) <i>cyan large open triangle</i> ²		$+1.27 \pm 0.08$ 1.35 – 2.1	$+2.28 \pm 0.05$ 2.1 – 6.5
Arches cluster*			
Figer et al. (1999), all radii <i>cyan large solid circle</i>			$+1.6 \pm 0.1$ 6.3 – 125
NGC 3603*			
Eisenhauer et al. (1998) <i>cyan small solid circle</i>		+1.73 1 – 30	+2.7 15 – 70
Globular clusters			
Piotto & Zoccali (1999) <i>yellow open triangles</i>	$+0.88 \pm 0.35$ 0.1 – 0.6	+2.3 0.6 – 0.8	
Galactic bulge			
Holtzman et al. (1998) <i>magenta filled square</i>	+0.9 0.3 – 0.7	+2.2 0.7 – 1.0	
Zoccali et al. (2000) <i>magenta filled square</i>	$+1.43 \pm 0.13$ 0.15 – 0.5	$+2.0 \pm 0.23$ 0.5 – 1.0	
Solar Neighbourhood (<i>magenta dotted lines</i>)			
Reid et al. (1999)	$+1.5 \pm 0.5$ 0.02 – 0.08		
Herbst et al. (1999)	$\leq +0.8$ 0.02 – 0.08		
Chabrier (2001, 2002)	$\leq +1$ 0.01 – 0.08	+1 / 0.10 – 0.35	+2 / 0.35 – 1.0

Table 1. $\alpha(<lm>)$ data obtained since 1998 and until 2002. The data are shown in Fig. 20 in addition to the previously available data set compiled by Scalo (1998). Each α value is obtained at $\langle lm \rangle = (lm_2 - lm_1)/2$, $lm \equiv \log_{10} m$, by the respective authors by fitting a power-law MF over the logarithmic mass range given by m_1 and m_2 listed above. Some authors do not quote uncertainties on their α values. Notes: * are star-burst clusters; ¹ thin green open circle emphasises the low-mass M35 datum which may be incomplete; ² the mass range $1.35 < m/M_{\odot} < 2.1$ may be incomplete and is emphasised by the cross through the cyan large open triangle.

mass range [M_\odot]	η_N [per cent]			η_M [per cent]			ρ^{st} [M_\odot/pc^3]	Σ^{st} [M_\odot/pc^2]
	α_3			α_3			α_3	α_3
	2.3	2.7	4.5	2.3	2.7	4.5	4.5	4.5
0.01–0.08	37.15	37.69	38.63	4.08	5.39	7.39	3.21×10^{-3}	1.60
0.08–0.5	47.81	48.50	49.71	26.61	35.16	48.21	2.09×10^{-2}	10.45
0.5–1	8.94	9.07	9.30	16.13	21.31	29.22	1.27×10^{-2}	6.35
1 – 8	5.70	4.60	2.36	32.38	30.30	15.09	6.54×10^{-3}	1.18
8 – 120	0.40	0.14	0.00	20.80	7.83	0.08	3.63×10^{-5}	6.53×10^{-3}
$\bar{m}/M_\odot =$	0.380	0.292	0.218				$\rho_{\text{tot}}^{\text{st}} = 0.043$	$\Sigma_{\text{tot}}^{\text{st}} = 19.6$
	m_{max} [M_\odot]	$\alpha_3 = 2.3$ N_{cl} M_{cl} [M_\odot]		$\alpha_3 = 2.7$ N_{cl} M_{cl} [M_\odot]		m_{to} [M_\odot]	$\Delta M_{\text{cl}}/M_{\text{cl}}$ [per cent]	
		$\alpha_3 = 2.3$		$\alpha_3 = 2.7$			$\alpha_3 = 2.3$	$\alpha_3 = 2.7$
	1	16	2.9	21	3.8	80	3.2	0.7
	8	245	74	725	195	60	4.9	1.1
	20	806	269	3442	967	40	7.5	1.8
	40	1984	703	1.1×10^4	2302	20	13	4.7
	60	3361	1225	2.2×10^4	6428	8	22	8.0
	80	4885	1812	3.6×10^4	1.1×10^4	3	32	15
	100	6528	2451	5.3×10^4	1.5×10^4	1	44	29
	120	8274	3136	7.2×10^4	2.1×10^4	0.7	47	33

Table 2. The number fraction $\eta_N = 100 \int_{m_1}^{m_2} \xi(m) dm / \int_{m_1}^{m_u} \xi(m) dm$, and the mass fraction $\eta_M = 100 \int_{m_1}^{m_2} m \xi(m) dm / M_{\text{cl}}$, $M_{\text{cl}} = \int_{m_1}^{m_u} m \xi(m) dm$, in per cent of BDs or main-sequence stars in the mass interval m_1 to m_2 , and the stellar contribution, ρ^{st} , to the Oort limit and to the Galactic-disk surface mass-density, $\Sigma^{\text{st}} = 2h\rho^{\text{st}}$, near to the Sun, taking $m_l = 0.01 M_\odot$, $m_u = 120 M_\odot$ and the Galactic-disk scale-height $h = 250$ pc ($m < 1 M_\odot$ Kroupa et al. 1993) and $h = 90$ pc ($m > 1 M_\odot$, Scalo 1986). Results are shown for the standard IMF (eq. 20), for the high-mass-star IMF approximately corrected for unresolved companions ($\alpha_3 = 2.7, m > 1 M_\odot$), and for the PDMF ($\alpha_3 = 4.5$, Scalo 1986; Kroupa et al. 1993) which describes the distribution of stellar masses now populating the Galactic disk. For gas $\Sigma^{\text{gas}} = 13 \pm 3 M_\odot/\text{pc}^2$ and remnants $\Sigma^{\text{rem}} \approx 3 M_\odot/\text{pc}^2$ (Weidemann 1990). The average stellar mass is $\bar{m} = \int_{m_l}^{m_u} m \xi(m) dm / \int_{m_l}^{m_u} \xi(m) dm$. N_{cl} is the number of stars that have to form in a star cluster such that the most massive star in the population has the mass m_{max} . The mass of this population is M_{cl} , and the condition is $\int_{m_{\text{max}}}^{\infty} \xi(m) dm = 1$ with $\int_{0.01}^{m_{\text{max}}} \xi(m) dm = N_{\text{cl}} - 1$. $\Delta M_{\text{cl}}/M_{\text{cl}}$ is the fraction of mass lost from the cluster due to stellar evolution, assuming that for $m \geq 8 M_\odot$ all neutron stars and black holes are kicked out due to an asymmetrical supernova explosion, but that white dwarfs are retained (Weidemann et al. 1992) and have masses $m_{\text{WD}} = 0.084 m_{\text{ini}} + 0.444 [M_\odot]$. This is a linear fit to the data in (Weidemann 2000, their table 3) for progenitor masses $1 \leq m/M_\odot \leq 7$ and $m_{\text{WD}} = 0.5 M_\odot$ for $0.7 \leq m/M_\odot < 1$. The evolution time for a star of mass m_{to} to reach the turn-off age is available in Fig. 20.

general	$dN = \xi(m) dm = \xi_L(m) dlm$ $\xi_L(m) = (m \ln 10) \xi(m)$ $\Gamma(m) \equiv \frac{d}{dlm} (\log_{10} \xi_L(lm))$ $\Gamma = -x = 1 + \gamma = 1 - \alpha$ e.g. for power-law form:	$\xi_L = A m^\Gamma = A m^{-x}$ $\xi = A' m^\alpha = A' m^{-\gamma}$ $A' = A/\ln 10$	<i>gen</i> <i>Gam</i> <i>ind</i>
Salpeter (1955)	$\xi_L(lm) = A m^\Gamma$ $A = 0.03 \text{ pc}^{-3} \log_{10}^{-1} M_\odot$; $0.4 \leq m/M_\odot \leq 10$	$\Gamma = -1.35$ ($\alpha = 2.35$)	<i>S</i>
Miller & Scalo (1979) <i>thick long-dash-dotted line</i>	$\xi_L(lm) = A \exp \left[-\frac{(lm-lm_o)^2}{2\sigma_{lm}^2} \right]$ $A = 106 \text{ pc}^{-2} \log_{10}^{-1} M_\odot$; $lm_o = -1.02$; $\sigma_{lm} = 0.68$	$\Gamma(lm) = -\frac{(lm-lm_o)}{\sigma_{lm}^2} \log_{10} e$	<i>MS</i>
Larson (1998) <i>thin short-dashed line</i>	$\xi_L(lm) = A m^{-1.35} \exp \left[-\frac{m_o}{m} \right]$ $A = -$; $m_o = 0.3 M_\odot$	$\Gamma(lm) = -1.35 + \frac{m_o}{m}$	<i>La</i>
Larson (1998) <i>thin long-dashed line</i>	$\xi_L(lm) = A \left[1 + \frac{m}{m_o} \right]^{-1.35}$ $A = -$; $m_o = 1 M_\odot$	$\Gamma(lm) = -1.35 \left(1 + \frac{m_o}{m} \right)^{-1}$	<i>Lb</i>
Chabrier (2001, 2002) <i>thick short-dash-dotted line</i>	$\xi(m) = A m^{-\delta} \exp \left[-\left(\frac{m_o}{m} \right)^\beta \right]$ $A = 3.0 \text{ pc}^{-3} M_\odot^{-1}$; $m_o = 716.4 M_\odot$; $\delta = 3.3$; $\beta = 0.25$	$\Gamma(lm) = 1 - \delta + \beta \left(\frac{m_o}{m} \right)^\beta$	<i>Ch</i>
Hollenbach et al. (2005) <i>not plotted in Fig. 20</i>	$\xi_L(m) = k m^{-\Gamma} (1 - \exp[-(m/m_{\text{ch}})^{\gamma+1}])$ $\gamma = 0.4, \Gamma = 1.35, m_{\text{ch}} = 0.18 M_\odot$		<i>Holl</i>

Table 3. Summary of different proposed analytical IMF forms (the modern power-law form, the standard IMF, is presented in eq. 20). Notation: $lm \equiv \log_{10}(m/M_\odot) = \ln(m/M_\odot)/\ln 10$; dN is the number of single stars in the mass interval m to $m + dm$ and in the logarithmic-mass interval lm to $lm + dlm$. The mass-dependent IMF indices, $\Gamma(m)$ (eq. *Gam*), are plotted in Fig. 20 using the line-types defined here. Eq. *MS* was derived by Miller&Scalo assuming a constant star-formation rate and a Galactic disk age of 12 Gyr (the uncertainty of which is indicated in the lower panel of Fig. 20a). Larson (1998) does not fit his forms (eqs. *La* and *Lb*) to solar-neighbourhood star-count data but rather uses these to discuss general aspects of likely systematic IMF evolution; the m_o in eq. *La* and *Lb* given here are approximate eye-ball fits to the standard IMF.

References

- Aarseth S. J., 1999, *PASP*, 111, 1333
- Adams F. C., Fatuzzo M., 1996, *ApJ*, 464, 256
- Adams F. C., Laughlin G., 1996, *ApJ*, 468, 586
- Adams F. C., Myers P. C., 2001, *ApJ*, 553, 744
- Allen P. R., Koerner D. W., Reid I. N., Trilling D. E., 2005, *ApJ*, 625, 385
- Andersen J., 1991, *A&A Rev.*, 3, 91
- Béjar V. J. S., Martín E. L., Zapatero Osorio M. R., Rebolo R., Barrado y Navascués D., Bailer-Jones C. A. L., Mundt R., Baraffe I., Chabrier C., Allard F., 2001, *ApJ*, 556, 830
- Baes M., Stamatellos D., Davies J. I., Whitworth A. P., Sabatini S., Roberts S., Linder S. M., Evans R., 2005, *New Astronomy*, 10, 523
- Bahcall J. N., 1984, *ApJ*, 287, 926
- Baraffe I., Chabrier G., Allard F., Hauschildt P. H., 1998, *A&A*, 337, 403
- Barrado y Navascués D., Stauffer J. R., Bouvier J., Martín E. L., 2001, *ApJ*, 546, 1006
- Barrado y Navascués D., Stauffer J. R., Jayawardhana R., 2004, *ApJ*, 614, 386
- Basri G., 2000, *ARA&A*, 38, 485
- Baumgardt H., Makino J., 2003, *MNRAS*, 340, 227
- Beech M., Mitalas R., 1994, *ApJS*, 95, 517
- Belikov A. N., Hirte S., Meusinger H., Piskunov A. E., Schilbach E., 1998, *A&A*, 332, 575
- Beuzit J.-L., Ségransan D., Forveille T., Udry S., Delfosse X., Mayor M., Perrier C., Hainaut M.-C., Roddier C., Roddier F., Martín E. L., 2004, *A&A*, 425, 997
- Binney J., Dehnen W., Bertelli G., 2000, *MNRAS*, 318, 658
- Binney J., Merrifield M., 1998, *Galactic astronomy. Galactic astronomy / James Binney and Michael Merrifield.* Princeton, NJ : Princeton University Press, 1998. (Princeton series in astrophysics) QB857 .B522 1998 (\$35.00)
- Boily C. M., Lançon A., Deiters S., Heggie D. C., 2005, *ApJ*, 620, L27
- Bonnell I. A., Bate M. R., 2002, *MNRAS*, 336, 659
- Bonnell I. A., Bate M. R., Vine S. G., 2003, *MNRAS*, 343, 413
- Bonnell I. A., Bate M. R., Zinnecker H., 1998, *MNRAS*, 298, 93
- Bonnell I. A., Clarke C. J., Bate M. R., Pringle J. E., 2001, *MNRAS*, 324, 573
- Bonnell I. A., Vine S. G., Bate M. R., 2004, *MNRAS*, 349, 735
- Bontemps S., André P., Kaas A. A. e. a., 2001, *A&A*, 372, 173
- Bosch G., Selman F., Melnick J., Terlevich R., 2001, *A&A*, 380, 137
- Boss A. R., 1986, *ApJS*, 62, 519
- Bouy H., Brandner W., Martín E. L., Delfosse X., Allard F., Basri G., 2003, *AJ*, 126, 1526
- Briceño C., Luhman K. L., Hartmann L., Stauffer J. R., Kirkpatrick J. D., 2002, *ApJ*, 580, 317
- Brocato E., Cassisi S., Castellani V., 1998, *MNRAS*, 295, 711
- Bromm V., Ferrara A., Coppi P. S., Larson R. B., 2001, *MNRAS*, 328, 969
- Casassus S., Bronfman L., May J., Nyman L.-Å., 2000, *A&A*, 358, 514
- Chabrier G., 2001, *ApJ*, 554, 1274
- Chabrier G., 2002, *ApJ*, 567, 304
- Chabrier G., 2003a, *PASP*, 115, 763
- Chabrier G., 2003b, *ApJ*, 586, L133
- Chabrier G., Baraffe I., 1997, *A&A*, 327, 1039
- Chabrier G., Baraffe I., 2000, *ARA&A*, 38, 337
- Chini R., Hoffmeister V., Kimeswenger S., Nielbock M., Nürnberger D., Schmidtobreick L., Sterzik M., 2004, *Nature*, 429, 155
- Clarke C. J., Pringle J. E., 1992, *MNRAS*, 255, 423
- Close L. M., Siegel N., Freed M., Biller B., 2003, *ApJ*, 587, 407
- Corbelli E., Palla F., Zinnecker H., eds, 2005, *The Initial Mass Function 50 years later*

- D'Antona F., Mazzitelli I., 1996, *ApJ*, 456, 329
- de Boer K. S., Fitzpatrick E. L., Savage B. D., 1985, *MNRAS*, 217, 115
- de La Fuente Marcos R., 1997, *A&A*, 322, 764
- de La Fuente Marcos R., 1998, *A&A*, 333, L27
- de Marchi G., Paresce F., 1995a, *A&A*, 304, 202
- de Marchi G., Paresce F., 1995b, *A&A*, 304, 211
- Delfosse X., Forveille T., Beuzit J.-L., Udry S., Mayor M., Perrier C., 1999, *A&A*, 344, 897
- Delfosse X., Forveille T., Ségransan D., Beuzit J.-L., Udry S., Perrier C., Mayor M., 2000, *A&A*, 364, 217
- Duchêne G., Simon T., Eislöffel J., Bouvier J., 2001, *A&A*, 379, 147
- Duquennoy A., Mayor M., 1991, *A&A*, 248, 485
- Eddington A. S., 1926, *The Internal Constitution of the Stars. The Internal Constitution of the Stars*, Cambridge: Cambridge University Press, 1926
- Egusa F., Sofue Y., Nakanishi H., 2004, *PASJ*, 56, L45
- Eisenhauer F., 2001, in *Starburst Galaxies: Near and Far Evidence in Favour of IMF Variations*. pp 24–+
- Eisenhauer F., Quirrenbach A., Zinnecker H., Genzel R., 1998, *ApJ*, 498, 278
- Elmegreen B. G., 1983, *MNRAS*, 203, 1011
- Elmegreen B. G., 1997, *ApJ*, 486, 944
- Elmegreen B. G., 1999, *ApJ*, 515, 323
- Elmegreen B. G., 2000, *ApJ*, 539, 342
- Elmegreen B. G., 2004, *MNRAS*, 354, 367
- Esteban C., Peimbert M., Torres-Peimbert S., Escalante V., 1998, *MNRAS*, 295, 401
- Fellhauer M., Lin D. N. C., Bolte M., Aarseth S. J., Williams K. A., 2003, *ApJ*, 595, L53
- Feltzing S., Gilmore G., Wyse R. F. G., 1999, *ApJ*, 516, L17
- Ferrini F., Marchesoni F., Vulpiani A., 1983, *MNRAS*, 202, 1071
- Figer D. F., 2003, in van der Hucht K., Herrero A., Esteban C., eds, *IAU Symposium Massive stars and the creation of our Galactic Center*. pp 487–+
- Figer D. F., 2005, *Nature*, 434, 192
- Figer D. F., Kim S. S., Morris M., Serabyn E., Rich R. M., McLean I. S., 1999, *ApJ*, 525, 750
- Fischer D. A., Marcy G. W., 1992, *ApJ*, 396, 178
- Fleck R. C., 1982, *MNRAS*, 201, 551
- Flynn C., Fuchs B., 1994, *MNRAS*, 270, 471
- Fuhrmann K., 2004, *Astronomische Nachrichten*, 325, 3
- García B., Mermilliod J. C., 2001, *A&A*, 368, 122
- García-Segura G., Langer N., Mac Low M.-M., 1996, *A&A*, 316, 133
- García-Segura G., Mac Low M.-M., Langer N., 1996, *A&A*, 305, 229
- Geyer M. P., Burkert A., 2001, *MNRAS*, 323, 988
- Gilmore G., Howell D., eds, 1998, *The Stellar Initial Mass Function (38th Herstmonceux Conference)*
- Gilmore G. F., Perryman M. A., Lindegren L., Favata F., Hoeg E., Lattanzi M., Luri X., Mignard F., Roeser S., de Zeeuw P. T., 1998, in *Proc. SPIE Vol. 3350*, p. 541-550, *Astronomical Interferometry*, Robert D. Reasenberg; Ed. GAIA: origin and evolution of the Milky Way. pp 541–550
- Gizis J. E., Kirkpatrick J. D., Burgasser A., Reid I. N., Monet D. G., Liebert J., Wilson J. C., 2001, *ApJ*, 551, L163
- Goodwin S. P., 1997, *MNRAS*, 284, 785
- Goodwin S. P., Bastian N., 2006, *MNRAS*, 373, 752
- Goodwin S. P., Kroupa P., 2005, *ArXiv Astrophysics e-prints*
- Goodwin S. P., Pagel B. E. J., 2005, *MNRAS*, 359, 707
- Goodwin S. P., Whitworth A. P., Ward-Thompson D., 2004, *A&A*, 414, 633
- Gouliermis D., Brandner W., Henning T., 2005, *ApJ*, 623, 846

- Grillmair C. J., Mould J. R., Holtzman J. A. e. a., 1998, *AJ*, 115, 144
- Halbwachs J. L., Arenou F., Mayor M., Udry S., Queloz D., 2000, *A&A*, 355, 581
- Hambly N. C., Hodgkin S. T., Cossburn M. R., Jameson R. F., 1999, *MNRAS*, 303, 835
- Hambly N. C., Jameson R. F., Hawkins M. R. S., 1991, *MNRAS*, 253, 1
- Hayashi C., Nakano T., 1963, *Progress of Theor. Phys.*, 30, 460
- Haywood M., Robin A. C., Creze M., 1997, *A&A*, 320, 440
- Henry T. J., Ianna P. A., Kirkpatrick J. D., Jahreiss H., 1997, *AJ*, 114, 388
- Herbst T. M., Thompson D., Fockenbrock R., Rix H.-W., Beckwith S. V. W., 1999, *ApJ*, 526, L17
- Hillenbrand L. A., 1997, *AJ*, 113, 1733
- Hillenbrand L. A., 2004, in *The Dense Interstellar Medium in Galaxies The Mass Function of Newly Formed Stars*. pp 601–+
- Hillenbrand L. A., Carpenter J. M., 2000, *ApJ*, 540, 236
- Hollenbach D., Parravano A., McKee C. F., 2005, in Corbelli E., Palla F., Zinnecker H., eds, *ASSL Vol. 327: The Initial Mass Function 50 Years Later An effective Initial Mass Function for galactic disks*. pp 417–424
- Holtzman J. A., Watson A. M., Baum W. A., Grillmair C. J., Groth E. J., Light R. M., Lynds R., O’Neil E. J., 1998, *AJ*, 115, 1946
- Hurley J. R., Pols O. R., Aarseth S. J., Tout C. A., 2005, *MNRAS*, 363, 293
- Hurley J. R., Pols O. R., Tout C. A., 2000, *MNRAS*, 315, 543
- Ivanova N., Belczynski K., Fregeau J. M., Rasio F. A., 2005, *MNRAS*, 358, 572
- Jahreiss H., 1994, *Ap&SS*, 217, 63
- Jahreiß H., Wielen R., 1997, in *ESA SP-402: Hipparcos - Venice ’97 The impact of HIPPARCOS on the Catalogue of Nearby Stars. The stellar luminosity function and local kinematics*. pp 675–680
- Janka H.-T., 2001, *A&A*, 368, 527
- Jao W., Henry T. J., Subasavage J. P., Bean J. L., Costa E., Ianna P. A., Méndez R. A., 2003, *AJ*, 125, 332
- Jijina J., Adams F. C., 1996, *ApJ*, 462, 874
- Kahn F. D., 1974, *A&A*, 37, 149
- Kim S. S., Figer D. F., Kudritzki R. P., Najarro F., 2006, *ApJ*, 653, L113
- Kim S. S., Figer D. F., Lee H. M., Morris M., 2000, *ApJ*, 545, 301
- Klessen R. S., 2001, *ApJ*, 550, L77
- Koen C., 2006, *MNRAS*, 365, 590
- Köppen J., Weidner C., Kroupa P., 2007, *MNRAS*, pp 1479–+
- Kroupa P., 1995a, *ApJ*, 453, 350
- Kroupa P., 1995b, *MNRAS*, 277, 1491
- Kroupa P., 1995c, *MNRAS*, 277, 1522
- Kroupa P., 1995d, *MNRAS*, 277, 1507
- Kroupa P., 1995e, *ApJ*, 453, 358
- Kroupa P., 2000, *New Astronomy*, 4, 615
- Kroupa P., 2001a, in *IAU Symposium Binary Stars in Young Clusters – a Theoretical Perspective*. pp 199–+
- Kroupa P., 2001b, *MNRAS*, 322, 231
- Kroupa P., 2001c, in *ASP Conf. Ser. 228: Dynamics of Star Clusters and the Milky Way The Local Stellar Initial Mass Function*. pp 187–+
- Kroupa P., 2002, *Science*, 295, 82
- Kroupa P., 2005, in *Proceedings of the Gaia Symposium "The Three-Dimensional Universe with Gaia" (ESA SP-576)*. Held at the Observatoire de Paris-Meudon, 4-7 October 2004. Editors: C. Turon, K.S. O’Flaherty, M.A.C. Perryman *The Fundamental Building Blocks of Galaxies*. pp 629–+
- Kroupa P., Aarseth S., Hurley J., 2001, *MNRAS*, 321, 699
- Kroupa P., Bouvier J., 2003, *MNRAS*, 346, 369
- Kroupa P., Bouvier J., Duchêne G., Moraux E., 2003, *MNRAS*, 346, 354
- Kroupa P., Gilmore G., Tout C. A., 1991, *MNRAS*, 251, 293

- Kroupa P., Tout C. A., 1997, *MNRAS*, 287, 402
- Kroupa P., Tout C. A., Gilmore G., 1990, *MNRAS*, 244, 76
- Kroupa P., Tout C. A., Gilmore G., 1993, *MNRAS*, 262, 545
- Kroupa P., Weidner C., 2003, *ApJ*, 598, 1076
- Kudritzki R., Puls J., 2000, *ARA&A*, 38, 613
- Kuijken K., 1991, *ApJ*, 372, 125
- Kumar S. S., 2003, in *IAU Symposium The Bottom of the Main Sequence and Beyond: Speculations, Calculations, Observations, and Discoveries (1958–2002)*. pp 3–+
- Lada C. J., Lada E. A., 2003, *ARA&A*, 41, 57
- Lada C. J., Margulis M., Dearborn D., 1984, *ApJ*, 285, 141
- Larson R. B., 1982, *MNRAS*, 200, 159
- Larson R. B., 1998, *MNRAS*, 301, 569
- Larson R. B., 2003, in *ASP Conf. Ser. 287: Galactic Star Formation Across the Stellar Mass Spectrum The Stellar Initial Mass Function and Beyond (Invited Review)*. pp 65–80
- Low C., Lynden-Bell D., 1976, *MNRAS*, 176, 367
- Luhman K. L., 2004, *ApJ*, 617, 1216
- Luhman K. L., Briceño C., Stauffer J. R., Hartmann L., Barrado y Navascués D., Caldwell N., 2003, *ApJ*, 590, 348
- Luhman K. L., Rieke G. H., Lada C. J., Lada E. A., 1998, *ApJ*, 508, 347
- Luhman K. L., Rieke G. H., Young E. T., Cotera A. S., Chen H., Rieke M. J., Schneider G., Thompson R. I., 2000, *ApJ*, 540, 1016
- Mac Low M., Klessen R. S., 2004, *Reviews of Modern Physics*, 76, 125
- Maeder A., Behrend R., 2002, in *ASP Conf. Ser. 267: Hot Star Workshop III: The Earliest Phases of Massive Star Birth Formation and pre-MS Evolution of Massive Stars with Growing Accretion*. pp 179–+
- Maeder A., Meynet G., 2000, *ARA&A*, 38, 143
- Maíz Apellániz J., Úbeda L., Walborn N. R., Nelan E. P., 2005, *ArXiv Astrophysics e-prints: stro-ph/0506283*
- Maíz Apellániz J., Walborn N. R., Morrell N. I., Niemela V. S., Nelan E. P., 2006, *ArXiv Astrophysics e-prints*
- Malkov O., Zinnecker H., 2001, *MNRAS*, 321, 149
- Martín E. L., Barrado y Navascués D., Baraffe I., Bouy H., Dahm S., 2003, *ApJ*, 594, 525
- Massey P., 1998, in *ASP Conf. Ser. 142: The Stellar Initial Mass Function (38th Herstmonceux Conference) The Initial Mass Function of Massive Stars in the Local Group*. pp 17–+
- Massey P., 2003, *ARA&A*, 41, 15
- Massey P., Hunter D. A., 1998, *ApJ*, 493, 180
- Maxted P. F. L., Jeffries R. D., 2005, *ArXiv Astrophysics e-prints*
- Mayor M., Duquennoy A., Halbwachs J.-L., Mermilliod J.-C., 1992, in *ASP Conf. Ser. 32: IAU Colloq. 135: Complementary Approaches to Double and Multiple Star Research CORAVEL Surveys to Study Binaries of Different Masses and Ages*. pp 73–+
- Megeath S. T., Herter T., Beichman C., Gautier N., Hester J. J., Rayner J., Shupe D., 1996, *A&A*, 307, 775
- Meyer M. R., Adams F. C., Hillenbrand L. A., Carpenter J. M., Larson R. B., 2000, *Protostars and Planets IV*, pp 121–+
- Meynet G., Maeder A., 2003, *A&A*, 404, 975
- Miller G. E., Scalo J. M., 1979, *ApJS*, 41, 513
- Moraux E., Bouvier J., Stauffer J. R., 2001, *A&A*, 367, 211
- Moraux E., Kroupa P., Bouvier J., 2004, *A&A*, 426, 75
- Motte F., Andre P., Neri R., 1998, *A&A*, 336, 150
- Muench A. A., Lada E. A., Lada C. J., 2000, *ApJ*, 533, 358
- Muench A. A., Lada E. A., Lada C. J., Alves J., 2002, *ApJ*, 573, 366

- Najarro F., Figuer D. F., Hillier D. J., Kudritzki R. P., 2004, *ApJ*, 611, L105
- Najita J. R., Tiede G. P., Carr J. S., 2000, *ApJ*, 541, 977
- Nakano T., 1989, *ApJ*, 345, 464
- Nordlund Å., Padoan P., 2003, *LNP Vol. 614: Turbulence and Magnetic Fields in Astrophysics*, 614, 271
- Oey M. S., Clarke C. J., 1998, *AJ*, 115, 1543
- Oey M. S., Clarke C. J., 2005, *ApJ*, 620, L43
- Onishi T., Mizuno A., Kawamura A., Tachihara K., Fukui Y., 2002, *ApJ*, 575, 950
- Padoan P., Nordlund Å., 2002, *ApJ*, 576, 870
- Padoan P., Nordlund Å., 2004, *ApJ*, 617, 559
- Paresce F., de Marchi G., Romaniello M., 1995, *ApJ*, 440, 216
- Park B., Sung H., Bessell M. S., Kang Y. H., 2000, *AJ*, 120, 894
- Parker J. W., Zaritsky D., Stecher T. P., Harris J., Massey P., 2001, *AJ*, 121, 891
- Penny L. R., Massey P., Vukovich J., 2001, *Bulletin of the American Astronomical Society*, 33, 1310
- Pflamm-Altenburg J., Kroupa P., 2006, *MNRAS*, 373, 295
- Phan-Bao N., Martin E. L., Reyle C., Forveille T., Lim J., 2005, *ArXiv Astrophysics e-prints*
- Pinfield D. J., Dobbie P. D., Jameson R. F., Steele I. A., Jones H. R. A., Katsiyannis A. C., 2003, *MNRAS*, 342, 1241
- Piotto G., Zoccali M., 1999, *A&A*, 345, 485
- Piskunov A. E., Belikov A. N., Kharchenko N. V., Sagar R., Subramaniam A., 2004, *MNRAS*, 349, 1449
- Portegies Zwart S. F., Makino J., McMillan S. L. W., Hut P., 2002, *ApJ*, 565, 265
- Portegies Zwart S. F., McMillan S. L. W., Hut P., Makino J., 2001, *MNRAS*, 321, 199
- Preibisch T., Balega Y., Hofmann K., Weigelt G., Zinnecker H., 1999, *New Astronomy*, 4, 531
- Ramspeck M., Heber U., Moehler S., 2001, *A&A*, 378, 907
- Reid I. N., Cruz K. L., Allen P., Mungall F., Kilkenny D., Liebert J., Hawley S. L., Fraser O. J., Covey K. R., Lowrance P., 2003, *AJ*, 126, 3007
- Reid I. N., Cruz K. L., Laurie S. P., Liebert J., Dahn C. C., Harris H. C., Guetter H. H., Stone R. C., Canzian B., Luginbuhl C. B., Levine S. E., Monet A. K. B., Monet D. G., 2003, *AJ*, 125, 354
- Reid I. N., Gizis J. E., 1997, *AJ*, 113, 2246
- Reid I. N., Gizis J. E., Hawley S. L., 2002, *AJ*, 124, 2721
- Reid I. N., Kirkpatrick J. D., Liebert J., Burrows A., Gizis J. E., Burgasser A., Dahn C. C., Monet D., Cutri R., Beichman C. A., Skrutskie M., 1999, *ApJ*, 521, 613
- Reid N., Gilmore G., 1982, *MNRAS*, 201, 73
- Reipurth B., Clarke C., 2001, *AJ*, 122, 432
- Reylé C., Robin A. C., 2001, *A&A*, 373, 886
- Sagar R., Richtler T., 1991, *A&A*, 250, 324
- Salpeter E. E., 1955, *ApJ*, 121, 161
- Sanner J., Geffert M., 2001, *A&A*, 370, 87
- Santiago B., Beaulieu S., Johnson R., Gilmore G. F., 2001, *A&A*, 369, 74
- Scalo J., 1998, in *ASP Conf. Ser. 142: The Stellar Initial Mass Function (38th Hermonceux Conference) The IMF Revisited: A Case for Variations*. pp 201–+
- Scalo J. M., 1986, *Fundamentals of Cosmic Physics*, 11, 1
- Schaller G., Schaerer D., Meynet G., Maeder A., 1992, *A&AS*, 96, 269
- Schwarzschild M., Härm R., 1959, *ApJ*, 129, 637
- Selman F., Melnick J., Bosch G., Terlevich R., 1999, *A&A*, 347, 532
- Siess L., Dufour E., Forestini M., 2000, *A&A*, 358, 593
- Sirianni M., Nota A., Leitherer C., De Marchi G., Clampin M., 2000, *ApJ*, 533, 203
- Slesnick C. L., Hillenbrand L. A., Carpenter J. M., 2004, *ApJ*, 610, 1045
- Smith L. J., Gallagher J. S., 2001, *MNRAS*, 326, 1027
- Soubiran C., Bienaymé O., Siebert A., 2003, *A&A*, 398, 141

- Stahler S. W., Palla F., Ho P. T. P., 2000, *Protostars and Planets IV*, pp 327–+
- Stobie R. S., Ishida K., Peacock J. A., 1989, *MNRAS*, 238, 709
- Stolte A., Grebel E. K., Brandner W., Figer D. F., 2002, *A&A*, 394, 459
- Stothers R. B., 1992, *ApJ*, 392, 706
- Sung H., Bessell M. S., 2004, *AJ*, 127, 1014
- Testi L., Sargent A. I., 1998, *ApJ*, 508, L91
- Tilley D. A., Pudritz R. E., 2004, *MNRAS*, 353, 769
- Vanbeveren D., 1982, *A&A*, 115, 65
- Vesperini E., Heggie D. C., 1997, *MNRAS*, 289, 898
- Vine S. G., Bonnell I. A., 2003, *MNRAS*, 342, 314
- Vogt S. S., Butler R. P., Marcy G. W., Fischer D. A., Pourbaix D., Apps K., Laughlin G., 2002, *ApJ*, 568, 352
- von Hippel T., Gilmore G., Tanvir N., Robinson D., Jones D. H. P., 1996, *AJ*, 112, 192
- Weidemann V., 1990, in *NATO ASIC Proc. 305: Baryonic Dark Matter White Dwarfs and the Local Mass Density*. pp 87–+
- Weidemann V., 2000, *A&A*, 363, 647
- Weidemann V., Jordan S., Iben I. J., Casertano S., 1992, *AJ*, 104, 1876
- Weidner C., Kroupa P., 2004, *MNRAS*, 348, 187
- Weidner C., Kroupa P., 2005, *ApJ*, 625, 754
- Weidner C., Kroupa P., 2006, *MNRAS*, 365, 1333
- Weidner C., Kroupa P., Larsen S. S., 2004, *MNRAS*, 350, 1503
- Weigelt G., Baier G., 1985, *A&A*, 150, L18
- White R. J., Basri G., 2003, *ApJ*, 582, 1109
- Whitworth A. P., Zinnecker H., 2004, *A&A*, 427, 299
- Wolfire M. G., Cassinelli J. P., 1986, *ApJ*, 310, 207
- Wolfire M. G., Cassinelli J. P., 1987, *ApJ*, 319, 850
- Wuchterl G., Klessen R. S., 2001, *ApJ*, 560, L185
- Wuchterl G., Tscharnuter W. M., 2003, *A&A*, 398, 1081
- Zheng Z., Flynn C., Gould A., Bahcall J. N., Salim S., 2001, *ApJ*, 555, 393
- Zinnecker H., 1984, *MNRAS*, 210, 43
- Zoccali M., Cassisi S., Frogel J. A., Gould A., Ortolani S., Renzini A., Rich R. M., Stephens A. W., 2000, *ApJ*, 530, 418
- Zucker S., Mazeh T., 2001, *ApJ*, 562, 1038

